THE FUNCTIONAL SIGNIFICANCE OF RAB PHOSPHORYLATION

A Dissertation

Presented to the Faculty of the Graduate School

of Cornell University

In Partial Fulfillment of the Requirements for the Degree of

Doctor of Philosophy

by

Dante Mariano Lepore

August 2016

THE FUNCTIONAL SIGNIFICANCE OF RAB PHOSPHORYLATION

Dante Mariano Lepore, Ph.D.
Cornell University 2016

The precise movement of vesicle-enclosed cargo to predetermined spatial and temporal locations within the cell is an essential eukaryotic process. Extensive regulatory mechanisms are required to coordinate membrane trafficking events to ensure proper cell growth, organelle identity, and homeostasis. Rab GTPases are a family of proteins responsible for controlling the specificity and regulation of each membrane trafficking step by utilizing a nucleotide-bound cycle. Proteomic mass spectrometry screens have identified many Rabs to be phosphorylated, but the functional significance of these modifications is not well characterized. Using the *Saccharomyces cerevisiae* Rabs Sec4p and Ypt7p as models for unique and conserved phosphorylation events respectively, we found that phosphorylation can regulate effector protein recruitment as well as membrane association of Rab GTPases.

Although phosphorylation negatively regulates the activity of both Sec4p and Ypt7p, two very different mechanisms of action were uncovered. Sec4p phosphorylation was found to be a cell-cycle dependent modification mediated by the polo-like kinase Cdc5p that disrupts the interaction with exocyst component Sec15p. Sec4p phosphorylation occurs exclusively during cytokinesis and is required for proper cell size maintenance. Ypt7p phosphorylation on the other hand significantly alters membrane association. Phosphomimetic Ypt7p mutants fail to become prenylated and thus cannot directly anchor to membranes, rendering them nonfunctional. This particular phosphorylation site (serine/threonine 73) is well conserved among Rabs and phosphomimetic mutation leads to membrane dissociation in several other Rabs including Sec4p, Ypt1p, and Ypt6p. Rab phosphorylation thus appears to be an additional regulatory mechanism to more tightly control membrane trafficking events.

BIOGRAPHICAL SKETCH:

Dante Lepore was born in Albany, New York, 1988. Growing up in East Greenbush, NY, Dante had an interest in forensic science and criminal investigation at a young age. This interest propelled him forward to attend the University of New Haven for Forensic Science, specializing in biological samples, such as DNA analysis. During his studies, he became a tutor in math, chemistry, and biology and later went on to pursue independent research with Dr. Carl Barratt and Dr. Pauline Schwartz. Releasing his innate interest in the pursuit of knowledge and enthusiasm to share science with those around him, Dante decided to pursue a career as a researcher and educator.

After graduating the University of New Haven with a Bachelor's degree in both Forensic Science and Biology, he went on to study at Cornell University in the Biochemistry, Molecular, and Cellular Biology Program. In 2012 he joined the Collins lab where he studied the functional significance of Rab phosphorylation for his Ph.D. During his time at Cornell, he received an honorable mention for an NSF graduate research award and a CALS outstanding TA award. After graduating from Cornell University, Dante plans to work as a postdoc in the Munson lab at the University of Massachusetts Medical College in Worcester.

ACKNOWLEDGEMENTS

Reflecting on the past five years of graduate study, I recall many cliché hallmarks: late nights, difficult experiments, deadline rushes, thrilling discoveries (sometimes), hard work, countless seminars, and crippling caffeine addiction. However, in background of all those struggles and successes resides the most important factor towards a successful graduate school experience: the support of those around you. I can honestly say that without the encouragement and help of so many wonderful friends, family members, and mentors, I would not have made it to the end. As such, I would like to briefly thanks those who have given me the will to keep going when I did not think I could, who believed in me when I failed to believe in myself, and who trained me to be the scientist I find myself to be today.

First, I have to thank my family whose love and support always pushed me forward. To my father who always wanted to hear about my experiments even though not understanding them, to my mother who never stopped giving me the confidence to keep moving forward, and to my sister on whose advice I have come to rely on, I can never say thank you enough, and you will never know just how much your support has meant to me.

Next, I am indebted to those who spent countless hours to train me as a researcher. My advisor, Dr. Ruth Collins, has been instrumental in this regard. From basic laboratory practices to critical thinking, experimental design to data presentation, and scientific writing to research presentations, Ruth has shaped me into an independent and competent researcher, and I thank her immeasurably. In addition to Ruth herself, all members of the Collins Lab, past and present, helped lay my foundation as a researcher. In particular, Duane Hoch, Fabio Rinaldi, Guste Urbonaite, Gabrielle Pinto, Aurelie Kengne, and Olya Spassibojko have all been incredibly supportive over the years, and I owe them quite a bit. In particular, Olya Spassibojko has been

instrumental in her efforts working with Ytp7p phosphorylation and pushing that project forward.

Outside of the Collins Lab itself, I have had the support of many Cornell professors who freely gave me their time and support. First, Dr. Carolyn Sevier has been extremely approachable and generous with her time to help me with experiments, reagents, and typical graduate student crises. Though incredibly busy, she always found the time to meet with me, planned or not, and I am very grateful to have her on my committee. Also on my committee is Dr. Hening Lin, in whose lab I had the pleasure of rotating. Hening helped instill in me a fascination in molecular mechanisms and biochemistry that I will keep with me throughout my scientific career. I would also like to thank Dr. Tony Bretscher, Dr. Tim Huffaker, Dr. Ken Kemphues, and Dr. Maria Garcia all of whom I had the absolute pleasure of working with in my capacity as a teaching assistant.

I would like to thank my fellow BMCB classmates for their support and camaraderie throughout the years. In particular, I would like to thank Margaret Gustafson, Bridget Kreger, and Aravind Sivakumar. These three in particular have been a constant source of support and advice; I would be lost without them.

Finally, in terms of the project and the work itself, I would like to thank the Whittaker Lab for their help in designing and isolating pan Sec4p antibodies, as well as the Huffaker and Bretscher lab for providing yeast strains. This work was supported by NIH Predoctoral Training in Cellular and Molecular Biology (5T32GM007273) and by a grant from the National Institutes of Health (5R01GM069596) to R.N.C.

TABLE OF CONTENTS

LIST OF FIGURES

LIST OF TABLES:

Chapter 1: Introduction

Membrane Trafficking is Essential for Organelle Function and Identity

In eukaryotic cells, the presence of membrane bound organelles allows for the compartmentalization of biochemical processes necessary for life. Due to the fact that lipid membranes are fluid and dynamic structures that can exchange material, there must be tight regulatory control to establish and maintain the correct structural morphology, lipid and protein composition, and sub-cellular localization necessary for ideal organelle function. The movement of pre-packaged vesicles with specific protein and lipid cargos to various destinations/organelles throughout the cell is a conserved and essential process referred to as membrane trafficking.

The importance of membrane trafficking to maintain organelle composition and identity was realized with the advent of electron microscopy to visualize individual membrane-bound organelles within cells, differential centrifugation experiments to show the distinct composition of each organelle, and pulse-chase experiments to illustrate the movement of cargo between organelles (Barrnett and Palade, 1958; Duve, 1975; Jamieson and Palade, 1968). These results, which formed the foundation of modern cell biology and membrane trafficking, implied an exchange of material between organelles via vesicles in such a way that limited random diffusion and mixing of lipids and proteins in the cell to maintain compartmentalization of cellular function. Therefore, it is critical that the cell employs mechanisms to package specific cargo into vesicles, transport vesicles to their correct spatial and temporal sub-cellular location, and tether and fuse vesicles to their pre-determined target membrane. Indeed, disruption of membrane trafficking can lead to a variety of diseases including, but not limited to Alzheimer's disease, cystic fibrosis, I-cell disease, Griscelli syndrome, and Huntington's disease (Ben-Yoseph et al., 1987; Gauthier et al., 2004; Heda et al., 2001; Howell et al., 2006; Menasche et al., 2000;

Uemura et al., 2004). Therefore, the cell employs many regulatory control mechanisms to ensure that membrane trafficking is carried out with high fidelity. One such regulatory mechanism is performed by a family of proteins called Rab GTPases.

Rab GTPases are Molecular Switches

Rab GTPases (Rabs) are a family of proteins that regulate the trafficking of vesicles to their correct cellular destination and subsequent tethering. Rabs are the largest subfamily of the Ras superfamily of GTPases, with each Rab having a specific membrane localization and controlling a specific membrane trafficking step/s (figure 1.1) (Colicelli, 2004). There are 11 yeast Rabs, at least 60 human Rabs, and they have high sequence homology (Pereira-Leal and Seabra, 2000; Zerial and McBride, 2001). As GTPases, Rabs act as molecular switches, alternating between two distinct protein conformations when either GTP or GDP is bound (figure 1.2) (Dumas et al., 1999). Nucleotide exchange is catalyzed by guanine nucleotide exchange factors (GEFs), and GTPase activating proteins or GAPs facilitate Rab catalyzed GTP hydrolysis. In their GTP-bound state, Rabs engage with a set of proteins including motor proteins and tethering complexes called effectors, which transport and specifically target vesicles to their correct destination membrane fusion (Gillingham et al., 2014).

Structural changes upon nucleotide binding are mainly confined to two regions within the GTPase domain of Rab proteins, referred to as the switch I and switch II regions. These two switch regions make contacts with the Mg^{2+} ion and the γ-phosphate of the GTP nucleotide, thus they are sensitive to the nucleotide bound state of the Rab (Stroupe and Brunger, 2000). The switch I and II regions have been shown to make contacts with effector proteins as well, coupling the nucleotide bound-state of Rabs with effector protein binding. Much of the switch I and II regions are conserved among Rabs, but there is some variation to allow the specific

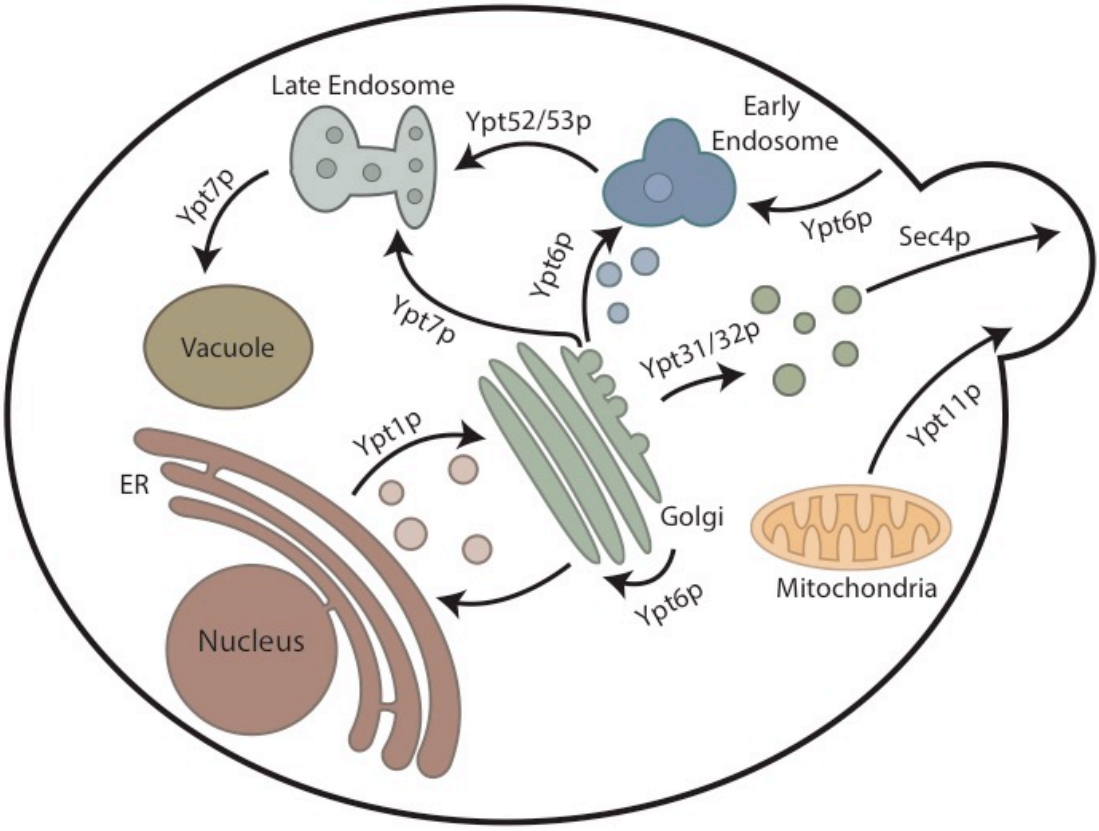

Figure 1.1: Rab GTPases participate in distinct membrane trafficking steps

Diagram of membrane trafficking steps in *S. cerevisiae* with relevant Rab GTPases listed for each step.

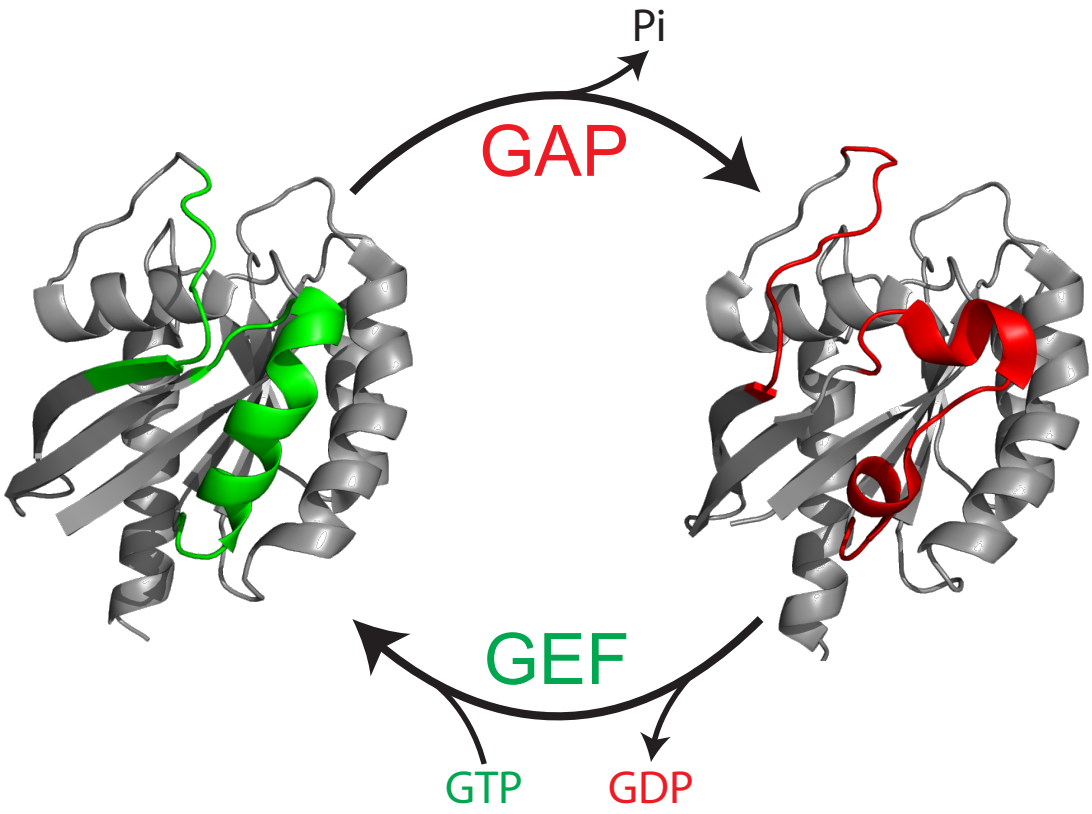

Figure 1.2: Rab GTPase nucleotide cycle
Protein crystal structures of the Rab GTPase Sec4p in a GDP-bound conformation (right) versus a GTP bound conformation (left) (PDB 3CPH and 1G17 respectively) (Ignatev et al., 2008; Stroupe and Brunger, 2000). Guanine nucleotide exchange factors (GEFs) exchange GDP for GTP in cells, while GTPase activating proteins stimulate Rabs to hydrolyze GTP to GDP, releasing an inorganic phosphate (Pi). The conformation changes between the two nucleotide-bound structures occur mainly in the switch I and switch II regions colored in green and red for the GTP and GDP bound structures respectively.

recruitment of distinct effector proteins for different membrane trafficking steps (Pereira-Leal and Seabra, 2000). Additionally, the COOH-terminus of Rabs (referred to as the hypervariable region) is thought to provide additional effector protein specificity as well as controlling the specific membrane localization of Rabs. The NH_2 terminus immediately preceding the GTPase domain (another intrinsically unstructured region of low sequence conservation among Rabs) is also thought to be involved in providing additional effector protein specificity. This was demonstrated by studying chimeric Rab proteins between Rab3/Rab5 and Sec4p/Ypt1p (Brennwald and Novick, 1993; Burton et al., 1997).

Effector Proteins Mediate Vesicle Movement and Tethering

Each individual Rab has a certain set of effector proteins for its particular membrane trafficking step. The definition of an effector protein is one that has a significantly higher affinity for GTP bound Rab as opposed to GDP bound Rab. As such, Rabs are considered to be in their active conformation when bound to GTP. By recruiting specific effector proteins, Rabs are able to control membrane trafficking events ranging from cargo selection, movement and tethering (Hutagalung and Novick, 2011).

Typically, vesicle formation and cargo selection is regulated by another family of small GTPases called Arf GTPases (Arfs) (Kawasaki et al., 2005). However, examples of Rabs facilitating cargo selection can be seen in Rab9 interacting with effector protein TIP47 to accumulate the mannose-6-phosphate receptor in vesicles moving between the late endosome and the trans-Golgi network (Aivazian et al., 2006; Carroll et al., 2001). Rabs also interact with motor proteins in a nucleotide dependent manner, such as the Rab Sec4p interacting with the class 5 myosin motor, Myo2p, to direct exocytic vesicles down actin cables towards sites of polarized exocytosis (Jin et al., 2011). A very common feature of Rabs is their ability to interact

with large tethering complexes as effectors in order to specifically hold vesicles at their target membrane to allow SNARE mediated fusion. Several different tethering complexes have been well explored, including the octameric exocyst complex, the HOPS complex, COG complex, and the GARP complex to name a few (Conibear and Stevens, 2000; Heider et al., 2016; Ho and Stroupe, 2015; Whyte and Munro, 2002). Although these complexes do not directly perform vesicle fusion, SNARE mediated fusion *in vivo* still requires their activity (Novick et al., 1981; Novick et al., 1980).

Rabs Exist as a Soluble Complex with GDI or Bound Directly to Membranes

In addition to their nucleotide binding cycle, Rabs can also cycle on and off membranes (figure 1.3). Through COOH-terminal 20 carbon geranylgeranyl modifications, Rabs can directly anchor to vesicles/membranes and facilitate trafficking steps through effector protein recruitment and tethering (Leung et al., 2006). Once a trafficking step has been completed, Rabs can be extracted from membranes for subsequent rounds of trafficking through an interaction with guanine nucleotide dissociation inhibitor proteins (GDIs). GDI proteins have increased affinity for Rabs in their GDP conformation and thus extraction is thought to take place after GTP hydrolysis (Shen and Seabra, 1996; Yamamoto et al., 1990). There is only one GDI protein in yeast (Gdi1p), and two isoforms in humans (*rab* GDI α and *rab* GDI β), thus GDI proteins are able to bind multiple Rabs to recycle them off membranes (Bachner et al., 1995; Garrett et al., 1994). GDI proteins recognize conserved sequences in the switch regions of Rabs in order to preferentially bind the GDP bound state, as well as to have affinity for all Rabs, although individual Rabs vary in affinity for GDI (Ignatev et al., 2008). GDI proteins also shield and make contacts with the hypervariable COOH-terminal and geranylgeranyl modification for membrane extraction (Pylypenko et al., 2006).

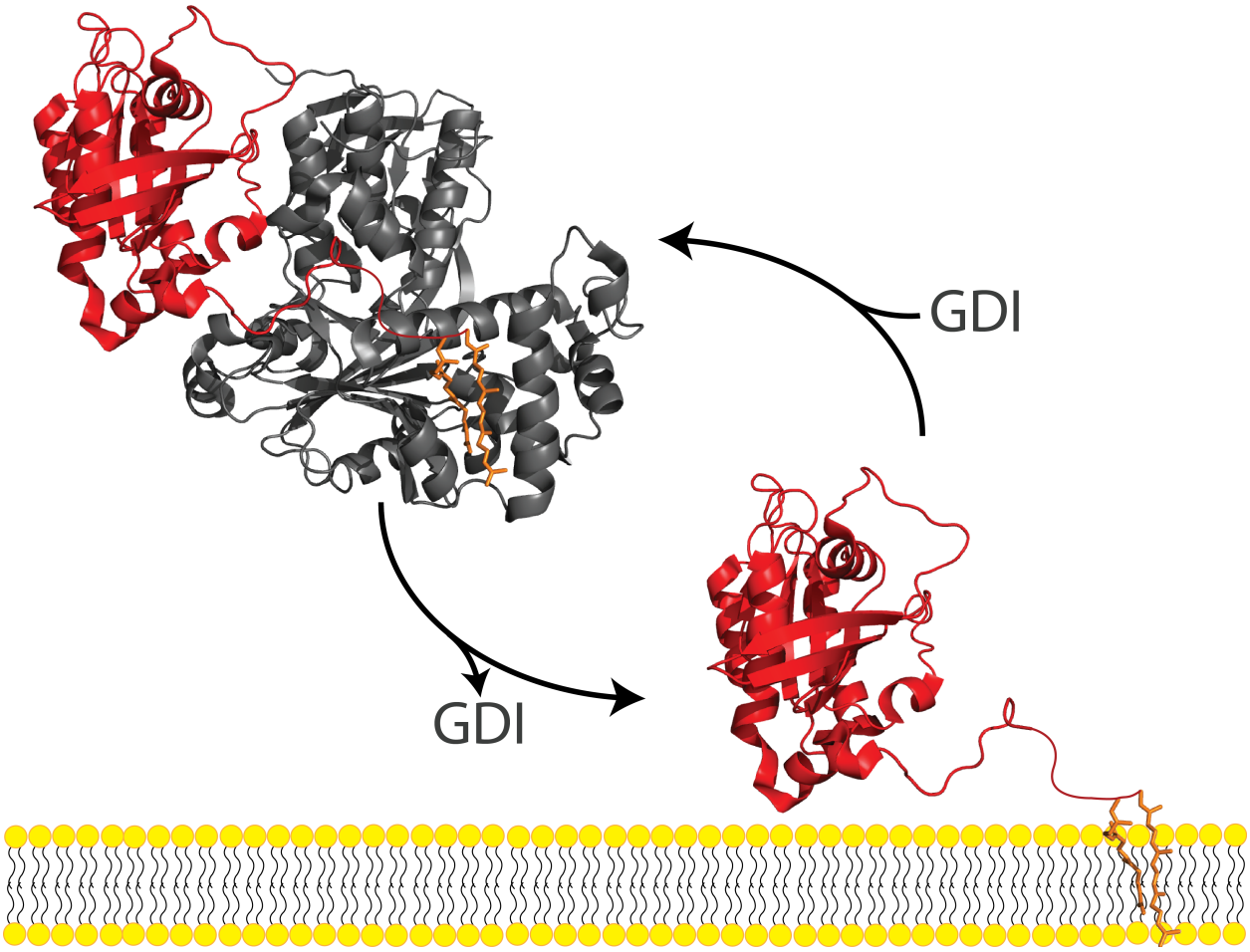

Figure 1.3: Rab GTPases exist bound either as soluble complexes with GDI or directly anchored to membranes

Diagram of Rab GTPase (red) in complex with GDI (gray) with shielded geranylgernanyl moiety (orange), and Rab GTPase directly anchored to a lipid bi-layer based on the crystal structure of Ypt1p in complex with Gdi1p (Pylypenko et al., 2006). The switch I and II regions are on the interface between the Rab and GDI, and the interaction prefers the GDP nucleotide-bound state of the Rab.

Geranylgeranylation of Rabs occurs in the hypervariable COOH-terminus and on one or two cysteine residues. In humans, there are six different motifs observed for the more common, double cysteine prenylation (XXCC, XCXC, CCXX, CCXXX, and XCCX where X is any amino acid), however Rab8 and Rab23 contain a single modified cysteine (Pereira-Leal and Seabra, 2001). It is important to mention that double prenylation is important for many Rabs to maintain their proper membrane localization and function. Substitution of the yeast Rabs Ypt1p and Sec4p prenylation sites with a single CAAX motif (a motif more common among other members of the Ras-superfamily of small GTPases for single geranylgeranylation or farnesylation), prevents normal membrane localization and renders these proteins non-functional (Calero et al., 2003; Casey and Seabra, 1996).

Geranylgeranyl Transferase II and Rab Escort Protein are Required to Prenylate Rabs

A single enzyme called geranylgeranyl transferase II (GGTase II) is responsible for transferring two geranylgeranyl groups onto cysteine residues of Rabs in the hypervariable region (Jiang and Ferro-Novick, 1994; Jiang et al., 1993; Jiang et al., 1995). GGTase II is a complex of Bet4p and Bet2p in *S. cerevisiae* and RABGGTA and RABGGTB in humans (Zhang et al., 2000). Since the motifs for prenylation and the surrounding amino acid sequence in Rabs are divergent in sequence, there is an accessory protein that binds Rabs in their GTPase domain and presents the Rab COOH-terminus to GGTase II for modification. This accessory protein is referred to as a Rab Escort Protein (REP). There is a single REP in *S. cerevisiae* (Mrs6p) and two in humans REP-1 and REP-2 (Benito-Moreno et al., 1994; Seabra et al., 1992).

GGTaseII uses geranylgeranyl pyrophosphate (GGpp) as a substrate and has increased affinity for the Rab-REP complex when GGpp is bound to the complex (Thoma et al., 2001). Upon transfer of the geranylgeranyl groups, the Rab can be directed onto membranes and the

REP recycled for further modification of newly synthesized Rabs. REP and GDI are very similar in this respect as they can solubilize prenylated Rabs and thus allow Rabs to find and anchor to their correct membrane compartment. Both REP and GDI proteins have high sequence homology and similar Rab recognition motifs, however GDI has a greatly increased affinity for prenylated Rabs, while REP can bind both prenylated and unprenylated Rabs (Sasaki et al., 1990; Waldherr et al., 1993). As such, it is fairly well established that REPs simply present Rabs to GGTase II for modification, then only initially deliver Rabs to membranes. Subsequent rounds of Rab membrane association and recycling are performed by GDI proteins.

Specific Recruitment of Rabs to Membrane

The main function of Rabs is to recruit effector proteins to their correct membrane compartment, but this raises the question as to how Rabs themselves are targeted to the correct membranes. This question still remains to be fully explored and there may be more than one type of mechanism involved. Recently, certain Rab GEFs have been shown to be sufficient to target Rab GTPases to a membrane using a GEF-Tom70 fusion protein to target a GEF to the mitochondria and measuring changes in Rab localization (Gerondopoulos et al., 2012). Depletion of Rab GEFs do disrupt normal Rab membrane localization, but do not completely preclude Rabs from associating with membranes (Cabrera and Ungermann, 2013). Furthermore, GEF cascade mechanisms, where the Rab from a previous membrane trafficking step recruits the GEF for a subsequent trafficking step as an effector protein has been observed via Ypt32p recruiting the GEF Sec2p for the Rab Sec4p to prepare post-Golgi secretory vesicles for polarize exocytosis (Ortiz et al., 2002). Membrane localization of Rabs has also been suggested to be influenced by membrane proteins that have high affinity prenylated Rabs (Calero and Collins, 2002). These

membrane proteins could facilitate the transition of Rabs from a soluble protein complex, to a membrane bound state.

Phosphorylation is an Additional Rab Post-Translational Modification

Post-translation modifications of Rabs extend beyond prenylation. Pathogens such as *Legionella pneumophila* can highjack membrane trafficking pathways through bacterial effector proteins that modify Rabs (Ge and Shao, 2011) (Goody et al., 2012; Mukherjee et al., 2011). Phosphocholination of Rab1a and Rab35 have been show to inhibit GEF mediated nucleotide exchange, while adenylation of Rab1b can completely block interaction with GDI (Oesterlin et al., 2012). If pathogens are capable of altering Rab function through post-translation modification, could endogenous regulatory systems be in place to regulate Rab function through covalent modification?

Phosphorylation is one of the most ubiquitous post-translation modifications observed in eukaryotes, affecting almost two-thirds of all proteins according to recent measurements (Newman et al., 2014; Sharma et al., 2014). Protein phosphorylation is performed by kinases that transfer the γ-phosphate from ATP to a serine, threonine, or tyrosine hydroxyl-group, though histidine phosphorylation has been observed in both prokaryotes and eukaryotes to a lesser extent (Besant and Attwood, 2005; Mukherjee et al., 2011; Stock et al., 2000). Phosphorylation is a dynamic modification, able to be removed by phosphatases, and thus act as an additional regulatory mechanism to control a protein's function. Many mass spectrometry proteomic screens have identified Rab GTPases as phosphoproteins, though the extent and ramifications of such modifications are not yet understood. We sought to investigate the cellular consequences of Rab phosphorylation and understand what cellular conditions lead to Rab phosphorylation.

Mass spectrometry confirmed phosphorylation events of Rab proteins occur in approximately 98% of human Rabs and 82% of yeast Rabs (Hornbeck et al., 2015; Sadowski et al., 2013) (figure 1.4A). These phosphorylation events also tend to accumulate in the intrinsically unstructured NH_2 and COOH termini of Rab GTPases, although phosphorylation in the GTPase domain itself is not uncommon. This is particular true for *S. cerevisiae* Rabs, but considering how the NH_2 and COOH termini consist of only a very small portion of the entire Rab, phosphorylation is still quite enriched. It is difficult to identify consensus motifs among Rabs for phosphorylation events in these NH_2 and COOH terminal intrinsically unstructured regions, as they are quite divergent (the COOH terminus is referred to as the hypervariable region). This does not mean it is unimportant, as phosphorylation could have different effects for individual Rabs using these regions.

There is very high sequence conservation within the GTPase domain of Rabs, making it easier to identify whether or not there are any conserved phosphorylation sites. Performing a ClustalX alignment of human and yeast Rabs, then superimposing all known phosphorylation sites reveals a highly conserved serine/threonine residue in the switch II region (figure 1.5). This particular phosphorylation event is present in approximately 20% of all Rabs, and is much more common in humans than in yeast. Indeed, only the yeast Rab Ypt7p has yet to be shown to have this particular modification, however this information is only based on proteomic screens not necessarily investigating Rabs in particular.

Combining the structure function information available for Rabs and the location of phosphorylation sites, it could be hypothesized that NH_2 and COOH terminal phosphorylation events could regulate specific effector protein recruitment or membrane localization, while phosphorylation of conserved switch regions could regulate nucleotide or membrane cycling of

A.

Homo sapiens	Percent of Phophorylation Events	29%	52%	28%
	Average Length (aa)	19	162	40
Saccharomyces cerevisiae	Percent of Phophorylation Events	44%	28%	28%
	Average Length (aa)	29	162	43

B.

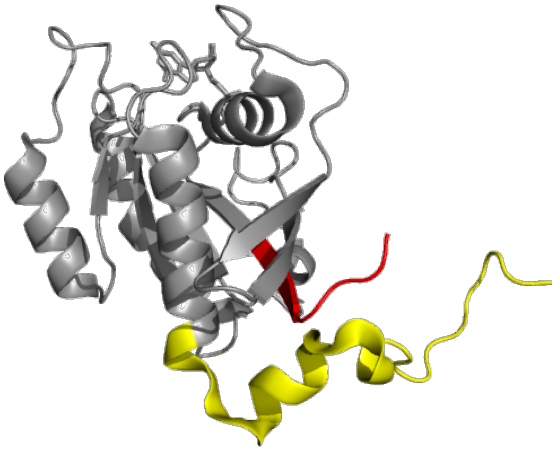

Figure 1.4: Phosphorylation of Rab GTPases

A. Table of complied phosphorylation data and representation of the domains of an average Rab GTPase where phosphorylation occurs (Hornbeck et al., 2015; Sadowski et al., 2013).

B. Crystal structure of a Rab GTPase with the GTPase domain in gray, NH_2 terminal intrinsically unstructured region in red, and COOH terminal hypervariable domain in yellow. Based on the PDB structure 2BCG (Pylypenko et al., 2006)

Figure 1.5: Rab phosphorylation of the switch II region

A. Representative image of the switch II domain from a Clustal X (Larkin et al., 2007) alignment of human and yeast Rab GTPases . Mass spectrometry confirmed phosphorylation sites are highlighted in red (Hornbeck et al., 2015; Sadowski et al., 2013).

B. Sequence logo of the switch II domain with the conserved S/T phosphorylation site highlighted (Crooks et al., 2004; Schneider and Stephens, 1990).

A.

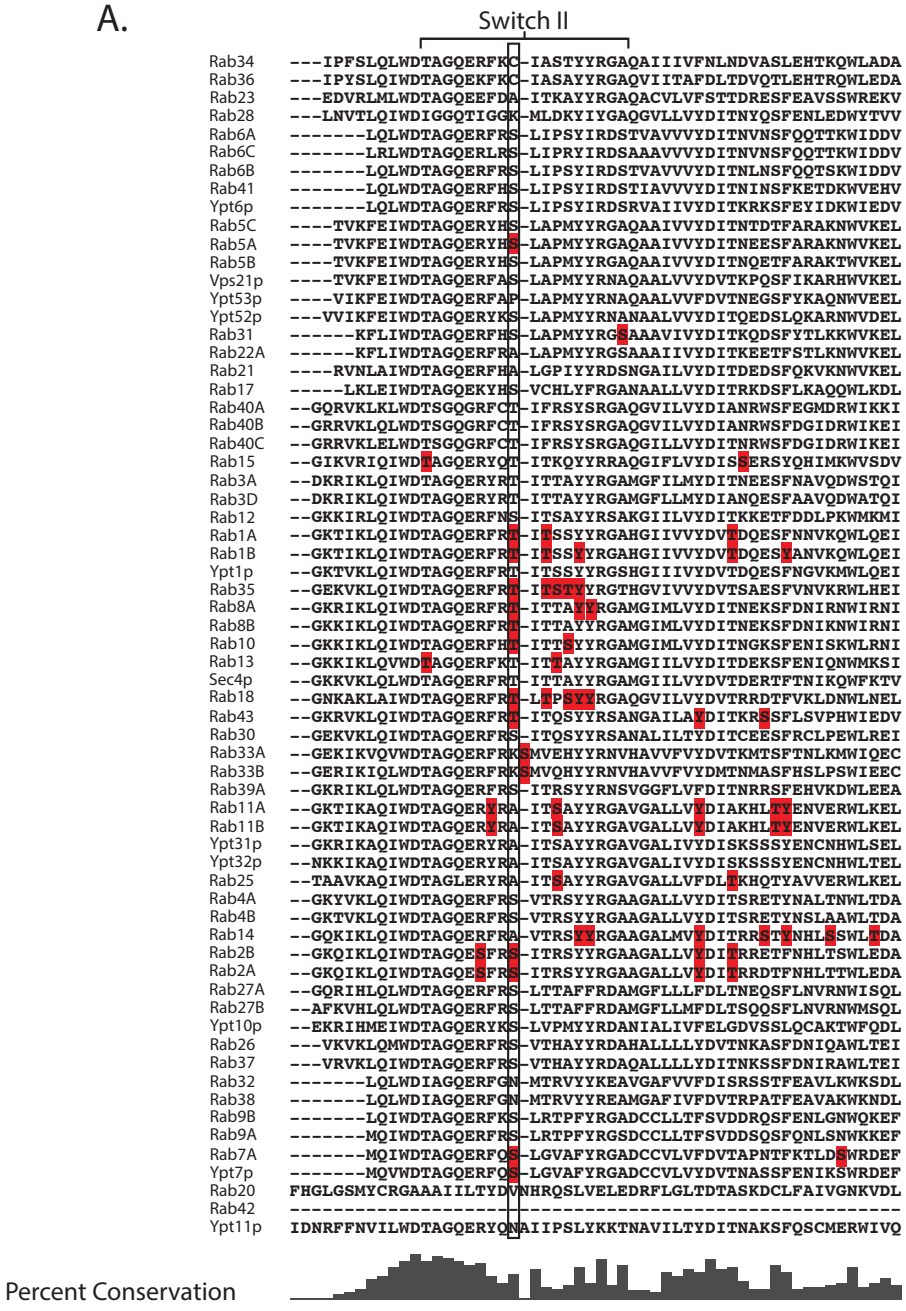
Switch II
Rab34 ---IPFSLQLWDTAGQERFKC-IASTYYRGAQAIIIVFNLNDVASLEHTKQWLADA
Rab36 ---IPYSLQIWDTAGQEKFKC-IASAYYRGAQVIITAFDLTDVQTLEHTRQWLEDA
Rab23 ---EDVRLMLWDTAGQEEFDA-ITKAYYRGAQACVLVFSTTDRESFEAVSSWREKV
Rab28 ---LNVTLQIWDIGGQTIGGK-MLDKYIYGAQGVLLVYDITNYQSFENLEDWYTVV
Rab6A -------LQLWDTAGQERFRS-LIPSYIRDSTVAVVVYDITNVNSFQQTTKWIDDV
Rab6C -------LRLWDTAGQERLRS-LIPRYIRDSAAAVVVYDITNVNSFQQTTKWIDDV
Rab6B -------LQLWDTAGQERFRS-LIPSYIRDSTVAVVVYDITNLNSFQQTSKWIDDV
Rab41 -------LQLWDTAGQERFHS-LIPSYIRDSTIAVVVYDITNINSFKETDKWVEHV
Ypt6p -------LQLWDTAGQERFRS-LIPSYIRDSRVAIIVYDITKRKSFEYIDKWIEDV
Rab5C ----TVKFEIWDTAGQERYHS-LAPMYYRGAQAAIVVYDITNTDTFARAKNWVKEL
Rab5A ----TVKFEIWDTAGQERYHS-LAPMYYRGAQAAIVVYDITNEESFARAKNWVKEL
Rab5B ----TVKFEIWDTAGQERYHS-LAPMYYRGAQAAIVVYDITNQETFARAKTWVKEL
Vps21p ----TVKFEIWDTAGQERFAS-LAPMYYRNAQAALVVYDVTKPQSFIKARHWVKEL
Ypt53p ----VIKFEIWDTAGQERFAP-LAPMYYRNAQAALVVFDVTNEGSFYKAQNWVEEL
Ypt52p ---VVIKFEIWDTAGQERYKS-LAPMYYRNANAALVVYDITQEDSLQKARNWVDEL
Rab31 ------KFLIWDTAGQERFHS-LAPMYYRGSAAAVIVYDITKQDSFYTLKKWVKEL
Rab22A ------KFLIWDTAGQERFRA-LAPMYYRGSAAAIIVYDITKEETFSTLKNWVKEL
Rab21 ----RVNLAIWDTAGQERFHA-LGPIYYRDSNGAILVYDITDEDSFQKVKNWVKEL
Rab17 -----LKLEIWDTAGQEKYHS-VCHLYFRGANAALLVYDITRKDSFLKAQQWLKDL
Rab40A --GQRVKLKLWDTSGQGRFCT-IFRSYSRGAQGVILVYDIANRWSFEGMDRWIKKI
Rab40B --GRRVKLQLWDTSGQGRFCT-IFRSYSRGAQGVILVYDIANRWSFDGIDRWIKEI
Rab40C --GRRVKLELWDTSGQGRFCT-IFRSYSRGAQGILLVYDITNRWSFDGIDRWIKEI
Rab15 --GIKVRIQIWDTAGQERYQT-ITKQYYRRAQGIFLVYDISSERSYQHIMKWVSDV
Rab3A --DKRIKLQIWDTAGQERYRT-ITTAYYRGAMGFILMYDITNEESFNAVQDWSTQI
Rab3D --DKRIKLQIWDTAGQERYRT-ITTAYYRGAMGFLLMYDIANQESFAAVQDWATQI
Rab12 --GKKIRLQIWDTAGQERFNS-ITSAYYRSAKGILVVYDITKKETFDDLPKWMKMI
Rab1A --GKTIKLQIWDTAGQERFRT-ITSSYYRGAHGIIVVYDVTDQESFNNVKQWLQEI
Rab1B --GKTIKLQIWDTAGQERFRA-ITSSYYRGAHGIIVVYDVTDQESYANVKQWLQEI
Ypt1p --GKTVKLQIWDTAGQERFRT-ITSSYYRGSHGIIIVYDVTDQESFNGVKMWLQEI
Rab35 --GEKVKLQIWDTAGQERFRT-ITSTYYRGTHGVIVVYDVTSAESFVNVKRWLHEI
Rab8A --GKRIKLQIWDTAGQERFRT-ITTAYYRGAMGIMLVYDITNEKSFDNIRNWIRNI
Rab8B --GKKIKLQIWDTAGQERFRT-ITTAYYRGAMGIMLVYDITNEKSFDNIKNWIRNI
Rab10 --GKKIKLQIWDTAGQERFHT-ITTSYYRGAMGIMLVYDITNGKSFENISKWLRNI
Rab13 --GKKIKLQVWDTAGQERFKT-ITTAYYRGAMGIILVYDITDEKSFENIQNWMKSI
Sec4p --GKKVKLQLWDTAGQERFRT-ITTAYYRGAMGIILVYDVTDERTFTNIKQWFKTV
Rab18 --GNKAKLAIWDTAGQERFRT-LTPSYYRGAQGVILVYDVTRRDTFVKLDNWLNEL
Rab43 --GKRVKLQIWDTAGQERFRT-ITQSYYRSANGAILAYDITKRSSFLSVPHWIEDV
Rab30 --GEKVKLQIWDTAGQERFRS-ITQSYYRSANALILTYDITCEESFRCLPEWLREI
Rab33A --GEKIKVQVWDTAGQERFRKSMVEHYYRNVHAVVFVYDVTKMTSFTNLKMWIQEC
Rab33B --GERIKIQLWDTAGQERFRKSMVQHYYRNVHAVVFVYDMTNMASFHSLPSWIEEC
Rab39A --GKRIKLQLWDTAGQERFRS-ITRSYYRNSVGGFLVFDITNRRSFEHVKDWLEEA
Rab11A --GKTIKAQIWDTAGQERYRA-ITSAYYRGAVGALLVYDIAKHLTYENVERWLKEL
Rab11B --GKTIKAQIWDTAGQERYRA-ITSAYYRGAVGALLVYDIAKHLTYENVERWLKEL
Ypt31p --GKRIKAQIWDTAGQERYRA-ITSAYYRGAVGALIVYDISKSSSYENCNHWLSEL
Ypt32p --NKKIKAQIWDTAGQERYRA-ITSAYYRGAVGALIVYDISKSSSYENCNHWLTEL
Rab25 --TAAVKAQIWDTAGLERYRA-ITSAYYRGAVGALLVFDLTKHQTYAVVERWLKEL
Rab4A --GKYVKLQIWDTAGQERFRS-VTRSYYRGAAGALLVYDITSRETYNALTNWLTDA
Rab4B --GKTVKLQIWDTAGQERFRS-VTRSYYRGAAGALLVYDITSRETYNSLAAWLTDA
Rab14 --GQKIKLQIWDTAGQERFRA-VTRSYYRGAAGALMVYDITRRSTYNHLSSWLTDA
Rab2B --GKQIKLQIWDTAGQESFRS-ITRSYYRGAAGALLVYDITRRETFNHLTSWLEDA
Rab2A --GKQIKLQIWDTAGQESFRS-ITRSYYRGAAGALLVYDITRRDTFNHLTTWLEDA
Rab27A --GQRIHLQLWDTAGQERFRS-LTTAFFRDAMGFLLLFDLTNEQSFLNVRNWISQL
Rab27B --AFKVHLQLWDTAGQERFRS-LTTAFFRDAMGFLLMFDLTSQQSFLNVRNWMSQL
Ypt10p --EKRIHMEIWDTAGQERYKS-LVPMYYRDANIALIVFELGDVSSLQCAKTWFQDL
Rab26 ---VKVKLQMWDTAGQERFRS-VTHAYYRDAHALLLLYDVTNKASFDNIQAWLTEI
Rab37 ---VRVKLQIWDTAGQERFRS-VTHAYYRDAQALLLLYDITNKSSFDNIRAWLTEI
Rab32 -------LQLWDIAGQERFGN-MTRVYYKEAVGAFVVFDISRSSTFEAVLKWKSDL
Rab38 -------LQLWDIAGQERFGN-MTRVYYREAMGAFIVFDVTRPATFEAVAKWKNDL
Rab9B -------LQIWDTAGQERFKS-LRTPFYRGADCCLLTFSVDDRQSFENLGNWQKEF
Rab9A -------MQIWDTAGQERFRS-LRTPFYRGSDCCLLTFSVDDSQSFQNLSNWKKEF
Rab7A -------MQIWDTAGQERFQS-LGVAFYRGADCCVLVFDVTAPNTFKTLDSWRDEF
Ypt7p -------MQVWDTAGQERFQS-LGVAFYRGADCCVLVYDVTNASSFENIKSWRDEF
Rab20 FHGLGSMYCRGAAAIILTYDVNHRQSLVELEDRFLGLTDTASKDCLFAIVGNKVDL
Rab42 ----------
Ypt11p IDNRFFNVILWDTAGQERYQNAIIPSLYKKTNAVILTYDITNAKSFQSCMERWIVQ
Percent Conservation

B.

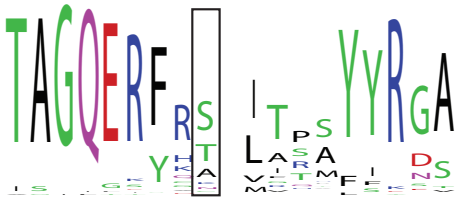
TAGQERFRS
YYRGA

Rabs. To test this idea, it is necessary to investigate specific Rabs that are representative of these general observations about phosphorylation. Using *S. cerevisiae* Rab Sec4p as a model for NH_2 and COOH terminal phosphorylation and Ypt7p as a model for the conserved switch II phosphorylation event, we sought to determine the physiological role for these phosphorylation events, the kinases responsible for this modification, and under what cellular context phosphorylation is up/down regulated.

Overview of thesis

Rab GTPases are highly conserved molecular switches that regulate membrane trafficking in eurkaryotes. Able to cycle between GTP/GDP nucleotide bound states, as well as soluble and membrane associated states, Rabs coordinate the recruitment of effector proteins such as motors and tethering complexes to facilitate each trafficking step. Recent mass spectrometry data show Rabs to be phosphoproteins, but the pathways involved, functional consequences, and cellular pathways involved remain unclear.

Rab phosphorylation accumulates in NH_2 and COOH terminal intrinsically unstructured regions. Using Sec4p as a model, the functional consequences, cellular conditions under which phosphorylation occurs, and a kinase responsible for modification have been elucidated. As hypothesized, modification of the intrinsically unstructured regions affected recruitment of the effector protein Sec15p, a component of the exocyst tethering complex. Furthermore, phosphorylation was enriched on the membrane-bound fraction of Sec4p, suggesting it plays a role while Sec4p is associated with vesicles/plasma membrane.

A global kinase overexpression screen of all 127 yeast kinases identified the cell-cycle regulated polo-like kinase, Cdc5p as a potential Sec4p kinase. Cdc5p was able to directly phosphorylate Sec4p substrates, and loss of Cdc5p activity ablated Sec4p phosphorylation.

Furthermore, cell-cycle block and release experiments show Sec4p phosphorylation to be cell cycle dependent, and exclusively taking place when Sec4p is localized to the bud neck along with Cdc5p during cytokinesis. While phosphomimetic mutations of Sec4p were known to be nonfunctional (Heger et al., 2011), a fully unphosphorylatable Sec4p mutant shows decreased cell size in a cytokinetic defective *hof1Δ* and wild-type genetic background. These data suggest that phosphorylation inhibits Sec4p function at the bud neck directly prior to completion of cytokinesis, and that this inhibition is required for proper maintenance of cell size.

Phosphorylation of the switch II region at a highly conserved serine/threonine residue was also investigated using Ypt7p as a representative Rab GTPase. Phosphomimetic mutants were found to be completely non-functional, while no adverse phenotypes were observed with an unphosphorylatable mutant. Indeed, the phosphomimetic mutant was unable to associate with membranes at all, and this was found to be a result of loss of Rab prenylation. Additionally, non-prenylated phosphomimetic Ypt7p has decreased affinity for Gdi1p, while unprenylated unphosphorylatable Ypt7p has a much higher affinity for Gdi1p compared to unprenylated wild type protein. These same mutations in other Rabs, regardless of observed phosphorylation events, confers the same phenotype; loss of membrane association. Taken together, the conserved phosphorylation site in the switch II domain may regulate interaction with GDI or regulate prenylation of Rabs.

References

Aivazian, D., R.L. Serrano, and S. Pfeffer. 2006. TIP47 is a key effector for Rab9 localization. *J Cell Biol*. 173:917-926.

Bachner, D., Z. Sedlacek, B. Korn, H. Hameister, and A. Poustka. 1995. Expression patterns of two human genes coding for different rab GDP-dissociation inhibitors (GDIs), extremely conserved proteins involved in cellular transport. *Hum Mol Genet*. 4:701-708.

Barrnett, R.J., and G.E. Palade. 1958. Applications of histochemistry to electron microscopy. *J Histochem Cytochem*. 6:1-12.

Ben-Yoseph, Y., M. Potier, D.A. Mitchell, B.A. Pack, S.B. Melancon, and H.L. Nadler. 1987. Altered molecular size of N-acetylglucosamine 1-phosphotransferase in I-cell disease and pseudo-Hurler polydystrophy. *Biochem J*. 248:697-701.

Benito-Moreno, R.M., M. Miaczynska, B.E. Bauer, R.J. Schweyen, and A. Ragnini. 1994. Mrs6p, the yeast homologue of the mammalian choroideraemia protein: immunological evidence for its function as the Ypt1p Rab escort protein. *Curr Genet*. 27:23-25.

Besant, P.G., and P.V. Attwood. 2005. Mammalian histidine kinases. *Biochim Biophys Acta*. 1754:281-290.

Brennwald, P., and P. Novick. 1993. Interactions of three domains distinguishing the Ras-related GTP-binding proteins Ypt1 and Sec4. *Nature*. 362:560-563.

Burton, J.L., V. Slepnev, and P.V. De Camilli. 1997. An evolutionarily conserved domain in a subfamily of Rabs is crucial for the interaction with the guanyl nucleotide exchange factor Mss4. *J Biol Chem*. 272:3663-3668.

Cabrera, M., and C. Ungermann. 2013. Guanine nucleotide exchange factors (GEFs) have a critical but not exclusive role in organelle localization of Rab GTPases. *J Biol Chem*. 288:28704-28712.

Calero, M., C.Z. Chen, W. Zhu, N. Winand, K.A. Havas, P.M. Gilbert, C.G. Burd, and R.N. Collins. 2003. Dual prenylation is required for Rab protein localization and function. *Mol Biol Cell*. 14:1852-1867.

Calero, M., and R.N. Collins. 2002. Saccharomyces cerevisiae Pra1p/Yip3p interacts with Yip1p and Rab proteins. *Biochem Biophys Res Commun*. 290:676-681.

Carroll, K.S., J. Hanna, I. Simon, J. Krise, P. Barbero, and S.R. Pfeffer. 2001. Role of Rab9 GTPase in facilitating receptor recruitment by TIP47. *Science*. 292:1373-1376.

Casey, P.J., and M.C. Seabra. 1996. Protein prenyltransferases. *J Biol Chem*. 271:5289-5292.

Colicelli, J. 2004. Human RAS superfamily proteins and related GTPases. *Sci STKE*. 2004:RE13.

Conibear, E., and T.H. Stevens. 2000. Vps52p, Vps53p, and Vps54p form a novel multisubunit complex required for protein sorting at the yeast late Golgi. *Mol Biol Cell*. 11:305-323.

Crooks, G.E., G. Hon, J.M. Chandonia, and S.E. Brenner. 2004. WebLogo: a sequence logo generator. *Genome Res*. 14:1188-1190.

Dumas, J.J., Z. Zhu, J.L. Connolly, and D.G. Lambright. 1999. Structural basis of activation and GTP hydrolysis in Rab proteins. *Structure*. 7:413-423.

Duve, C. 1975. Exploring cells with a centrifuge. *Science*. 189:186-194.

Garrett, M.D., J.E. Zahner, C.M. Cheney, and P.J. Novick. 1994. GDI1 encodes a GDP dissociation inhibitor that plays an essential role in the yeast secretory pathway. *EMBO J*. 13:1718-1728.

Gauthier, L.R., B.C. Charrin, M. Borrell-Pages, J.P. Dompierre, H. Rangone, F.P. Cordelieres, J. De Mey, M.E. MacDonald, V. Lessmann, S. Humbert, and F. Saudou. 2004. Huntingtin controls neurotrophic support and survival of neurons by enhancing BDNF vesicular transport along microtubules. *Cell*. 118:127-138.

Ge, J., and F. Shao. 2011. Manipulation of host vesicular trafficking and innate immune defence by Legionella Dot/Icm effectors. *Cell Microbiol*. 13:1870-1880.

Gerondopoulos, A., L. Langemeyer, J.R. Liang, A. Linford, and F.A. Barr. 2012. BLOC-3 mutated in Hermansky-Pudlak syndrome is a Rab32/38 guanine nucleotide exchange factor. *Curr Biol*. 22:2135-2139.

Gillingham, A.K., R. Sinka, I.L. Torres, K.S. Lilley, and S. Munro. 2014. Toward a comprehensive map of the effectors of rab GTPases. *Dev Cell*. 31:358-373.

Goody, P.R., K. Heller, L.K. Oesterlin, M.P. Muller, A. Itzen, and R.S. Goody. 2012. Reversible phosphocholination of Rab proteins by Legionella pneumophila effector proteins. *EMBO J*. 31:1774-1784.

Heda, G.D., M. Tanwani, and C.R. Marino. 2001. The Delta F508 mutation shortens the biochemical half-life of plasma membrane CFTR in polarized epithelial cells. *Am J Physiol Cell Physiol*. 280:C166-174.

Heger, C.D., C.D. Wrann, and R.N. Collins. 2011. Phosphorylation provides a negative mode of regulation for the yeast Rab GTPase Sec4p. *PLoS One*. 6:e24332.

Heider, M.R., M. Gu, C.M. Duffy, A.M. Mirza, L.L. Marcotte, A.C. Walls, N. Farrall, Z. Hakhverdyan, M.C. Field, M.P. Rout, A. Frost, and M. Munson. 2016. Subunit connectivity, assembly determinants and architecture of the yeast exocyst complex. *Nat Struct Mol Biol*. 23:59-66.

Ho, R., and C. Stroupe. 2015. The HOPS/class C Vps complex tethers membranes by binding to one Rab GTPase in each apposed membrane. *Mol Biol Cell*. 26:2655-2663.

Hornbeck, P.V., B. Zhang, B. Murray, J.M. Kornhauser, V. Latham, and E. Skrzypek. 2015. PhosphoSitePlus, 2014: mutations, PTMs and recalibrations. *Nucleic Acids Res*. 43:D512-520.

Howell, G.J., Z.G. Holloway, C. Cobbold, A.P. Monaco, and S. Ponnambalam. 2006. Cell biology of membrane trafficking in human disease. *Int Rev Cytol*. 252:1-69.

Hutagalung, A.H., and P.J. Novick. 2011. Role of Rab GTPases in membrane traffic and cell physiology. *Physiol Rev*. 91:119-149.

Ignatev, A., S. Kravchenko, A. Rak, R.S. Goody, and O. Pylypenko. 2008. A structural model of the GDP dissociation inhibitor rab membrane extraction mechanism. *J Biol Chem*. 283:18377-18384.

Jamieson, J.D., and G.E. Palade. 1968. Intracellular transport of secretory proteins in the pancreatic exocrine cell. IV. Metabolic requirements. *J Cell Biol*. 39:589-603.

Jiang, Y., and S. Ferro-Novick. 1994. Identification of yeast component A: reconstitution of the geranylgeranyltransferase that modifies Ypt1p and Sec4p. *Proc Natl Acad Sci U S A*. 91:4377-4381.

Jiang, Y., G. Rossi, and S. Ferro-Novick. 1993. Bet2p and Mad2p are components of a prenyltransferase that adds geranylgeranyl onto Ypt1p and Sec4p. *Nature*. 366:84-86.

Jiang, Y., G. Rossi, and S. Ferro-Novick. 1995. Characterization of yeast type-II geranylgeranyltransferase. *Methods Enzymol*. 257:21-29.

Jin, Y., A. Sultana, P. Gandhi, E. Franklin, S. Hamamoto, A.R. Khan, M. Munson, R. Schekman, and L.S. Weisman. 2011. Myosin V transports secretory vesicles via a Rab GTPase cascade and interaction with the exocyst complex. *Dev Cell*. 21:1156-1170.

Kawasaki, M., K. Nakayama, and S. Wakatsuki. 2005. Membrane recruitment of effector proteins by Arf and Rab GTPases. *Curr Opin Struct Biol*. 15:681-689.

Larkin, M.A., G. Blackshields, N.P. Brown, R. Chenna, P.A. McGettigan, H. McWilliam, F. Valentin, I.M. Wallace, A. Wilm, R. Lopez, J.D. Thompson, T.J. Gibson, and D.G. Higgins. 2007. Clustal W and Clustal X version 2.0. *Bioinformatics*. 23:2947-2948.

Leung, K.F., R. Baron, and M.C. Seabra. 2006. Thematic review series: lipid posttranslational modifications. geranylgeranylation of Rab GTPases. *J Lipid Res*. 47:467-475.

Menasche, G., E. Pastural, J. Feldmann, S. Certain, F. Ersoy, S. Dupuis, N. Wulffraat, D. Bianchi, A. Fischer, F. Le Deist, and G. de Saint Basile. 2000. Mutations in RAB27A cause Griscelli syndrome associated with haemophagocytic syndrome. *Nat Genet*. 25:173-176.

Mukherjee, S., X. Liu, K. Arasaki, J. McDonough, J.E. Galan, and C.R. Roy. 2011. Modulation of Rab GTPase function by a protein phosphocholine transferase. *Nature*. 477:103-106.

Newman, R.H., J. Zhang, and H. Zhu. 2014. Toward a systems-level view of dynamic phosphorylation networks. *Front Genet*. 5:263.

Novick, P., S. Ferro, and R. Schekman. 1981. Order of events in the yeast secretory pathway. *Cell*. 25:461-469.

Novick, P., C. Field, and R. Schekman. 1980. Identification of 23 complementation groups required for post-translational events in the yeast secretory pathway. *Cell*. 21:205-215.

Oesterlin, L.K., R.S. Goody, and A. Itzen. 2012. Posttranslational modifications of Rab proteins cause effective displacement of GDP dissociation inhibitor. *Proc Natl Acad Sci U S A*. 109:5621-5626.

Ortiz, D., M. Medkova, C. Walch-Solimena, and P. Novick. 2002. Ypt32 recruits the Sec4p guanine nucleotide exchange factor, Sec2p, to secretory vesicles; evidence for a Rab cascade in yeast. *J Cell Biol*. 157:1005-1015.

Pereira-Leal, J.B., and M.C. Seabra. 2000. The mammalian Rab family of small GTPases: definition of family and subfamily sequence motifs suggests a mechanism for functional specificity in the Ras superfamily. *J Mol Biol*. 301:1077-1087.

Pereira-Leal, J.B., and M.C. Seabra. 2001. Evolution of the Rab family of small GTP-binding proteins. *J Mol Biol*. 313:889-901.

Pylypenko, O., A. Rak, T. Durek, S. Kushnir, B.E. Dursina, N.H. Thomae, A.T. Constantinescu, L. Brunsveld, A. Watzke, H. Waldmann, R.S. Goody, and K. Alexandrov. 2006. Structure of doubly prenylated Ypt1:GDI complex and the mechanism of GDI-mediated Rab recycling. *EMBO J*. 25:13-23.

Sadowski, I., B.J. Breitkreutz, C. Stark, T.C. Su, M. Dahabieh, S. Raithatha, W. Bernhard, R. Oughtred, K. Dolinski, K. Barreto, and M. Tyers. 2013. The PhosphoGRID Saccharomyces cerevisiae protein phosphorylation site database: version 2.0 update. *Database (Oxford)*. 2013:bat026.

Sasaki, T., A. Kikuchi, S. Araki, Y. Hata, M. Isomura, S. Kuroda, and Y. Takai. 1990. Purification and characterization from bovine brain cytosol of a protein that inhibits the dissociation of GDP from and the subsequent binding of GTP to smg p25A, a ras p21-like GTP-binding protein. *J Biol Chem*. 265:2333-2337.

Schneider, T.D., and R.M. Stephens. 1990. Sequence logos: a new way to display consensus sequences. *Nucleic Acids Res*. 18:6097-6100.

Seabra, M.C., M.S. Brown, C.A. Slaughter, T.C. Sudhof, and J.L. Goldstein. 1992. Purification of component A of Rab geranylgeranyl transferase: possible identity with the choroideremia gene product. *Cell*. 70:1049-1057.

Sharma, K., R.C. D'Souza, S. Tyanova, C. Schaab, J.R. Wisniewski, J. Cox, and M. Mann. 2014. Ultradeep human phosphoproteome reveals a distinct regulatory nature of Tyr and Ser/Thr-based signaling. *Cell Rep*. 8:1583-1594.

Shen, F., and M.C. Seabra. 1996. Mechanism of digeranylgeranylation of Rab proteins. Formation of a complex between monogeranylgeranyl-Rab and Rab escort protein. *J Biol Chem*. 271:3692-3698.

Stock, A.M., V.L. Robinson, and P.N. Goudreau. 2000. Two-component signal transduction. *Annu Rev Biochem*. 69:183-215.

Stroupe, C., and A.T. Brunger. 2000. Crystal structures of a Rab protein in its inactive and active conformations. *J Mol Biol*. 304:585-598.

Thoma, N.H., A. Iakovenko, A. Kalinin, H. Waldmann, R.S. Goody, and K. Alexandrov. 2001. Allosteric regulation of substrate binding and product release in geranylgeranyltransferase type II. *Biochemistry*. 40:268-274.

Uemura, K., A. Kuzuya, and S. Shimohama. 2004. Protein trafficking and Alzheimer's disease. *Curr Alzheimer Res*. 1:1-10.

Waldherr, M., A. Ragnini, R.J. Schweyer, and M.S. Boguski. 1993. MRS6--yeast homologue of the choroideraemia gene. *Nat Genet*. 3:193-194.

Whyte, J.R., and S. Munro. 2002. Vesicle tethering complexes in membrane traffic. *J Cell Sci*. 115:2627-2637.

Yamamoto, T., K. Kaibuchi, T. Mizuno, M. Hiroyoshi, H. Shirataki, and Y. Takai. 1990. Purification and characterization from bovine brain cytosol of proteins that regulate the GDP/GTP exchange reaction of smg p21s, ras p21-like GTP-binding proteins. *J Biol Chem*. 265:16626-16634.

Zerial, M., and H. McBride. 2001. Rab proteins as membrane organizers. *Nat Rev Mol Cell Biol*. 2:107-117.

Zhang, H., M.C. Seabra, and J. Deisenhofer. 2000. Crystal structure of Rab geranylgeranyltransferase at 2.0 A resolution. *Structure*. 8:241-251.

Chapter 2: Sec4p Phosphorylation is a Cell Cycle Dependent Modification Regulated by the Polo-like Kinase Cdc5p

Introduction

Phosphorylation is a known modification of Rabs, with 55 of the approximately 60 human Rabs containing at least one phosphorylated residue (Hornbeck et al., 2015). However, very little is known about the kinases and cellular pathways involved in regulating phosphorylation, or how these modifications affect function. Phosphorylation of Rabs accumulates in their NH_2 and COOH-terminal intrinsically unstructured regions (see chapter 1, figure 1.4A). To investigate the functional significance of this phenomenon, we chose to investigate the *S. cerevisiae* Rab Sec4p as a model for this type of Rab phosphorylation, as Sec4p has multiple phosphorylation sites in its NH_2 and COOH termini. We investigated the kinase/kinases involved in modifying Sec4p to elucidate the cellular pathway(s) that control Sec4p phosphorylation.

Sec4p is involved in trafficking post-Golgi secretory vesicles to the site of polarized exocytosis and is a founding member of the Rab family of GTPases (Goud et al., 1988; Guo et al., 1999; Salminen and Novick, 1987). This trafficking step is spatially and temporally regulated to the sites of active growth. Reflecting this fact, Sec4p is found at the tip of newly growing cells and at the neck region between dividing cells (Novick and Brennwald, 1993). The closest mammalian orthologs of Sec4p are Rab3A, Rab8 and Rab13 (Collins, 2005), and these proteins also regulate post-Golgi trafficking pathways.

Sec4p is recruited to membranes via its GEF, Sec2p. Sec2p is first recruited to membranes via interaction with the Rab, Ypt31/32, and also by interacting with phosphatidylinositol-4-phosphate (Mizuno-Yamasaki et al., 2010; Ortiz et al., 2002). Once recruited to vesicles and activated by nucleotide exchange, GTP-bound Sec4p is able to engage with a set of effector

proteins to traffic vesicles to the site of polarized exocytosis, including exocyst component Sec15p, the lethal-giant larva homolog Sro7p, and the class 5 myosin motor Myo2p (Grosshans and Novick, 2008; Jin et al., 2011; Salminen and Novick, 1989; Watson et al., 2015). Using actin cables, Myo2p bound to Sec4p brings vesicles to the site of polarized exocytosis, whereby vesicles can be tethered to the plasma membrane through interactions between Sec4p and exocyst component Sec15p. This interaction is not sufficient for vesicle fusion, as that process is facilitated by the exocytic SNARE complex consisting of Sso1/2p, Sec9p, and Snc1/2p (Jahn and Scheller, 2006; Munson et al., 2000; Munson and Hughson, 2002). The exocyst complex is also an effector for other Ras-related small GTPases and is known to be a central player that serves as an intersection point for multiple signal transduction pathways (Bao et al., 2007; Blankenship et al., 2007; Chang et al., 2004; Chien et al., 2006; Goehring et al., 2007; Gromley et al., 2005; He et al., 2007; Jiang et al., 2007; Nejsum and Nelson, 2007; Stuart et al., 2007).

Sec4p has four serine phosphorylation sites situated within two stretches close to the NH_2- and COOH-termini, ^{5}TVpSASpSGNGK^{15}, and ^{196}EGNIpSINpSGSGNS^{209} (Ficarro et al., 2002). Previous work studying Sec4p phosphorylation using serine to aspartic acid residue mutations to mimic the constitutively phosphorylated state of the protein (phosphomimetic) illustrated a negative regulatory role for Sec4p phosphorylation (Heger et al., 2011). However, the physiological role of Sec4p phosphorylation, cellular pathways involved in modifying Sec4p, and the kinase/phosphatase responsible remained unclear. We demonstrate that Sec4p phosphorylation is a cell cycle dependent modification occurring exclusively during cytokinesis. Furthermore, we identified the polo-like kinase Cdc5p as a Sec4p kinase and show phosphorylation is required for coordinating cell size and growth with cell cycle progression.

Methods and Materials

Yeast strains, media and reagents

The *Saccharomyces cerevisiae* strains used in this study are listed in Table 2.1 and were created using standard manipulations. Plasmids used in this study are listed in Table 2.2. For Western blot analysis, gels were transferred to PVDF Immobilon membrane (Millipore) prior to probing with antibodies including anti-GFP antibody (abcam, ab6556), pS8 antibody (21st Century Biochemicals), and anti-Sec4p (this study). Blots were subsequently incubated with the appropriate secondary antibody coupled to alkaline phosphatase and imaged using CDP-Star chemiluminescence reagent (Perkin Elmer) and recorded with Fuji LAS3000.

Antibody testing

For characterization of pS8 antibody, 100μg of synthetic peptides were loaded onto a nitrocellulose membrane using a Bio-Rad Dot-Blot apparatus (Bio-Dot, Catalog number 170-6545). The membrane was probed with the pS8 antibody at a 1:1000 dilution, and a 1:2500 goat-anti-Ig rabbit HRP secondary prior to ECL detection and imaging.

Nutrient starvation and rapamycin treatments

For nutrient starvation assays, one culture of cells (RCY3651) was grown overnight, split into four different media conditions with a starting OD_{600} of 0.3, then allowed to grown for 3 hours at 25˚C. Yeast extract peptone (YP) media with 2% glucose, 2% sucrose, or 2% glycerol were used to compare different carbon sources. SD-N (0.17% yeast nitrogen base without amino acids, 2% glucose) was used to observe the effects of nitrogen starvation. Rapamycin was obtained from Calbiochem: 553210.

Table 2.1: Strain list

Strain	Genotype	Source
NY605	*MAT***a** *ura3-52 leu2-3,112*	Novick Lab
RCY1507	*MATα ura3-52 leu2-3,112 his3Δ200 sec4ΔHIS3* [*YCP50 SEC4*]	Calero et al.
RCY3918	*MATα leu2-3,112 ura3-52,*	Novick Lab
CUY318	*MAT***a** *ade1 ade2 lys2 tyr1 gal1 his7 cdc5^{ts}*	Huffaker Lab
RCY3343	*MAT***a** *ura3-52 leu2-3,112 his3Δ0*	Collins lab
RCY3350	*MAT***a** *ura3Δ0 leu2-3,112 cdc55ΔKAN^{R}*	Heger et al
RCY5066	*MAT***a** *ura3-52 leu2-3,112 his3Δ0 bar1ΔHIS3*	This study
RCY5009	*MATα ura3-52 leu2-3,112 his3Δ200 sec4ΔHIS3* [*pRS315 MBP-SEC4*]	This study
RCY5010	*MATα ura3-52 leu2-3,112 his3Δ200 sec4ΔHIS3* [*pRS315 MBP-SEC4 S8,10,11,201,204A*]	This study
RCY5085A	*MAT***a** *ura3-52 leu2-3,112 his3Δ0 sch9ΔHIS3*	This study
RCY5090	*MATα his3Δ1 leu2Δ0 ura3Δ0 env7ΔKAN^{R}*	Resgen
RCY5091	*MATα his3Δ1 leu2Δ0 ura3Δ0 sky1ΔKAN^{R}*	Resgen
RCY5092	*MATα his3Δ1 leu2Δ0 ura3Δ0 pkh3ΔKAN^{R}*	Resgen
RCY5081	*MATα his3Δ1 leu2Δ0 ura3Δ0 sak1ΔKAN^{R}*	Resgen
RCY5093	*MATα his3Δ1 leu2Δ0 ura3Δ0 slt2ΔKAN^{R}*	Resgen
RCY5094	*MATα his3Δ1 leu2Δ0 ura3Δ0 psk2ΔKAN^{R}*	Resgen
RCY5095	*MATα his3Δ1 leu2Δ0 ura3Δ0 ste11ΔKAN^{R}*	Resgen
RCY5096	*MATα his3Δ1 leu2Δ0 ura3Δ0 vps15ΔKAN^{R}*	Resgen
RCY4607	*MATα his3Δ1 leu2Δ0 ura3Δ0 kcc4KAN^{R}*	Resgen
RCY5097	*MATα his3Δ1 leu2Δ0 ura3Δ0 bub1ΔKAN^{R}*	Resgen
RCY5120	*MATα ura3-52 leu2-3,112 his3Δ200 sec4ΔHIS3*	This study
RCY5126	*MAT***α** *ura3-52 ade2-101 myo1ΔLEU2 his3Δ200 sec4ΔHIS3* [*YCP50 SEC4*]	This study
RCY5130	*MAT***a** *ura3-52 leu2-3,112 his3Δ200 hof1ΔKAN^{R} sec4ΔHIS3* [*YCP50 SEC4*]	This study

Table 2.2: Plasmid List

Plasmid ID	Description	Source
pRC5316	MBP-Sec4p/pRS315	This study
pRC5313D	MBP-Sec4p S8,10,11,201,204A/pRS315	This study
pRC1820	Sec4p/pRS315	Collins lab
pRC5411A	pRS316 GFP-atg8	This study
pRC2568	Sec4p S8,10,11,201,204A/pRS315	Collins Lab
pRC2569	Sec4p S8,10,11,201,204D/pRS315	Collins Lab
pRC3423	Sec4p Q79L/pRS315	Heger et al.
pRC5475	Sec4p S29V/pRS315	This study
pRC5464A	Sec4p S10,11A/pRS315	This study
pRC5463A	ppSUMO Cdc5p/pRS426	This study
pRC651	GFP-Sec4p/pRS315	Collins lab
pRC3000	GFP-Sec4p S8,11,201,204D/pRS315	Heger et al.
pRC5473	GFP-Sec4p S8,10,11,201,204D/pRS315	This Study
pRC5472	GFP-Sec4p S8,10,11,201,204A/pRS315	This Study
pRC5474	Sec15p-MBP/pRS426	This study
pRC5460	Cdc5p-3xmCherry/pRS316	This study
pRC5483	Vph1-mCherry/pRS426	This study

Protein purification

The protocol for Cdc5p purification was adapted from previous published studies (St-Pierre et al., 2009). Briefly, 6X-His-SUMO tagged Cdc5p under a *GAL1/10* promoter (pRC5463A) was expressed in 2 Liters of yeast culture, pelleted at 3000xg for 10min, re-suspended in 30mM KPO_4, 0.5M NaCl, 10mM Tris pH 8.0, 5% glycerol, 1mM PMSF, 5mM β-glycerol phosphate, and lysed using glass beads. Cdc5p was purified using PrepEASE agarose conjugated Ni resin (Affymetrix) and eluting with 250mM imidazole. MBP-Sec4p (both wild type and Ala mutants) for pS8 antibody characterization was purified from 50mL of RCY5009 and RCY5010. Cells were harvested by glass bead lysis into 10mM Tris pH 7.5, 10mM NaN_3, 1mM PMSF, 1mM benzamidine, 0.2mM DTT, and 1mM $MgCl_2$. MBP-Sec4p was purified using amylose resin (New England BioLabs, E8021L) and eluted into 10mM Maltose, 100mM NaCl, 50mM Tris pH 9.5, 1mM $MgCl_2$, and 0.2mM DTT. Phosphatase treatment was preformed by adding 20 units of Calf Intestinal Alkaline Phosphatse from New England BioLabs M0290S and incubating samples for 1 hour at 37˚C.

Membrane fractionation

MBP-Sec4p wild type and alanine mutants were grown to mid-log phase OD, and 15 OD units of cells were lysed using glass beads into 10mM Tris pH 7.5, 10mM NaN_3, 200mM sorbitol, 1mM PMSF, 1mM benzamidine, 0.2mM DTT, 5mM β-glycerol phosphate, 50mM NaF, and 2mM EDTA. Samples were clarified for 10 min at 4˚C 10,000xg. The supernatant was then spun for 1 hour at 100,000xg to separate the insoluble membrane fraction from the cytosolic fraction. The supernatant was removed and the membrane was re-suspended in the original lysis buffer prior to preparation for western blot.

Fluorescence microscopy

Fluorescence microscopy and differential interference contrast microscopy were achieved using an Eclipse E600 Nikon microscopy, 1X optivar (0.08μm/pixel), 60X Oil objective (1.4 numerical aperture), 10X/25 Nikon eye piece (CFIUW), and imaged with a Clara CCD camera from Andor Technology (DR-328G-C01-SIL). A C-FL GFP HC HISN zero shift filter set and C-FL Texas Red HC HISN zero shift filter set was used for GFP and mCherry image acquisition respectively. Images were taken as a series of z-stacks in 0.6μm increments over 8μm using NIS-Elements Advanced Research imaging software. Images were deconvolved using AutoQuant X software. For heat-shock experiments and cell-synchrony and release experiments, cells were fixed in 4% paraformaldehyde for 30 minutes prior to washes and re-suspension in PBS for imaging. Cdc5p and Sec4p co-localization experiments were performed on live cells.

GFP-Atg8p autophagy assay

Yeast strains of RCY3918 expressing Sec4p or Sec4p mutants (pRC1820, pRC2568, pRC2569) and pRC5411A were grown in SCD-Leu-Ura until mid-log phase. Each sample was then sub-cultured into either YPD or SD-N for 3 hours at 23˚C. Samples were harvested, and 10 OD_{600} units of cells were spun down, washed in 10mM Tris pH 7.5, 10mM NaN_3, then resuspended in 10mM Tris pH 7.5, 10mM NaN_3, 1mM PMSF, 1mM benzamidine, 0.2mM DTT, 5mM β-glycerol phosphate, 50mM NaF, and 2mM EDTA for glass bead lysis. GFP-Atg8p degradation status was evaluated via western blot analysis using anti-GFP antibody abcam ab6556.

Kinase over-expression library preparation and screen

127 yeast kinases were individually cloned into a pRS426 multi-copy 2μ plasmid using homologous recombination. The endogenous promoter and terminator were included for all kinases (except *KNS1*, *PBS2*). A full list of library kinases and the primers used to generate the library can be found in Table 2.3. Plasmids were transformed into the yeast strain NY605 then single colonies were picked and grown up in SCD-Ura medium overnight. Samples were harvested in mid-log phase, and 10 OD_{600} units of cells were spun down, washed in TAZ buffer, 10mM Tris pH 7.5, 10mM NaN_3, then resuspended in 10mM Tris pH 7.5, 10mM NaN_3, 200mM sorbitol, 1mM PMSF, 1mM benzamidine, 0.2mM DTT, 5mM β-glycerol phosphate, 50mM NaF, and 2mM EDTA for glass bead lysis.

Pull-down assay:

Sec15-MBP and GFP-Sec4p wild type, ala, and asp (all Sec4p mutants expressed ectopically) were expressed in RCY3651 cells and grown in YPD to mid-log phase. 200 mls culture was harvested, were lysed with glass beads in 10mM Tris pH 7.5, 10mM NaN_3, 1mM PMSF, 1mM benzamidine, 0.2mM DTT, and 1mM $MgCl_2$, 5mM β-glycerol phosphate, and 50mM NaF lysis buffer. Triton X-100 was added to a final concentration of 1% to solubilize membranes. Cell lysate was clarified at 2,000xg for 30 minutes then Sec15-MBP was purified using amylose resin (New England BioLabs, E8021L) and eluted directly from resin with SDS-PAGE sample buffer containing DTT. GFP-Sec4p was probed for via western blot with Abcam anti-GFP antibody (Ab6556).

Table 2.3: Kinases and primers for over-expression screen

Note: For certain large kinases or kinases with introns, more than one PCR was performed and the two PCR products were combined using homologous recombination. For these cases, the following table lists additional forward and reverse primer pairs as “Kinase Cont.”.

Table 2.3: Kinases and primers for over-expression screen

RCK#	Kinase	Forward Primer	Reverse Primer
1	KIN1	CGGCCGCTCTAGAACTAGTGGATCCT TGCCACCACTCCCACAGG	GGTACCGGGCCCCCCCTCGAGAATCCGG AGGCAATGATGGTG
2	KIN2	CGGCCGCTCTAGAACTAGTGGATCCT TTTGACGCTCTCGCATTCC	GGTACCGGGCCCCCCCTCCATATGTGTT ATTGGAGCCTCGG
3	YCK1	CGGCCGCTCTAGAACTAGTGGATCCC GACTGTGTCATTGACGAAGAC	GGTACCGGGCCCCCCCTCGAGAGATGAT CGCTGGTGCGG
4	YCK2	CGGCCGCTCTAGAACTAGTGGATCCG CTCTGAAGGCGATCCTGTATGC	GGTACCGGGCCCCCCCTCGGGCGCTTCC TTAAGAGTCAC
5	YCK3	CGGCCGCTCTAGAACTAGTGGATCCG TGTCGTCGAAAATGACC	ACCGGGCCCCCCCTCGAGGTCGCTCACG GTTTCTCCAATTCTTG
6	HRR25	CGGCCGCTCTAGAACTAGTGGATCCG GTTCGACACTCGAGGAAAGCA	TACCGGGCCCCCCCTCGAGGTCGTCTCG TGATTGTTTCCTAATCAG
7	CKA1	CGGCCGCTCTAGAACTAGTGGATCCA GGCAGAGGTAATCAGAGGTTTAC	TACCGGGCCCCCCCTCGAGCTGCATCCT TTCTTTTCTG
8	CKA2	CGGCCGCTCTAGAACTAGTGGATCCT GCCAACAGGCCTTTATCA	TACCGGGCCCCCCCTCGAGGTCGAAACT CCTCGGAACACGC
9	CDC7	CGGCCGCTCTAGAACTAGTGGATCCT ACGCGATCATACTGATACGTTC	TACCGGGCCCCCCCTCGAGGTCGACTGT TTCAACAGCTCAAATGTACG
10	CDC5	CGGCCGCTCTAGAACTAGTGGATCCT TTTGTGTCAAATTCTGATTCTGC	TACCGGGCCCCCCCTCGAGGTTATGTAT GGGATGATAACCTGTCG
11	IPL1	CGGCCGCTCTAGAACTAGTGGATCCA TTTTCCGATACAGCATTGCTTA	TACCGGGCCCCCCCTCGAGGTCGACAAT TGAATGTTCAATTGAGAGAGC
12	IRE1	CCGCTCTAGAACTAGTGGATCCAAGA CGGAGCGTAAGCCTC	TACCGGGCCCCCCCTCGAGCAGTGTTGA ATAACTGGAGTAGTATG
13	VPS15	CGGCCGCTCTAGAACTAGTGGATCCA AGAGTACTGTTCAGAAATC	TACCGGGCCCCCCCTCGAGGTCGACATT TGAGGGTCCATCGATG
14	ENV7	CGGCCGCTCTAGAACTAGTGGATCCC GTGTGAATGTACAGTC	TACCGGGCCCCCCCTCGAGGCAGACTGT TCTTTATGGTCTGTA
15	MPS1	CCGCTCTAGAACTAGTGGATCCACAA CAAATGGTGATTCTGGAGA	GGGCCCCCCCTCGAGGTCGACCACATGT GGTTGTCTAAG
16	SLT2	CGGCCGCTCTAGAACTAGTGGATCCA GCTAAGCCTACGTATGCGGC	GCTTTCCACCAAGAAACTCCGC
16	SLT2 cont.	CAAGGATATACCAAGGCGATTGACG	TACCGGGCCCCCCCTCGAGTTTGTCCAG TTGGCAATTGCCTG
17	CDC28	CGGCCGCTCTAGAACTAGTGGATCCG AGACCTTTGGCGTTTACTC	ACCGGGCCCCCCCTCGAGGTCGATCAAT TGAGGCCCCAGCATAC

Table 2.3: Kinases and primers for over-expression screen (continued)

RCK#	Kinase	FORWARD PRIMER	REVERSE PRIMER
18	DBF20	CGGCCGCTCTAGAACTAGTGGATCCC CTACTTACTTTCATGCACTTGA	ACCGGGCCCCCCCTCGAGGTCGAGACGC TGAAGAAGAGATAGCC
19	SCH9	CGGCCGCTCTAGAACTAGTGGATCCG GTGGATCGGTCATTTACGATAAC	ACCGGGCCCCCCCTCGAGGTCGACCATG TACGCGCATCGATGAGC
20	MEK1	CGGCCGCTCTAGAACTAGTGGATCCG CGCAGTGCGTAAGAAAGC	ACCGGGCCCCCCCTCGAGGTCGGCCAAT ACGATTCAACAACGC
21	TPK1	CGGCCGCTCTAGAACTAGTGGATCCG AAGCTGTGCTGCTATTCGTTC	ACCGGGCCCCCCCTCGAGGTCGATGGCG TGAAAGCTTCTCATCTCCC
22	SAK1 (PAK1)	CGGCCGCTCTAGAACTAGTGGATCCG CTCATCACATTCTAAAGATCAC	TACCGGGCCCCCCCTCGAGGTCGACCTT CTCATGGCTTAGTGGTG
23	PRK1	CGGCCGCTCTAGAACTAGTGGATCCA ATGTCGTTAGTTTGCACTAGCTG	GCAAATTCATCAGAAAGTGGAACGG
23	PRK1 cont.	TGCTGGCTTACAGGTTGGAAGCC	TACCGGGCCCCCCCTCGAGGTCGACGCT GTTCAGAGAACCACAATG
24	ELM1	CGGCCGCTCTAGAACTAGTGGATCCG CTTAAGTCAATTGCCGCACC	TACCGGGCCCCCCCTCGAGGTCGACCTG TTGACGTTACTGAGTGATC
25	PCK1	CGGCCGCTCTAGAACTAGTGGATCCC CATACAATTCTGACCAGAGCAC	TACCGGGCCCCCCCTCGAGGTCGACGGT GAATCATTCCGGTAACC
26	HAL5	CGGCCGCTCTAGAACTAGTGGATCCC AACTACGGTGTTCAAGGTGAAG	TACCGGGCCCCCCCTCGAGGTCGACGCA ACGACCTCATCTCTCGAAC
27	VHS1	CGGCCGCTCTAGAACTAGTGATCCCT CGCTTGTGTATCTAGGTC	TACCGGGCCCCCCCTCGAGGTCGACAAC GACGAAACTGACTGTGAC
28	YAK1	CGGCCGCTCTAGAACTAGTGGATCCA CTATTGTCGCGTTGCACG	TACCGGGCCCCCCCTCGAGGTCGACGCA CCTTCCTCTCAACCTC
29	TPK2	CGGCCGCTCTAGAACTAGTGGATCCG TACACACAATTCCATATCGAG	TACCGGGCCCCCCCTCGAGGTCGACGCA CTGAGATCATGAGATCAG
30	SGV1	CGGCCGCTCTAGAACTAGTGGATCCT GGACACAACTGTGAATCTTGG	AAGGATCTAACGCTAACAACTGTCC
30	SGV1 cont.	CAACTAATTACAAGCCAACGTTGAGG	TACCGGGCCCCCCCTCGAGGTCGACGCA GTGATCGTTGTATCGAGG
31	AKL1	CGGCCGCTCTAGAACTAGTGGATCCG TACTAGGCTTGCTAGCTTTGC	TACCGGGCCCCCCCTCGAGGTCGACCTT AGTGGTGGGTATGTACACC
32	KIN82	CGGCCGCTCTAGAACTAGTGGATCCT CCTGCTGGCTCTTCAACTC	TACCGGGCCCCCCCTCGAGGTCGACTGG CGAGGACTGGATGAG

Table 2.3: Kinases and primers for over-expression screen (continued)

RCK#	Kinase	FORWARD PRIMER	REVERSE PRIMER
33	YPL150W	CGGCCGCTCTAGAACTAGTGGATCCG CTCCTCTTGTCACATTGAATGC	TACCGGGCCCCCCCTCGAGGTCGACGAT ACCAGCACATTAAGCTCACC
34	YPK1	CGGCCGCTCTAGAACTAGTGGATCCG ACGAACCAACAGTCCGCAC	TACCGGGCCCCCCCTCGAGGTCGACATC TTGTCAGCTGTTGTCTTGC
35	YPK3	CGGCCGCTCTAGAACTAGTGGATCCT TATGCACGCTATACTACTCT	CGGGCCCCCCCTCGAGGTCGACCTGGGT ACACCACTCGT
36	CLA4	CGGCCGCTCTAGAACTAGTGGATCCG GAACGTGCAGGAGAGTCTG	CGGGCCCCCCCTCGAGGTCGACTAGAAG CTGAAGCATGGACG
37	SWE1	CGGCCGCTCTAGAACTAGTGGATCCG TCTCTAGTACTGGTAAGCC	GAATCGGTGGAAGATATGGAATGCG
37	SWE1 cont.	CCATCGTGACAAACACAACAAGTGC	CGGGCCCCCCCTCGAGGTCGACCATTGC CACAATGGATCAG
38	PKC1	CGGCCGCTCTAGAACTAGTGGATCCC ACTCCAGGTTGCACCTG	CGGGCCCCCCCTCGAGGTCGACCATTTG AGACGTCATGAACTCTC
39	STE7	CCGCTCTAGAACTAGTGGATCCTCGT TATAAGTGATTCGTG	CGGGCCCCCCCTCGAGGTCGACGCAAGC TTCTCTCAATCGTG
40	CAK1	CGGCCGCTCTAGAACTAGTGGATCCT CAGTGGTCTACGCTACAC	CGGGCCCCCCCTCGAGGTCGACATATGG GTGTGACCGCT
41	PKH1	CGGCCGCTCTAGAACTAGTGGATCCG GCTTGGACCCTAAAGGTTGC	CGGGCCCCCCCTCGAGGTCGACGGGATC TGCTGAGAGACGACAA
42	HOG1	CGGCCGCTCTAGAACTAGTGGATCCT CTGGTTACCCTACATGGTCTG	CGGGCCCCCCCTCGAGGTCGACGCCATA AGTGACGGTTCTTGG
43	HSL1	CGGCCGCTCTAGAACTAGTGGATCCC TTTGGATCGTAAGTTCGCT	CTCTCTCATGGGTCCAGTGAGAG
43	HSL1 cont.	TCTTTGCCTAATGATCAAGGTAAACC G	CGGGCCCCCCCTCGAGGTCGACGGATGA CGAATCTTCTTGAGCTC
44	KIN3	CGGCCGCTCTAGAACTAGTGGATCCA ACGCATCTGTTTGGAAAAGAGATC	CGGGCCCCCCCTCGAGGTCGACAAGACA TTGTCGACAGGACAAGG
45	SAT4	CGGCCGCTCTAGAACTAGTGGATCCG ACGATTTCCTGTCGGTTTCGTT	CGGGCCCCCCCTCGAGGTCGACGCTCTA TCTGACCAACCGACTC
46	CDC15	CGGCCGCTCTAGAACTAGTGGATCCG GGCCTATCAACTCATTAGCACTC	CGGGCCCCCCCTCGAGGTCGACTGTGCC ACTGCAATCATGTC
47	BUB1	CGGCCGCTCTAGAACTAGTGGATCCG ACTCCATAACTTGTGCC	CGGGCCCCCCCTCGAGGTCGACACATCC CAATTGGCTCTGCAG

Table 2.3: Kinases and primers for over-expression screen (continued)

RCK#	Kinase	FORWARD PRIMER	REVERSE PRIMER
48	RTK1	CGGCCGCTCTAGAACTAGTGGATCCTTCTTGAATGGAGGCCAG	CGGGCCCCCCCTCGAGGTCGACGTCGGGTGACTTCAATTTGGC
49	RIO1	CGGCCGCTCTAGAACTAGTGGATCCATTCAAGCGGATTTCTGGGAC	CGGGCCCCCCCTCGAGGTCGACGAGAAGCTTGGGAGAAGACCG
50	PTK2	CGGCCGCTCTAGAACTAGTGGATCCGGAGCTGCAAGTACTACG	CGGGCCCCCCCTCGAGGTCGACGTGGGTGAGACATGGTGGTC
51	DBF2	CGGCCGCTCTAGAACTAGTGGATCCGGTCATGGTTAGGGCTC	CGGGCCCCCCCTCGAGGTCGACCTTCTAAGAGAGCTACCTTGCG
52	PSK2	CGGCCGCTCTAGAACTAGTGGATCCTGGTGTGAGTAATCAGTACG	CGGGCCCCCCCTCGAGGTCGACGTAGTACGTTCTGCTAGTGCCTC
53	HRK1	CGGCCGCTCTAGAACTAGTGGATCCGTTCGTTTACATTTCACACACACAG	CGATTCCATGAGCCATCGTTACGC
53	HRK1 cont.	CTCGTGGCGAGATCAACTGTTGC	CGGGCCCCCCCTCGAGGTCGACATTCAGTGAGAAATGGGGTGTC
54	SKS1	CGGCCGCTCTAGAACTAGTGGATCCGTTGGACAGATACTTGAGCAG	CGGGCCCCCCCTCGAGGTCGACCCATTCAAATGCGCCGTCG
55	PTK1	CGGCCGCTCTAGAACTAGTGGATCCATTGTGCGAGCACGCAGGAC	CGGGCCCCCCCTCGAGGTCGACGGAGGATTCTTTGCGCCGGTT
56	YPK2	CGGCCGCTCTAGAACTAGTGGATCCTAGGAACTGAAGAACCAACGGTTC	CGGGCCCCCCCTCGAGGTCGACGCCGTTTGGCGAATTCCGGTA
57	PRR1	CGGCCGCTCTAGAACTAGTGGATCCGCGTTGCGTTACAGAATAAGGC	CCATGACGGCAGCTAATAAGTCTCC
57	PRR1 cont.	CTCTGACTAGGGAATTGCAGGTGC	CGGGCCCCCCCTCGAGGTCGACCTTTACCTGTTTGTTATTGGCTGCC
58	PHO85	CGGCCGCTCTAGAACTAGTGGATCCATAGTCCGTCCAGACACG	CTGCTTAAATTGTGAAGAAGAAGACATTGGTATTGCTC
58	PHO85 cont.	CTTCTTCACAATTTAAGCAGTTAGAAAAGCTTGGCAATGG	CGGGCCCCCCCTCGAGGTCGACGCGTTTACGTTCTGCTCTCTCAC
59	BCK1	CGGCCGCTCTAGAACTAGTGGATCCGAAATAGACGGGTCCGTCATGC	CGGGCCCCCCCTCGAGGTCGACGCCGTCCTTTATAGAGACTGTGC
60	SPS1	CGGCCGCTCTAGAACTAGTGGATCCATATTTCGGAGCTGTCCCAGGTTC	CGGGCCCCCCCTCGAGGTCGACGGTCCACCATTAGGTTCAACTGC
61	PSK1	CGGCCGCTCTAGAACTAGTGGATCCTTTGTTTCAGGCGTCGTTGC	GCTAACGATTGGCTTATACTCTTGACGTC

Table 2.3: Kinases and primers for over-expression screen (continued)

RCK#	Kinase	FORWARD PRIMER	REVERSE PRIMER
61	PSK1 Cont.	CTGAACCATCGCTGTCATCATCGC	CGGGCCCCCCCTCGAGGTCGACAGGGCATTCCGGGTATTATCGTCTG
62	SSK2	CGGCCGCTCTAGAACTAGTGGATCCGCGTTTCATACCCTGAAACAGTG	GTCTCTGCAGCCTCGTCAGC
62	SSK2 cont.	GGATGAATGGGAGGACCGTGG	GATCAGTCGGATCACAGTCTTCAGC
62	SSK2 cont.	AATGATGCGGTTAAGTATCGGATGG	CGGGCCCCCCCTCGAGGTCGACATTTTCGACAAGACCCCTACCG
63	STE11	CGGCCGCTCTAGAACTAGTGGATCCATGAGACTGTTCATGGTGCC	CGGGCCCCCCCTCGAGGTCGATTCGTGCTTCCATCTGTGCG
64	GIN4	CGGCCGCTCTAGAACTAGTGGATCCGCGCCAAGTTTCGTCTGAC	CGGGCCCCCCCTCGAGGTCGAGAGAGTAACTTCTTGTCGGCCTC
65	FMP48	CGGCCGCTCTAGAACTAGTGGATCCGGAACGATGATGCTGCCTGAG	CGGGCCCCCCCTCGAGGTCGACTCGCGGTGCATTTGCATG
66	FRK1	CGGCCGCTCTAGAACTAGTGGATCCTGAAACCCAGATCAACACCTG	CGGGCCCCCCCTCGAGGTCGAATCTCGCTGTAAGCGCAGTG
67	SKY1	CGGCCGCTCTAGAACTAGTGGATCCATGAGTCGGCTACTTGACAACC	CGGGCCCCCCCTCGAGGTCGAGCTTAGGTATCACACCCATCATCC
68	PRR2	CGGCCGCTCTAGAACTAGTGGATCCGTCACCTTCGGCTGTGG	CGGGCCCCCCCTCGAGGTCGACGCTTGTCAGTGTTGATGTCG
69	KSP1	CGGCCGCTCTAGAACTAGTGGATCCTACTCTTCCAATCTAGTGTCGC	CGGGCCCCCCCTCGAGGTCGAGAGGGAAGAAGTAGAGGTCGACG
70	CBK1	CGGCCGCTCTAGAACTAGTGGATCCGTTTGATCTGCAGTCCAGCG	CGGGCCCCCCCTCGAGGTCGACCGAGATTGTGCTATTGTGCG
71	KCC4	CGGCCGCTCTAGAACTAGTGGATCCGTTTCTGTCCTTGCCACAGCTC	TCATCAATCAGTGTAGCGAAGTTGG
71	KCC4 cont.	GTCCCGAATCCTCACAAGAGG	CGGGCCCCCCCTCGAGGTCGAGTTCTCCTCGAGGATATAGGAATCCTC
72	TDA1	CGGCCGCTCTAGAACTAGTGGATCCGGTTATTCCGCCGATTCCACG	CGGGCCCCCCCTCGAGGTCGACTTTGAGCCTCTGTGAGCCAC
73	MKK2	CGGCCGCTCTAGAACTAGTGGATCCGCCAGACTCTCAAAGGTGAACTG	CGGGCCCCCCCTCGAGGTCGAATCATAAGGGTTGTCCCGTGG
74	CHK1	CGGCCGCTCTAGAACTAGTGGATCCTTTTCAGCCACTGGTCATCCC	CGGGCCCCCCCTCGAGGTCGACTACATCTAGGGAAGCCACACC

Table 2.3: Kinases and primers for over-expression screen (continued)

RCK#	Kinase	FORWARD PRIMER	REVERSE PRIMER
74	CHK1	CGGCCGCTCTAGAACTAGTGGATCCTTTTCAGCCACTGGTCATCCC	CGGGCCCCCCCTCGAGGTCGACTACATCTAGGGAAGCCACACC
75	KKQ8	CGGCCGCTCTAGAACTAGTGGATCCATGAAGGCTCCGTTGTAGAGAC	CGGGCCCCCCCTCGAGGTCGACGTTGCATTCGGAGATACTGC
76	FUS3	CGGCCGCTCTAGAACTAGTGGATCCAGAGTTAACTGGAGAGGGCAG	CGGGCCCCCCCTCGAGGTCGAGGAGTTGCGTAACTGCTCC
77	SCY1	CGGCCGCTCTAGAACTAGTGGATCCGCTCACCCGTACATATGCTCC	CGGGCCCCCCCTCGAGGTCGACTGTGAACGATTGTATACGGACTG
78	SKM1	CGGCCGCTCTAGAACTAGTGGATCCGTTGTCATCACGGGTGTTATGG	CGGGCCCCCCCTCGAGGTCGACATCCGTAAATCCGCCTAACG
79	NPR1	CGGCCGCTCTAGAACTAGTGGATCCGGATTAGTCAGTGGCGTACC	CGGGCCCCCCCTCGAGGTCGAGGAATTGTCGCCTTGGTAAGAC
80	KSS1	CGGCCGCTCTAGAACTAGTGGATCCGAACATCTTTCCTCCACATTCCTG	CGGGCCCCCCCTCGAGGTCGACCATTCACTGTTGAATAGTGCTGG
81	KIN28	CGGCCGCTCTAGAACTAGTGGATCCGATTCGTCCATTGGATGAACCTAC	CGGGCCCCCCCTCGAGGTCGACAAACTTACTGACAAACCTCTGC
82	SSN3	CGGCCGCTCTAGAACTAGTGGATCCAGTTGAAGTTGCGCACTCG	CGGGCCCCCCCTCGAGGTCGACGAAATTCGCATACATCTGCG
83	MRK1	CGGCCGCTCTAGAACTAGTGGATCCGTTAGGATCTACCGGAGAGC	CCGTTTATGAATAGTCCTTTCCTTGGTTTTAATATACCTATAATC
83	MRK1 cont.	GGAAAGGACTATTCATAAACGGGTTTATAAACATGACCGC	CGGGCCCCCCCTCGAGGTCGACTTACAGTTGCCAAGGTTCTGC
84	PKH2	CGGCCGCTCTAGAACTAGTGGATCCGAAGCGAACATTTCCCGATCC	CGGGCCCCCCCTCGAGGTCGAGCCTTTGTGAGCTGTCATCC
85	PAN3	CGGCCGCTCTAGAACTAGTGGATCCAAGACGCTATCCGTGATAGC	CGGGCCCCCCCTCGAGGTCGATCGCCGTGCACAATATCACC
86	RAD53	CGGCCGCTCTAGAACTAGTGGATCCGGTTGGTGCATTAATAGCCTGC	ATTGGTCCTGTGTGCTACCAC
86	RAD53	GGATATGTGGTCAATGGGATGTCTTG	CGGGCCCCCCCTCGAGGTCGACTTGTTGTACCACATCAAGCAGG
87	CMK1	CGGCCGCTCTAGAACTAGTGGATCCGATACGTCTGCATACTACGAGG	CGGGCCCCCCCTCGAGGTCGAGTGAAACTCCTTACAGGCTGCA
88	TOS3	CGGCCGCTCTAGAACTAGTGGATCCACAACGTCCTTCAGCAAGC	CGGGCCCCCCCTCGAGGTCGAGCGTTTAGTACTTGCCTTTGGC
89	PKH3	CGGCCGCTCTAGAACTAGTGGATCCGCACACGTACTGATGACTAGAGATG	CGGGCCCCCCCTCGAGGTCGAGAGGTCGTAGGCAATTGGAATGG

Table 2.3: Kinases and primers for over-expression screen (continued)

RCK#	Kinase	FORWARD PRIMER	REVERSE PRIMER
90	SMK1	CGGCCGCTCTAGAACTAGTGGATCCT TCTTTAACAGTCGGTACCAGT	CGGGCCCCCCCTCGAGGTCGAGACTGTT TATGGAAAGACCACGTC
91	ATG1	CGGCCGCTCTAGAACTAGTGGATCCT AGAACGCCACATTTCATCACC	CGGGCCCCCCCTCGAGGTCGACCAAAGG CAAGTACTAAACGCAAC
92	SSK22	CGGCCGCTCTAGAACTAGTGGATCCA TATTTCGTATTAACCCTATGTCTCG	CGGGCCCCCCCTCGAGGTCGAAGGAATC AGGGTGGACATCTG
93	RCK1	CGGCCGCTCTAGAACTAGTGGATCCG TGCATGAGATTGACATCTCGG	CGGGCCCCCCCTCGAGGTCGAGTAAGAT CCATTGAGCTCGAGAC
94	FPK1	CGGCCGCTCTAGAACTAGTGGATCCA CACCTGGTATAAATCAAGCGAG	CGGGCCCCCCCTCGAGGTCGACACACTA CTGACTAACTGACAGAGG
95	RIM15	CGGCCGCTCTAGAACTAGTGGATCCA ACTTCTGCATTGTCTGCCG	CAAGTTTCCTTCGAGGTGTCGG
95	Rim15 cont.	TAGCAACACCGTTATGAAACTACCG	CTTTTCGCAGGATCCACAACCAAC
95	RIM15 cont.	GCGAGAATTCCTAACACCAGAGGC	CGGGCCCCCCCTCGAGGTCGATGGGAGA ACTATTCTTCCAGAGG
96	CTK1	CGGCCGCTCTAGAACTAGTGGATCCT CATGCTTGTGGATACTGG	CGGGCCCCCCCTCGAGGTCGAGTTGGTA CGATGGACAAACAGC
97	BUD32	CGGCCGCTCTAGAACTAGTGGATCCT CTCGTAATATGGATCGCTGGAC	CGGGCCCCCCCTCGAGGTCGAACTCGGA CACGCTTTGATGG
98	RIM11	CGGCCGCTCTAGAACTAGTGGATCCG AAGGAGTGGTAGGAAGACCAG	CGGGCCCCCCCTCGAGGTCGACAGCTCG ATGATGAACCTTCAC
99	RCK2	CGGCCGCTCTAGAACTAGTGGATCCA GTGATTAAGAGGAAACCTCGTC	CGGGCCCCCCCTCGAGGTCGACGGGAAT CAACATTCACTTGC
100	SNF1	CGGCCGCTCTAGAACTAGTGGATCCT ATGGCACATCAACAGGTAGCG	CGGGCCCCCCCTCGAGGTCGAGTGTTGG CAGTACATGTAGTAGG
101	KIN4	CGGCCGCTCTAGAACTAGTGGATCCG TTCACTGTTTATTGAGCTTACTGTG	CGGGCCCCCCCTCGAGGTCGAAGACTTT CGGTGCCTCTGTC
102	TPK3	CGGCCGCTCTAGAACTAGTGGATCCA GCCTCATTATGCAGTTTCCG	CGGGCCCCCCCTCGAGGTCGAGAACGTC CCAGTCTTCTGAGG
103	MCK1	CGGCCGCTCTAGAACTAGTGGATCCG TATGTAATGACAGTTCAGTGAC	CGGGCCCCCCCTCGAGGTCGAGCAATTT ATTACAAGCCACGTAGGC
104	NNK1	CGGCCGCTCTAGAACTAGTGGATCCG GAACTTTGTGTATGGCGTTG	TCCATATGGCTACTTCTCTCAGCAC

Table 2.3: Kinases and primers for over-expression screen (continued)

RCK#	Kinase	FORWARD PRIMER	REVERSE PRIMER
104	NNK1	CGGTTGGGTAAAATCATAGGTTTCG	CGGGCCCCCCCTCGAGGTCGACACGAGTCGCAATGAATAGCG
105	MKK1	CGGCCGCTCTAGAACTAGTGGATCCGGATCGACTGATTATCATTAAGGC	CGGGCCCCCCCTCGAGGTCGATCGCTGGAAATTGCGTTGCG
106	GCN2	CGGCCGCTCTAGAACTAGTGGATCCTTAGGAAGCAGTTGAGTAGCTG	CGGGCCCCCCCTCGAGGTCGACGTAGGAGCTAGAGGAGCCTCA
107	IME2	CGGCCGCTCTAGAACTAGTGGATCCGGACACTCCAGTCGGTTAAGG	CGGGCCCCCCCTCGAGGTCGACCGAACACAAAGATCTCGTTCTAC
108	DUN1	CGGCCGCTCTAGAACTAGTGGATCCATTATGTGCTGGAGAAATCAGAGG	CGGGCCCCCCCTCGAGGTCGACTCAAGATTATGGACACAATGCC
109	STE20	CGGCCGCTCTAGAACTAGTGGATCCGAAAGTCTACCGCTTTTGGC	TGTGCGAATCACTTGTCGACG
109	STE20	CTTTCAACACAACCACAGGATTGCC	CGGGCCCCCCCTCGAGGTCGAGTGTAATGGTACCCGACACTCG
110	PBS2	CGGCCGCTCTAGAACTAGTGGATCCTAGTGAGCGATTTCGTGAGCCA	CGGGCCCCCCCTCGAGGTCGAGTCCACATCGCTTCACTTGCC
111	KNS1	CGGCCGCTCTAGAACTAGTGGATCCAGTGCAGTAACTCCTCGTGC	CGGGCCCCCCCTCGAGGTCGAGCCAAATGTACAAAGGAGCTGG
112	ARK1	CGGCCGCTCTAGAACTAGTGGATCCGCTAACCACGGCTTATTTAGG	CGGGCCCCCCCTCGAGGTCGATTCGGCAACCTTCATGCCTT
113	KDX1	CGGCCGCTCTAGAACTAGTGGATCCTCAATGCAGGAAGCACCGTAGG	CGGGCCCCCCCTCGAGGTCGACGAACTGCAAAACCGCCGAGAG
114	CMK2	CGGCCGCTCTAGAACTAGTGGATCCAGTCGTTGAGCATCATATGG	CGGGCCCCCCCTCGAGGTCGACATCTTCTCAGAACCCGTTAGGC
115	IKS1	CGGCCGCTCTAGAACTAGTGGATCCGTAAGAAGGGCGGTTTTCAGG	CGGGCCCCCCCTCGAGGTCGACGGTCAATTGGCGTTTCTGTCACC
116	ISR1	CGGCCGCTCTAGAACTAGTGGATCCAGCTAGATTGTGATGTATGGG	CGGGCCCCCCCTCGAGGTCGACGGAGTTCTTGTCCTAGACGGCAT
117	KIC1	CGGCCGCTCTAGAACTAGTGGATCCCAGGTTTCGCCACATCTG	CGGGCCCCCCCTCGAGGTCGACGAGGTTTGGTAACTGCGCC
118	YGK3	CGGCCGCTCTAGAACTAGTGGATCCAACAAGGTTGCTATATCGGGC	CGGGCCCCCCCTCGAGGTCGACGAGGCCAATTAAGGCGATCTG
119	COQ8	CGGCCGCTCTAGAACTAGTGGATCCACAGCAAACGAATACAGAGCG	CGGGCCCCCCCTCGAGGTCGATGGCAGAAGGATTAGCGTTGC
120	MEC1	CGGCCGCTCTAGAACTAGTGGATCCAAGGCTCCATAACTATATGGAGC	CGGGCCCCCCCTCGAGGTCGAGCTCTTCTAAGGGAACCTTACGAG

Table 2.3: Kinases and primers for over-expression screen (continued)

RCK#	Kinase	FORWARD PRIMER	REVERSE PRIMER
121	PKP1	CGGCCGCTCTAGAACTAGTGGATCCG CTTATTCCACTCCTCTGCCTAC	CGGGCCCCCCCTCGAGGTCGAGAACTTG AAGAGCAAAGGCACG
122	PKP2	CGGCCGCTCTAGAACTAGTGGATCCG GGATTTGGGTCTGTTAACACTCATC	CGGGCCCCCCCTCGAGGTCGATCTAGCT GGTGTGGACATGACG
123	RIO2	CGGCCGCTCTAGAACTAGTGGATCCT GAATGGCTCAACAGAGTGAGTG	CGGGCCCCCCCTCGAGGTCGATGAAGAT GATGAGGATGGATCCG
124	SLN1	CGGCCGCTCTAGAACTAGTGGATCCG CGCGTTAATATTTCCTCTTCG	CGGGCCCCCCCTCGAGGTCGAGTGGTCA CACCAACCAATTGCG
125	TEL1	CGGCCGCTCTAGAACTAGTGGATCCT GAGAAACAAGTATGGCACCAGCC	CGGGCCCCCCCTCGAGGTCGAAGTCCTA GCAATAGTTGGTGCC
126	TOR1	CGGCCGCTCTAGAACTAGTGGATCCA TTGTCCATGACAACAGCG	CGGGCCCCCCCTCGAGGTCGACCTATTG TGAAAAGTACCATGTGCC
127	TOR2	CGGCCGCTCTAGAACTAGTGGATCCG AATAGAGACTGACATATATGGCAGC	CGGGCCCCCCCTCGAGGTCGAGCGTAAC GAGCGAGTACTTGACAG

***In vitro* kinase assay**

For each reaction, samples were incubated in 15mM KPO_4, 5mM Tris pH 8.0, 250mM NaCl, 2.5% glycerol, 10mM $MgCl_2$, and 200μM ATP. 2μg of substrate peptides and 100μL of Cdc5p purification prep were added, and reactions were brought to a final volume of 200μL. Reactions were started with the addition of Cdc5p and incubated for 1 hour at 30˚C. Aliquots were then assayed on nitrocellulose using Bio-Rad Dot-Blot apparatus (Bio-Dot, Catalog number 170-6545) and pS8 antibody analysis.

Cell-cycle synchrony and release

To achieve cell synchrony, cells were treated with either 10μg/mL nocodazole (Cayman Chemical) or 1μg/mL alpha-factor (Bachem 4003514) and grown at 30˚C for 2 hours. Cells were imaged with DIC microscopy and checked to ensure greater than 95% synchrony (large budded cells or shmoo formation for nocodazole and alpha-factor respectively). Cells were washed and re-suspended in pre-warmed 30˚C YPD to initiate the release. Cells were grown in a 30˚C shaker and 3 OD_{600} units of cells were taken every ten minutes, pelleted, washed in 10mM Tris pH 7.5, 10mM NaN_3, pelleted once again, then snap frozen in liquid nitrogen (for each sample, it took about 3 minutes to take cells from incubator until the pellet was snap frozen in liquid nitrogen). For immunofluorescence preparation, aliquots were taken every 10 minutes and mixed with 2X fixative (8% paraformaldehyde). Alpha-factor synchrony experiments were performed in *bar1Δ* cells (RCY5066) for efficient synchrony and release. Endogenous Sec4p was monitored for phosphorylation via western blot in both synchrony experiments, but nocodazole release localization experiments used GFP-Sec4p as the sole copy of Sec4p. Alpha-factor release experiments monitored endogenous Sec4p localization via immunofluorescence. For immunofluorescence experiments, cells were spheroblasted in 100mM KPi pH 7.5, 1.2M

sorbitol, zymolyase, and 0.2% 2-mercaptoethanol for 30 minutes, permeabilized with 0.1% SDS, and blocked in 10% Goat serum PBS (30 min). Sec4p was detected using 1:500 mouse anti-Sec4p (generated in collaboration with Whittaker lab) and a goat anti-mouse Ig 488 Alexa fluor secondary.

Results

Identification of phosphorylated Sec4p *in vivo*

To investigate and measure the phosphorylation status of Sec4p, antibodies were raised against phosphorylated Sec4p (figure 2.1). Phospho-peptides representing both NH_2 and COOH terminally phosphorylated Sec4p were injected into rabbits and subsequent test bleeds were analyzed for specificity to modified Sec4p (21^{st} Century Biochemicals). To screen the bleeds, yeast purified MBP (maltose binding protein) tagged Sec4p and Sec4p with serine 8, 10, 11, 201, and 204 mutated to alanine residues (an unphosphorylatable mutant hereby referred to as $Sec4p^{Ala}$) were probed, and specificity for the wild type phosphorylated protein was assessed. NH_2 terminal phospho-antibodies for either phosphorylated serine 8, 10, or 11 along with COOH terminal phospho-antibodies for serine 201 were specific to wild type Sec4p and did not produce a signal for the unphosphorylatable $Sec4p^{Ala}$ (figure 2.1B). However, the rabbits used for the generation of phospho-antibodies for serine 204 had significant detection for the $Sec4p^{Ala}$ protein (Rabbit 9828) or little to no detection for either protein (Rabbit 9829). These antibodies were thus not used further in this study.

Figure 2.1: Screening phospho-Sec4p antibodies

A. Schematic of the Rab GTPase Sec4p showing relative positions of the GTPase domain and phosphorylation sites. NH_2-terminal and COOH-terminal phosphorylation sites highlighted in red were targeted for antibody production.
B. Western blots of yeast purified MBP-Sec4p^{WT} and MBP-Sec4p^{Ala} probed with different test bleeds from rabbits to determine specificity for phosphorylated Sec4p at positions S8, 10, 11, 201, and 204. An MBP antibody was used to detect total protein as a loading control.

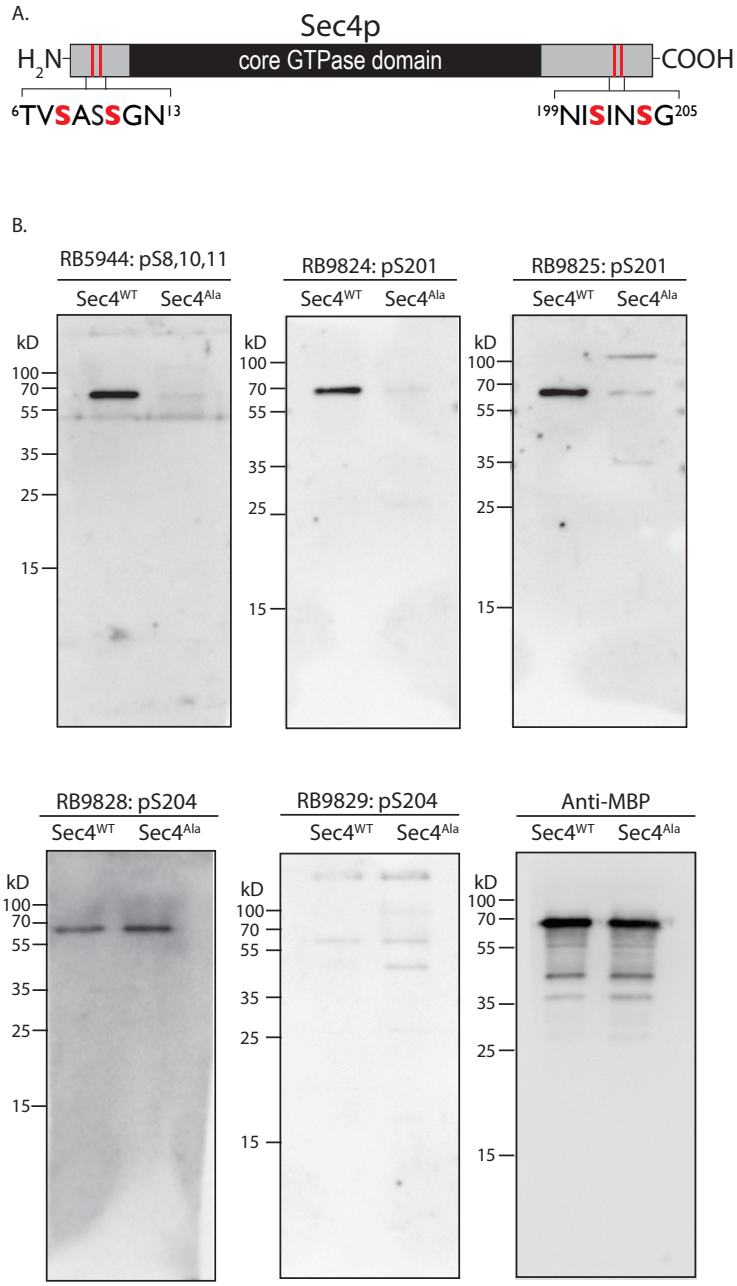
A.
Sec4p
H2N
core GTPase domain
COOH
6TVSASSGN13
199NISINSG205
B.
RB5944: pS8,10,11
RB9824: pS201
RB9825: pS201
Sec4WT
Sec4Ala
kD
100
70
55
35
25
15
RB9828: pS204
RB9829: pS204
Anti-MBP

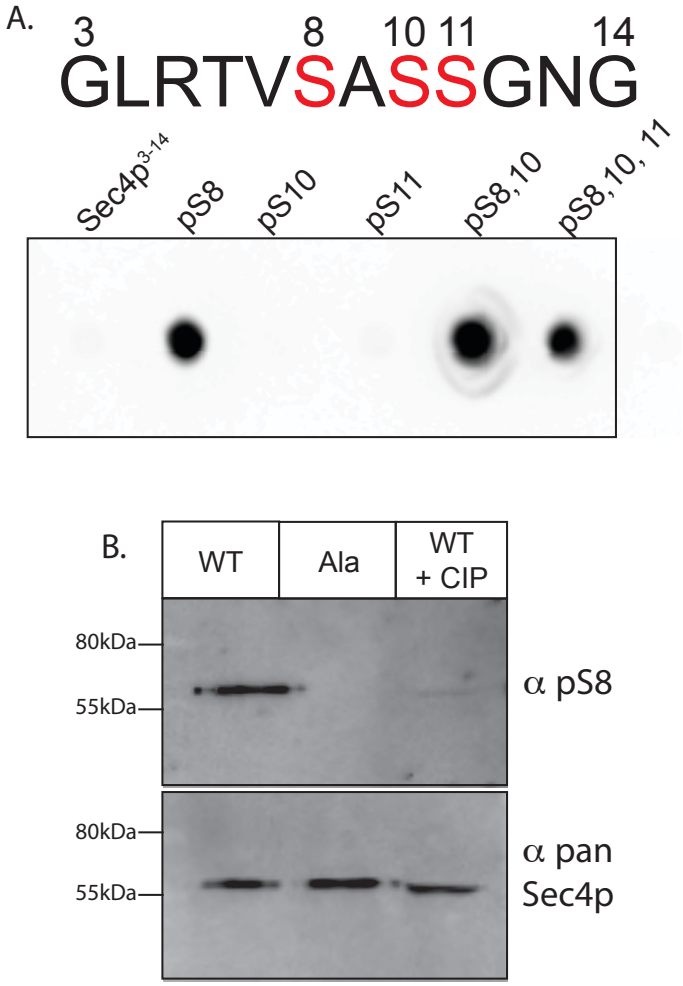

Figure 2.2: Detecting phosphorylation in the NH_2 terminus of the Rab GTPase Sec4p

A. Dot-blot of phosphate modified peptides (sequence shown and site of phosphate modifications highlighted in red) representing $Sec4p^{3-14}$ probed with a custom antibody raised against phosphorylated Sec4p peptide sequences.

B. Western blot of *S. cerevisiae* purified MBP-Sec4p (with and without alkaline phosphatase treatment) and MBP-$Sec4p^{Ala}$ (S8, 10, 11, 201, and 204A) using pS8 antibody and pan-Sec4p antibody. MBP-Sec4p is expressed from an exogenous plasmid (pRS315 backbone) as the only cellular copy of Sec4p.

NH_2-terminal phospho-antibodies are specific to serine 8

The results are shown for an antibody specifically raised to detect phosphorylation at the NH_2-terminus of Sec4p (figure 2.2). Characterization of this custom antibody using chemically modified Sec4p peptides (residues 3-14 of Sec4p) reveals specific detection of serine 8 phosphorylation (pS8), and this detection is independent of the phosphorylation status of nearby serine residues (figure 2.2A). Furthermore, affinity-tagged, purified Sec4p protein was found to produce a robust pS8 signal, however this signal was lost upon serine 8 to alanine mutation, in additional to alkaline phosphatase treatment of the purified wild type protein (figure 2.2B). These data demonstrate a pool of phosphorylated Sec4p exists *in vivo*, however the dynamics of this modification, and sensitivity to signaling pathways remained unknown.

COOH-terminal phosphorylation on serine 201 cannot be detected in cell lysate

Sec4p phospho-antibodies for serine 201 were shown to have specificity for wild type Sec4p over $Sec4p^{Ala}$, but attempts to detect phosphorylated Sec4p in cell lysates were unsuccessful, and resulted in mostly non-specific detection of protein species at the wrong molecular weight (figure 2.3). Various growth conditions were attempted to elicit a response and increase detection, but no change in band intensity around the expected molecular weight was observed. It is possible that COOH-terminal phosphorylation is present, but below the detection limit with this particular antibody, or that phosphorylation of serine 201 requires some yet unknown stimulus. Regardless, we chose to pursue the effects of phosphorylation of serine 8, as it was the only residue where we could get reliable detection of phosphorylated Sec4p in cell lysates. It would be possible to use this COOH-terminal antibody for experiments where Sec4p was first purified, but this cumbersome technique was not conducive for

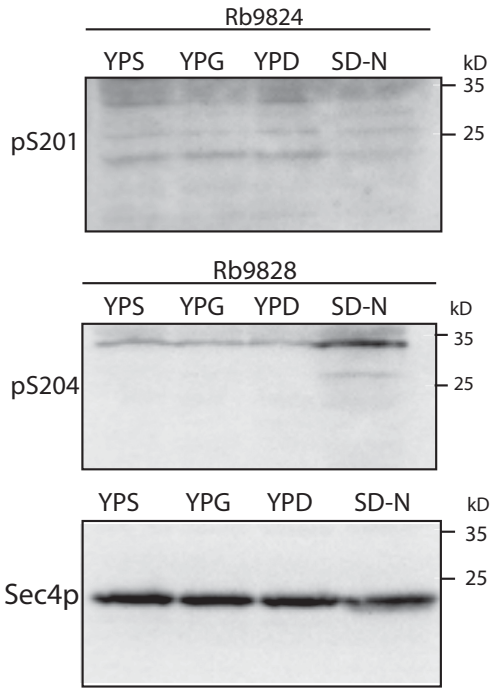

Figure 2.3: Detecting phosphorylation in the COOH-terminus of the Rab GTPase Sec4p

Western blot using yeast protein lysate derived from carbon and nitrogen starved wild type cells and probing with COOH-terminal phospho-antibodies. For each blot, the rabbit identification number is listed (Rb#) for the COOH-terminal antibodies. The third blot uses a pan Sec4p antibody to show equal loading of total Sec4p protein. Cells were split and incubated at 25˚C for 3 hours in YPD, YPG, YPS, and SD-N media prior to lysis.

early experiments trying to determine the physiological relevance and regulation of phosphorylation.

Sec4p phosphorylation is sensitive to nutrient availability

Considering that Sec4p is directly responsible for cellular growth by delivering membrane to the site of polarized exocytosis on the plasma membrane, we reasoned that phosphorylation may be sensitive to signaling pathways activated or inhibited under different nutrient availability conditions. To test this hypothesis, cells were grown under carbon and nitrogen starvation conditions for 3 hours, and then the phosphorylation status of Sec4p was accessed via western blot (figure 2.4A). Phosphorylation was significantly reduced upon both starvation conditions. No significant change in phosphorylation was observed when sucrose was the only carbon source. Additionally, the nitrogen starvation conditions contained ample glucose, but still showed a significant decrease in Sec4p phosphorylation, suggesting that glucose repression was not responsible for the changes observed (Gancedo, 1998). Nutrient availability typically signals through the TOR pathway, leading to the regulation cell growth, translation initiation, cell-cycle progression from G1, and autophagy (Barbet et al., 1996; Cardenas et al., 1999; Kamada et al., 2000). Inhibition of TORC1 using rapamycin shows a dose dependent ablation of Sec4p phosphorylation (figure 2.4B). Taken together, the status of Sec4p phosphorylation is altered in response to general nutrient availability, and downstream of the TORC1 signaling pathway.

Autophagy is not regulated by Sec4p phosphorylation

Sec4p has previously been shown to be required for autophagy (Geng et al., 2010). Both nutrient starvation and rapamycin treatment stimulate autophagy (Klionsky et al., 2007; Mizushima and Komatsu, 2011), therefore we investigated whether or not phosphorylation was involved in this specific action of Sec4p. Autophagy is a general term referring to the

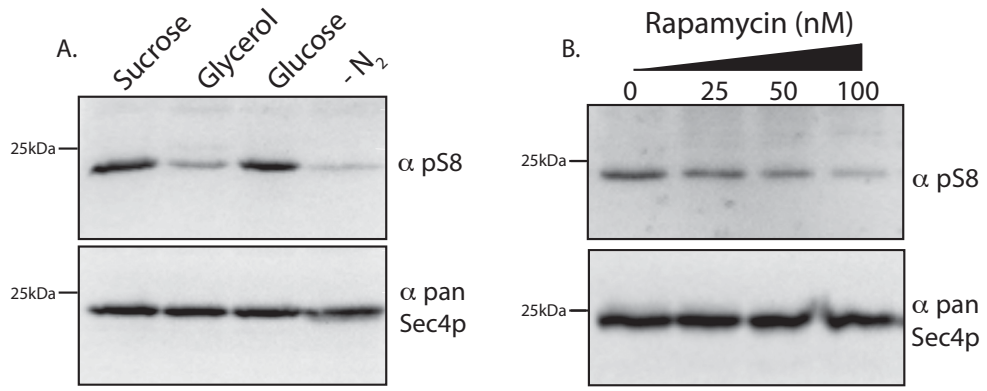

Figure 2.4: Sec4p phosphorylation is sensitive to nutrient starvation signaling via TORC1

A. Regulatory control of Sec4p phosphorylation in response to nutrient depravation. Carbon and nitrogen starvation of wild type cells. Cells were split and incubated at 25˚C for 3 hours in YPD, YP + 2% glycerol, YP + 2% sucrose, and SD-N media prior to lysis.

B. Effects of TORC1 inhibition on Sec4p phosphorylation. Cells were split into media containing different concentrations of the TORC1 inhibitor rapamycin and incubated for 3 hours at 25˚C prior to lysis.

degradation of proteins, organelles, and macromolecular complexes via trafficking to the vacuole or lysosome (Hutagalung and Novick, 2011; Reggiori and Klionsky, 2013). Upon induction of autophagic processes, a dynamic re-arrangement of cellular membranes occurs in order to form autophagosomes for lysosomal/vacuolar delivery (Kim et al., 2002; Stolz et al., 2014; Suzuki et al., 2001). Autophagosomes are double membrane structures that surround cellular components destined for degradation and fuse with the lysosome/vacuole for degradation.

Upon nutrient starvation, we found a dramatic Sec4p localization change to the vacuole, supporting the idea that Sec4p is indeed involved in the delivery of membrane components to the vacuole during autophagy, but phosphorylation was not required for this localization change (figure 2.5A). To determine if phosphorylation affects autophagy more directly, we employed a GFP-Atg8 assay (Klionsky, 2011) to measure autophagosome formation in a *sec4-8* genetic background. Briefly, GFP-Atg8 is degraded upon autophagosome formation, and this can be observed by the appearance of a GFP degradation band via western blot with a GFP antibody. *Sec4-8* cells were shown to be deficient for autophagy (Geng et al., 2010), thus we ectopically expressed Sec4p, Sec4p^{Ala}, and Sec4p^{Asp} (a phosphomimetic mutant of with S8, 10, 11, 201, and 204 mutated to aspartic acid residues to mimic the constitutively phosphorylated state of Sec4p) to determine if these mutants could rescue autophagy. Indeed, a vector only control confirmed Sec4p was required for autophagy, however all versions of Sec4p tested were able to rescue autophagy, thus we determined phosphorylation did not affect Sec4p's role in autophagy (figure 2.5B).

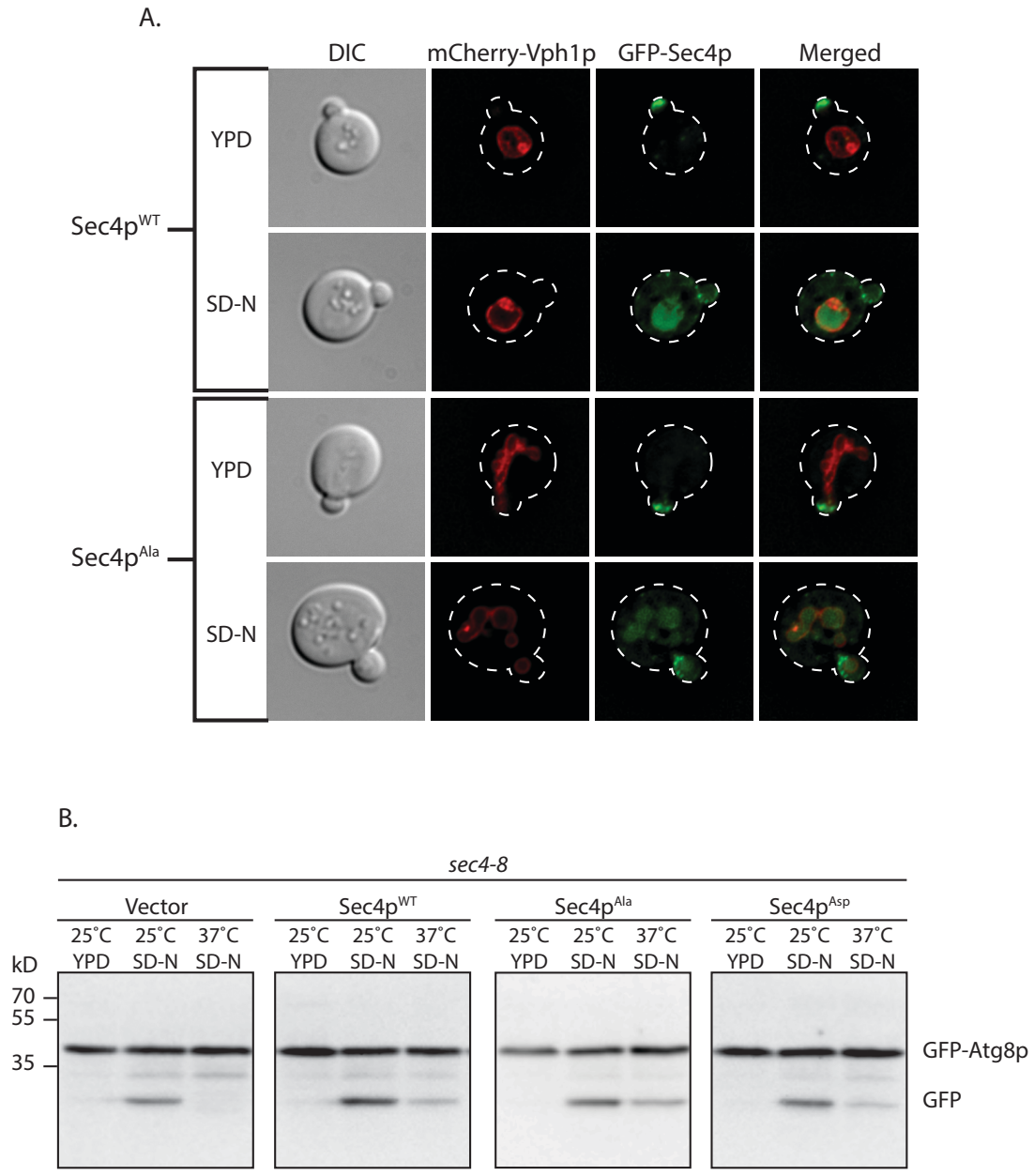

Figure 2.5: Phosphorylation of Sec4p is not related to Sec4p's role in autophagy

A. Localization of GFP-Sec4p and GFP-Sec4p^{Ala} as the sole copy of Sec4p under optimal growth conditions (YPD media) and in nutrient starvation conditions (SD-N) to induce autophagy. mCherry tagged Vph1p is used as a vacuolar marker.

B. GFP-Atg8p assay to test for autophagy induction in a *sec4-8* genetic background. Sec4p^{WT}, Sec4p^{Ala}, Sec4^{Asp}, and a vector only control plasmid were transformed into a *sec4-8* strain (RCY3918) and their ability to rescue autophagy was assessed by the appearance of a GFP only band as a degradation product from GFP-Atg8p.

Sec4p phosphorylation accumulates on membrane bound Sec4p and interrupts the interaction with effector protein Sec15p

Sec4p phosphorylation has previously been shown to negatively regulate Sec4p function (Heger et al., 2011). Sec4p^{Asp} failed to functionally replace the wild type protein, while Sec4p^{Ala} was able to functionally replace wild type Sec4p. However, the molecular mechanism by which phosphorylation negatively affects function is not understood. Using the pS8 antibody, we began to investigate how phosphorylation affects function. First, we investigated whether the nucleotide-bound state of the protein affected phosphorylation. Previous work had shown that nucleotide hydrolysis and exchange rates of phophomimetic Sec4p was indistinguishable from wild type protein in the presence of the GAP and GEF respectively (Heger et al., 2011). However, the effect of the nucleotide-bound state of Sec4p on phosphorylation was not investigated. Using GTP-hydrolysis (Q79L) and GDP exchange deficient (S29V) (Rinaldi et al., 2015) mutants of Sec4p as the sole copy, subsequent western blot analysis revealed no significant change in Sec4p phosphorylation levels (figure 2.6A). However, membrane fractionation experiments to separate the soluble and membrane bound Sec4p protein pools showed that phosphorylation was enriched on the membrane-bound fraction of Sec4p (figure 2.6B). Furthermore, using a GFP-tagged, temperature sensitive phosphomimetic mutant of Sec4p previously characterized (Heger et al., 2011), we found the Sec4p mutant accumulated on vesicles in the cytosol at the restrictive (but not permissive) temperature (figure 2.6C).

Figure 2.6: Sec4p phosphorylation accumulates on membrane bound Sec4p and interrupts the interaction with effector protein Sec15p

a. Phosphorylation status of GTP hydrolysis deficient (Q79L) and GDP exchange deficient (S29V) Sec4p mutants.

b. Membrane fractionation of MBP-Sec4p and MBP-Sec4p^{Ala} as the only copy of Sec4p and subsequent western blot. 100,000x*g* centrifugation was used to separate the cytosolic and membrane fractions. This experiment was replicated in triplicate and a representative western blot is shown

c. Localization of GFP-Sec4p and temperature sensitive phosphomimetic GFP-Sec4p$^{DASD\ DIND}$ (S8, 11, 201, 204D) at permissive (25˚C) and restrictive (37˚C) temperatures. Cells were split, incubated at designated temperature for 2 hours, then fixed in 4% PFA prior to microscopy.

d. Pull-down of Sec15p-MBP that was co-expressed with GFP-Sec4p, GFP-Sec4p^{Ala}, or GFP-Sec4p^{Asp} and subsequent western blot analysis using GFP antibody to determine Sec15p interaction with Sec4p.

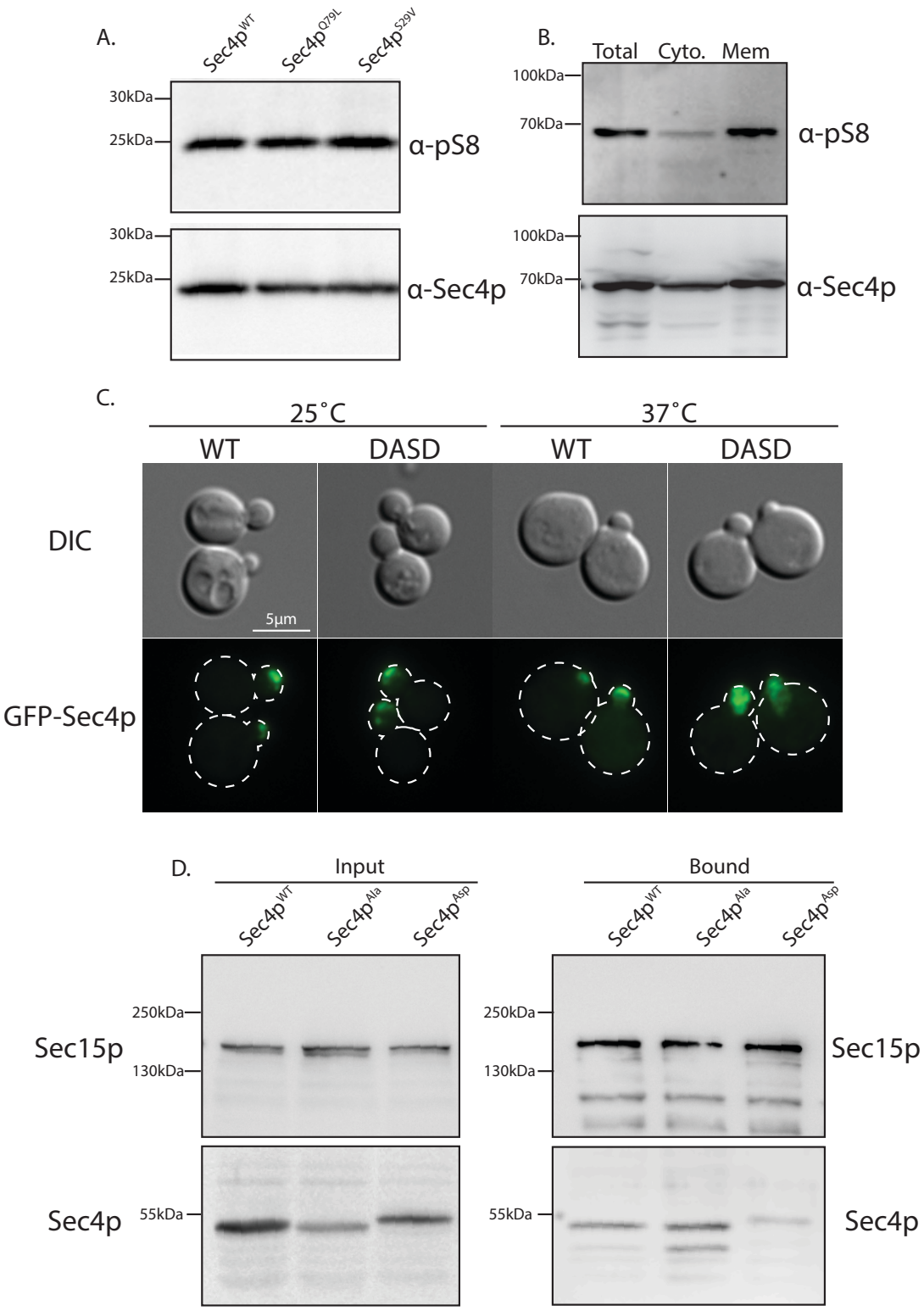
A.
Sec4p^WT
Sec4p^Q79L
Sec4p^S29V
30kDa
25kDa
α-pS8
30kDa
25kDa
α-Sec4p
B.
Total
Cyto.
Mem
100kDa
70kDa
α-pS8
100kDa
70kDa
α-Sec4p
C.
25˚C
37˚C
WT
DASD
WT
DASD
DIC
5μm
GFP-Sec4p
D.
Input
Bound
Sec4p^WT
Sec4p^Ala
Sec4p^Asp
Sec4p^WT
Sec4p^Ala
Sec4p^Asp
250kDa
130kDa
Sec15p
250kDa
130kDa
Sec15p
Sec4p
55kDa
Sec4p
55kDa
Sec4p

Since it appeared that Sec4p phosphorylation was negatively affecting the function of Sec4p on membranes, but prior to vesicle fusion, we decided to investigate the effector binding capacity of the phosphomimetic protein. Yeast-two hybrid analysis had previously implicated the exocyst component Sec15p as being disrupted by Sec4p phosphorylation (Heger et al., 2011). To investigate this suggestion biochemically, affinity tagged Sec15p was affinity purified from cells ectopically expressing GFP-tagged $Sec4p^{WT}$, $Sec4p^{Ala}$, and phosphomimetic Sec4p (figure 2.6D). The results of this experiment show phosphomimetic Sec4p, but not $Sec4p^{Ala}$ has a diminished affinity for Sec15p. Failure of Sec4p to effectively engage with Sec15p is known to result in severe membrane trafficking defects leading to cell death and could explain why the phosphomimetic Sec4p is a non-functional replacement of Sec4p.

General secretory defects lead to a decrease in Sec4p phosphorylation

Based on the observation that Sec4p phosphorylation accumulated on membranes, we sought to determine if it was possible to increase/decrease Sec4p phosphorylation by forcing Sec4p to membranes or the cytosol. To accomplish this, we used temperature sensitive alleles of various secretory proteins (Novick et al., 1981; Novick et al., 1980) to either deplete post-Golgi secretory vesicles (*sec12-4*, *ypt1-3*, $sec26^{TS}$, *sec18-1*, and *sec21-1*), prevent Sec4p from associating with post-Golgi vesicles (*sec2-41* and *sec19-1*), or to enrich the cell with Sec4p loaded post-Golgi secretory vesicles (*sec6-4*, *sec15-1*, *sec3-2*, *sec10-2*, *sec1-1*, and *sec9-4*). We found that in almost all membrane trafficking defects, Sec4p phosphorylation was reduced, and under no circumstance was phosphorylation increased (figure 2.7). Based on these data it appears that general membrane trafficking pathways must be intact and cellular growth active for proper Sec4p phosphorylation.

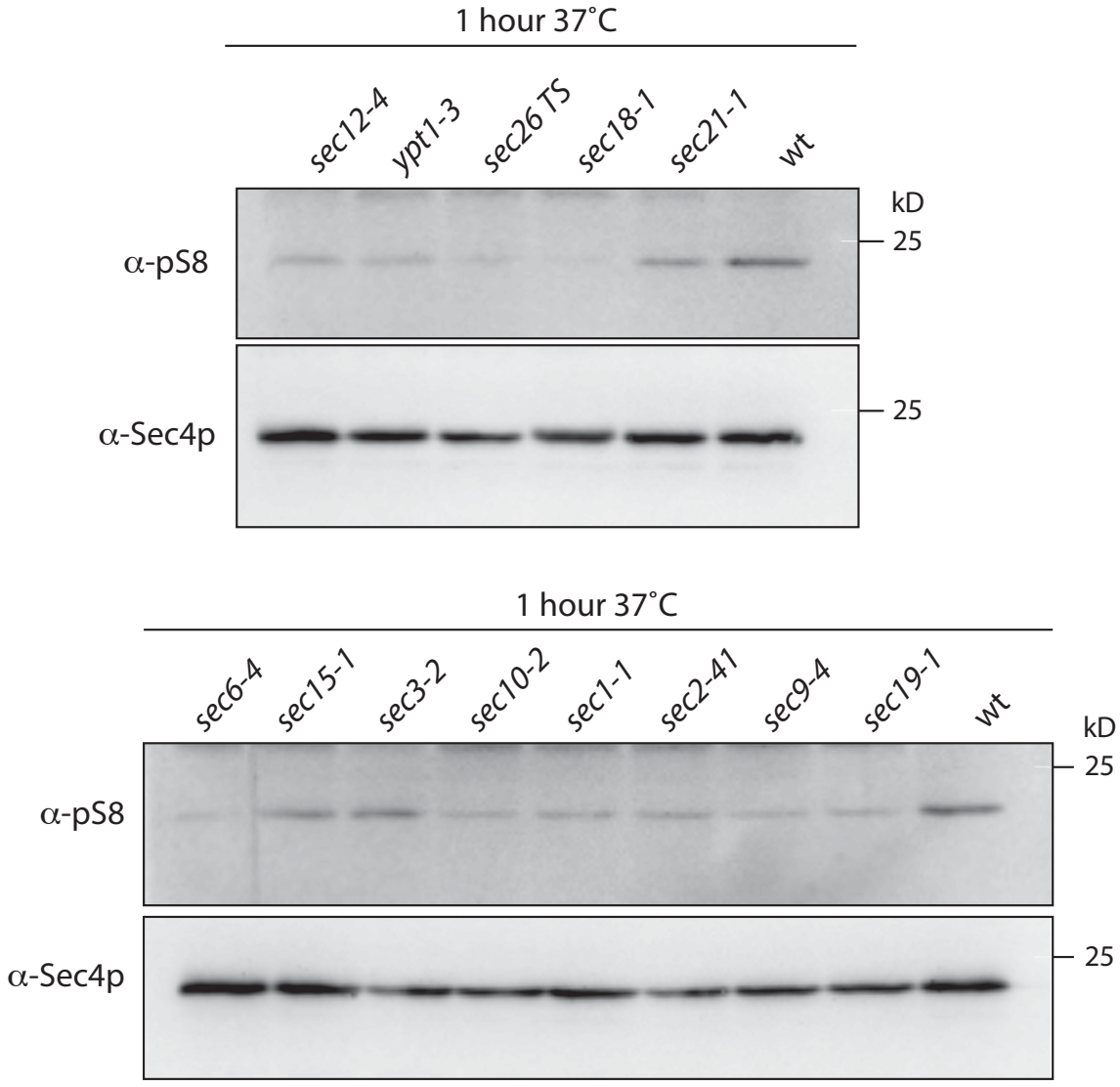

Figure 2.7: Sec4 pS8 levels in cells with membrane trafficking defects

Western blot analysis of pS8 and Sec4p levels in the following membrane trafficking temperature sensitive strains after 1 hour shift to 37˚C: sec12-4, ypt1-3, sec26 ts , sec18-1, sec21-1, sec6-4, sec15-1, sec3-2, sec10-2, sec1-1, sec2-41, sec9-4, sec19-1.

Kinase over-expression screen to identify Sec4p kinases

Our data indicate that effector binding, which is already known to be under the control of the nucleotide-bound state of Sec4p, can also be controlled by the phosphorylation status of Sec4p. This suggests that additional cellular pathways may impinge upon membrane trafficking through Sec4p effector protein recruitment, independent of its nucleotide bound state. Indeed, the nutrient starvation phenotype and sensitivity to rapamycin suggests a pathway downstream of TORC1, of which there are many, could be involved. We have ruled out phosphorylation playing a role in autophagy and shown that membrane trafficking must be intact for phosphorylation of Sec4p to occur. To elucidate the particular cellular pathways/processes responsible for controlling Sec4p phosphorylation, we sought to identify the kinase/s directly responsible for modifying Sec4p. To accomplish this, a kinase over-expression library was constructed, and a screen performed to measure the phosphorylation status of Sec4p in each over-expression strain. Due to the redundancy of many *S. cerevisiae* kinases, an over-expression screen was favored as opposed to a deletion screen where paralogous kinases have the potential to moderate the effects of individual kinase deletions. Additionally, all essential kinases can be included in an over-expression screen, which is not the case for a deletion library. 127 kinases and predicted kinases were cloned onto multi-copy plasmids with their endogenous promoters for the over-expression library (figure 2.8A and Table 2.4). For each kinase over-expression strain, the levels Sec4p pS8 and total Sec4p protein were measured in duplicate via western blot and normalized to a vector only control (figure 2.8B). Several kinases were found to significantly increase Sec4p phosphorylation, making them prime candidates for bona fide Sec4p kinases (a significant increase was defined as a doubling of Sec4p phosphorylation per total Sec4p protein, relative to a vector only control). Gene ontology of these kinases and kinases that significantly lowered Sec4p

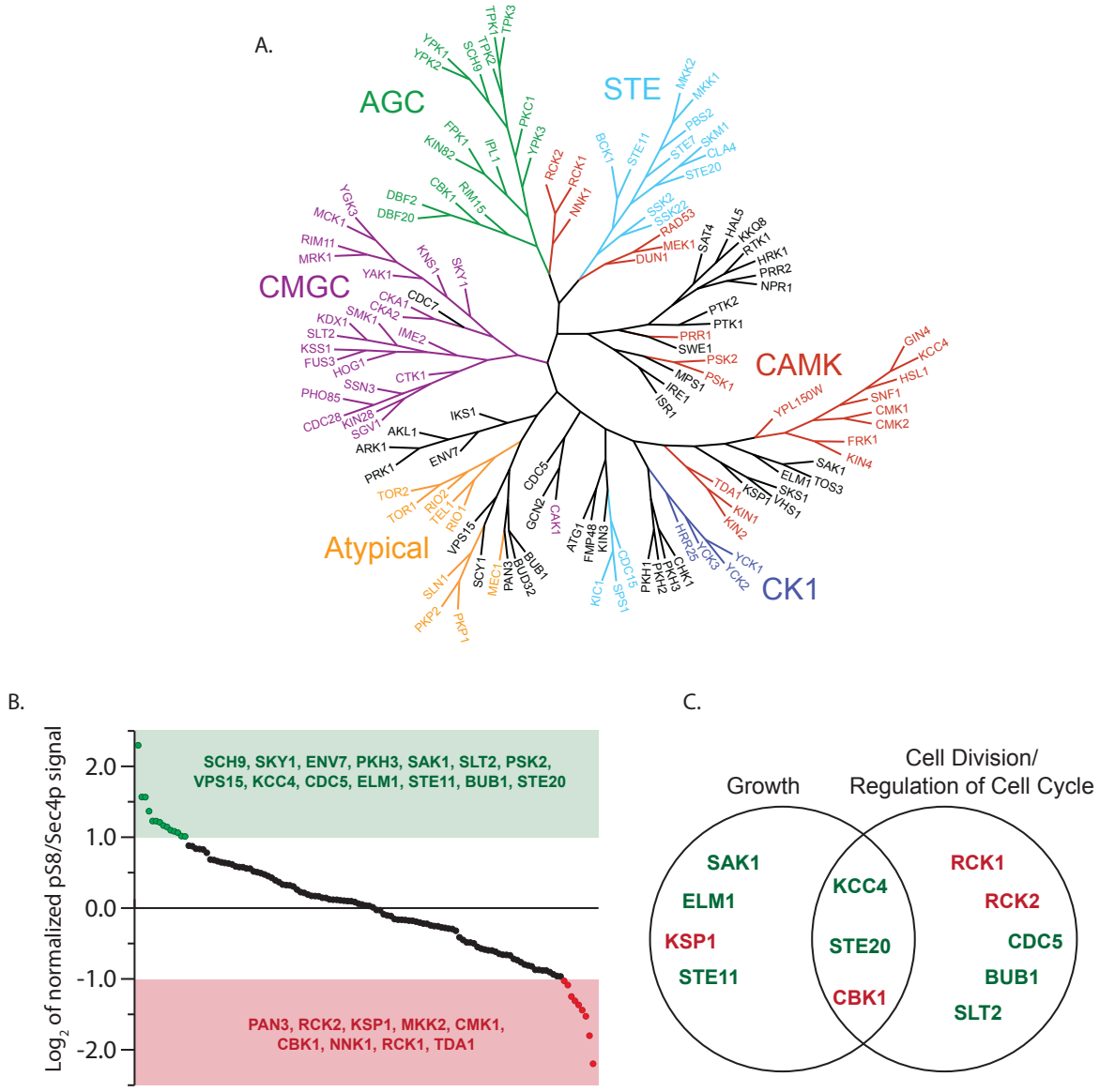

Figure 2.8: Kinase over-expression screen to identify entities responsible for Sec4p phosphorylation

a. Tree view of all 127 kinases/predicted kinases used in this study.

b. Summary of kinase overexpression screen with each point representing results from a single kinase assay. Kinases are ordered from most significant increase to most significant decrease in Sec4p phosphorylation relative to total Sec4p signal. The graph shows the $\log_2$ of average western blot quantified pS8/Sec4p levels relative to a vector only control .

c. Gene ontology (SGD Gene Ontology Term Finder) of kinases that significantly impact Sec4p phosphorylation.

Table 2.4: Quantitative measure of pS8/Sec4p ratio for kinase overexpression screen

Each number is the relative deviation of the ratio pS8/Sec4p levels from a vector only control as measured by quantification of western blot data.

Table 2.4: Quantitative measure of pS8/Sec4p ratio for kinase overexpression screen

RCK#	Kinase	YGD #	Trial I (A)	Trial II (B)	Average
1	KIN1	YDR122W	-0.368180345	-0.272581358	-0.320380851
2	KIN2	YLR096W	0.63250812	0.099633421	0.36607077
3	YCK1	YHR135C	0.23422238	0.619854836	0.427038608
4	YCK2	YNL154C	0.95741147	0.716563018	0.836987244
5	YCK3	YER123W	-0.74717631	-0.781108238	-0.764142274
6	HRR25	YPL204W	-0.575157781	-0.71649621	-0.645826995
7	CKA1	YIL035C	-0.214364456	0.314435837	0.050035691
8	CKA2	YOR061W	-0.596054498	0.108650793	-0.243701852
9	CDC7	YOR061W	0.602541802	0.554156518	0.57834916
10	CDC5	YMR001C	0.774803167	1.421924214	1.098363691
11	IPL1	YPL209C	-0.534319361	-0.899438656	-0.716879009
12	IRE1	YHR079C	0.621842751	0.018764474	0.320303612
13	VPS15	YBR097W	1.14320799	1.185797994	1.164502992
14	ENV7	YPL236C	2.497844408	0.63338866	1.565616534
15	MPS1	YDL028C	-0.276190311	0.099616465	-0.088286923
16	SLT2	YHR030C	1.397511262	1.057254896	1.227383079
17	CDC28	YBR160W	0.462396778	0.89249804	0.677447409
18	DBF20	YPR111W	0.172925106	1.479505749	0.826215427
19	SCH9	YHR205W	2.099017096	2.495078521	2.297047809
20	MEK1	YOR351C	1.122577581	0.638375904	0.880476743
21	TPK1	YJL164C	-0.165281936	-0.807218468	-0.486250202
22	SAK1 (PAK1)	YER129W	1.559474285	0.896768	1.228121143

Table 2.4: Quantitative measure of pS8/Sec4p ratio for kinase overexpression screen (continued)

RCK#	Kinase	YGD #	Trial I (A)	Trial II (B)	Average
23	PRK1	YIL095W	-0.202776002	-0.006279997	-0.104528
24	ELM1	YKL048C	1.424839516	0.739994016	1.082416766
25	PCK1	YKR097W	0.179522557	0.933642728	0.556582642
26	HAL5	YJL165C	-0.687546335	-1.05673993	-0.872143132
27	VHS1	YDR247W	-0.321738995	-0.1153942	-0.218566598
28	YAK1	YJL141C	0.314374183	0.113712673	0.214043428
29	TPK2	YPL203W	-0.203909829	-0.696521874	-0.450215851
30	SGV1	YPR161C	-0.586434503	-0.73145126	-0.658942881
31	AKL1	YBR059C	0.082794935	0.114572252	0.098683594
32	KIN82	YCR091W	-0.0293549	0.315405508	0.143025304
33	YPL150W	YPL150W	0.059201462	-1.027852149	-0.484325343
34	YPK1	YKL126W	-0.012610943	-0.396544688	-0.204577815
35	YPK3	YBR028C	-0.016568098	0.076959261	0.030195581
36	CLA4	YNL298W	-0.695883385	-1.047091846	-0.871487616
37	SWE1	YJL187C	0.654458065	0.637854491	0.646156278
38	PKC1	YBL105C	-1.124714932	0.535454177	-0.294630378
39	STE7	YDL159W	-1.66272995	0.465932431	-0.59839876
40	CAK1	YFL029C	0.549510908	0.059364103	0.304437505
41	PKH1	YDR490C	-0.173610464	-0.334424156	-0.25401731
42	HOG1	YLR113W	0.027636143	1.342433596	0.68503487
43	HSL1	YKL101W	-0.005903966	-0.348400854	-0.17715241
44	KIN3	YAR018C	-0.519856785	-0.813694543	-0.666775664
45	SAT4	YCR008W	0.627516105	0.321412476	0.474464291

Table 2.4: Quantitative measure of pS8/Sec4p ratio for kinase overexpression screen (continued)

RCK#	Kinase	YGD #	Trial I (A)	Trial II (B)	Average
46	CDC15	YAR019C	-0.55290846	0.214294208	-0.169307126
47	BUB1	YGR188C	0.489463876	1.541540671	1.015502274
48	RTK1	YDL025C	1.020919982	0.645354784	0.833137383
49	RIO1	YOR119C	-0.180539502	0.519885918	0.169673208
50	PTK2	YJR059W	0.469828971	0.432398953	0.451113962
51	DBF2	YGR092W	-0.06870188	0.449468251	0.190383186
52	PSK2	YOL045W	1.385774417	1.033628734	1.209701575
53	HRK1	YOR267C	-0.193291728	0.427470385	0.117089328
54	SKS1	YPL026C	-0.132218497	-1.335341651	-0.733780074
55	PTK1	YKL198C	-0.398685492	-0.144646105	-0.271665799
56	YPK2	YMR104C	-0.641715601	-0.528128722	-0.584922161
57	PRR1	YKL116C	0.714719386	0.268680489	0.491699938
58	PHO85	YPL031C	0.664994538	-1.10941832	-0.222211891
59	BCK1	YJL095W	-1.34679326	-0.296806306	-0.821799783
60	SPS1	YDR523C	0.443274322	0.078278769	0.260776545
61	PSK1	YAL017W	1.23163428	0.041352303	0.636493291
62	SSK2	YNR031C	-0.570944965	-0.750607098	-0.660776031
63	STE11	YLR362W	1.726241485	0.40106025	1.063650868
64	GIN4	YDR507C	-0.058291353	0.181643442	0.061676044
65	FMP48	YGR052W	0.76287766	0.983270599	0.873074129
66	FRK1	YPL141C	0.496420622	0.736458716	0.616439669
67	SKY1	YMR216C	1.839992555	1.294761012	1.567376783
68	PRR2	YDL214C	-0.392293471	-0.187262045	-0.289777758

Table 2.4: Quantitative measure of pS8/Sec4p ratio for kinase overexpression screen (continued)

RCK#	Kinase	YGD #	Trial I (A)	Trial II (B)	Average
69	KSP1	YHR082C	-0.875988671	-1.621040856	-1.248514763
70	CBK1	YNL161W	-1.092301472	-1.788645427	-1.440473449
71	KCC4	YCL024W	1.384637716	0.902527041	1.143582379
72	TDA1	YMR291W	-2.13909864	-2.255439897	-2.197269268
73	MKK2	YPL140C	-0.99605401	-1.623703112	-1.309878561
74	CHK1	YBR274W	-1.231824317	-0.575636481	-0.903730399
75	KKQ8	YKL168C	-0.413749617	0.085693743	-0.164027937
76	FUS3	YBL016W	-0.252051316	0.273883833	0.010916258
77	SCY1	YGL083W	0.336093274	0.312992674	0.324542974
78	SKM1	YOL113W	0.61566553	0.53812983	0.57689768
79	NPR1	YNL183C	0.685251606	0.573659706	0.629455656
80	KSS1	YGR040W	0.186381404	0.263585363	0.224983384
81	KIN28	YDL108W	-1.621723521	-0.296704537	-0.959214029
82	SSN3	YPL042C	0.1069089	0.67535919	0.391134045
83	MRK1	YDL079C	-0.290578972	0.067405745	-0.111586614
84	PKH2	YOL100W	0.791238964	-0.852683365	-0.0307222
85	PAN3	YKL025C	-0.58955808	-1.463946028	-1.026752054
86	RAD53	YPL153C	0.192326525	-0.550631239	-0.179152357
87	CMK1	YFR014C	-0.957226755	-1.776020359	-1.366623557
88	TOS3	YGL179C	0.837172281	0.485010563	0.661091422
89	PKH3	YDR466W	1.989654379	0.744579623	1.367117001
90	SMK1	YPR054W	0.025793534	-1.125284396	-0.549745431
91	ATG1	YGL180W	0.448963556	0.66845364	0.558708598

Table 2.4: Quantitative measure of pS8/Sec4p ratio for kinase overexpression screen (continued)

RCK#	Kinase	YGD #	Trial I (A)	Trial II (B)	Average
92	SSK22	YCR073C	0.28476469	-0.338603598	-0.026919454
93	RCK1	YGL158W	-2.261197508	-1.340683314	-1.800940411
94	FPK1	YNR047W	0.28561224	0.00475451	0.145183375
95	RIM15	YFL033C	0.424647473	-0.079879506	0.172383984
96	CTK1	YKL139W	0.297840026	-0.627420308	-0.164790141
97	BUD32	YGR262C	-0.849584996	-0.293722525	-0.57165376
98	RIM11	YMR139W	0.760124208	0.80090386	0.780514034
99	RCK2	YLR248W	-1.042667074	-1.130591551	-1.086629313
100	SNF1	YDR477W	-1.08231521	-0.677422956	-0.879869083
101	KIN4	YOR233W	0.020756305	0.149766702	0.085261503
102	TPK3	YKL166C	-1.982869269	0.111145444	-0.935861912
103	MCK1	YNL307C	-0.465837862	-0.359880517	-0.41285919
104	NNK1	YKL171W	-1.718154131	-1.335757317	-1.526955724
105	MKK1	YOR231W	0.062292681	-0.373419949	-0.155563634
106	GCN2	YDR283C	-0.307016651	0.543261731	0.11812254
107	IME2	YJL106W	0.591896037	0.441576083	0.51673606
108	DUN1	YDL101C	-0.628529827	-0.368992533	-0.49876118
109	STE20	YHL007C	0.883257038	1.137493371	1.010375205
110	PBS2	YJL128C	-0.016353449	-1.744239424	-0.880296436
111	KNS1	YLL019C	1.142416363	-0.129846428	0.506284967
112	ARK1	YNL020C	-1.199334154	-0.420273611	-0.809803882
113	KDX1	YKL161C	-0.855721101	-0.735963721	-0.795842411

Table 2.4: Quantitative measure of pS8/Sec4p ratio for kinase overexpression screen (continued)

RCK#	Kinase	YGD #	Trial I (A)	Trial II (B)	Average
114	CMK2	YOL016C	-0.17022358	-1.062052331	-0.616137955
115	IKS1	YJL057C	-0.628181961	0.82210542	0.096961729
116	ISR1	YPR106W	-0.268418096	0.486480124	0.109031014
117	KIC1	YHR102W	0.17012192	0.074765796	0.122443858
118	YGK3	YOL128C	0.390526859	-0.774514677	-0.191993909
119	COQ8	YGL119W	0.434283969	0.229390025	0.331836997
120	MEC1	YBR136W	-1.613411992	-0.316290315	-0.964851154
121	PKP1	YIL042C	0.622750058	0.55204766	0.587398859
122	PKP2	YGL059W	-0.650197754	0.090517636	-0.279840059
123	RIO2	YNL207W	0.332928552	-0.000294924	0.166316814
124	SLN1	YIL147C	-0.228159745	0.299742018	0.035791136
125	TEL1	YBL088C	-0.046258215	0.2543441	0.104042943
126	TOR1	YJR066W	-0.63058747	0.118263862	-0.256161804
127	TOR2	YKL203C	-0.685446814	-0.509380722	-0.597413768

phosphorylation was conducted, and cellular processes like growth and mitotic cell cycle were enriched (figure 2.8C), which is consistent with the observations of Sec4p phosphorylation status being sensitive to nutrient availability.

Identification of the polo-like kinase Cdc5p

To better understand the relationship between kinase over-expression and Sec4p phosphorylation, we sought to reduce the activity of each kinase and look for a subsequent reduction of Sec4p phosphorylation. Of the subset of kinases whose over-expression significantly increased Sec4p phosphorylation, all but one were non-essential. Using the Research Genetics haploid deletion collection, pS8 levels were measured for each kinase deletion strain. Surprisingly, most kinase deletions did not significantly reduce Sec4p phosphorylation, with the exception of Vps15p and, to a lesser extent, Sch9p, but neither kinase deletion strain completely lost Sec4p phosphorylation (figure 2.9A). Vps15p is a vacuolar membrane associated kinase whose deletion results in membrane trafficking defects (Herman et al., 1991). General membrane trafficking defects have been shown to attenuate pS8 levels in a similar fashion (figure 2.7), thus we believe this to be a secondary effect. Additionally, Sec4p is not associated with vacuolar traffic. *Sch9Δ* only causes a minor reduction in phosphorylation, thus we also believe this to be a secondary affect, although overexpression does increase Sec4p phosphorylation. Sch9p is a direct substrate of TORC1, and TORC1 activity was shown to be required for Sec4p phosphorylation, thus potentially explaining the over-expression phenotype (Urban et al., 2007).

The only essential kinase that significantly increased Sec4p phosphorylation upon over-expression was the polo-like kinase Cdc5p. Cdc5p is responsible for regulating a variety of

Figure 2.9: Cdc5p is responsible for Sec4p phosphorylation

A. Sec4p phosphorylation status in cells deleted for non-essential kinases identified in over-expression screen as measured by western blot with pS8 antibody.
B. i) Sec4p phosphorylation status in wild type and *cdc5*^{ts} cell at the permissive (25˚C) and restrictive (37˚C) temperatures. Cell were split and grown in YPDA for 2 hours at the specified temperature prior to lysis and western blot analysis. ii) Quantification of Sec4p phosphorylation relative to total Sec4p protein in *cdc5*^{ts} cells at both permissive and restrictive temperature.
C. i) Western blot of cells overexpressing Cdc5p under a Gal4 promoter with galactose as the sole carbon source compared to vector only control. ii) Quantification of pS8 levels from three separate western blot experiments. Error bars are standard deviation.
D. i) Disruption of hypothetical polo-box binding motif on Sec4p (S10,11A) and subsequent western blot analysis to measure changes in Sec4p phosphorylation. ii) Quantification of three separate experiments measuring phosphorylation status relative to total Sec4p protein. Error bars are standard deviation.
E. *In vitro* kinase assay with purified Cdc5p and peptides representing Sec4p$^{3\text{-}14}$ as substrates. Samples were incubated at 30˚C for 1 hour then analyzed via dot-blot of products probed with Sec4p pS8 antibody.

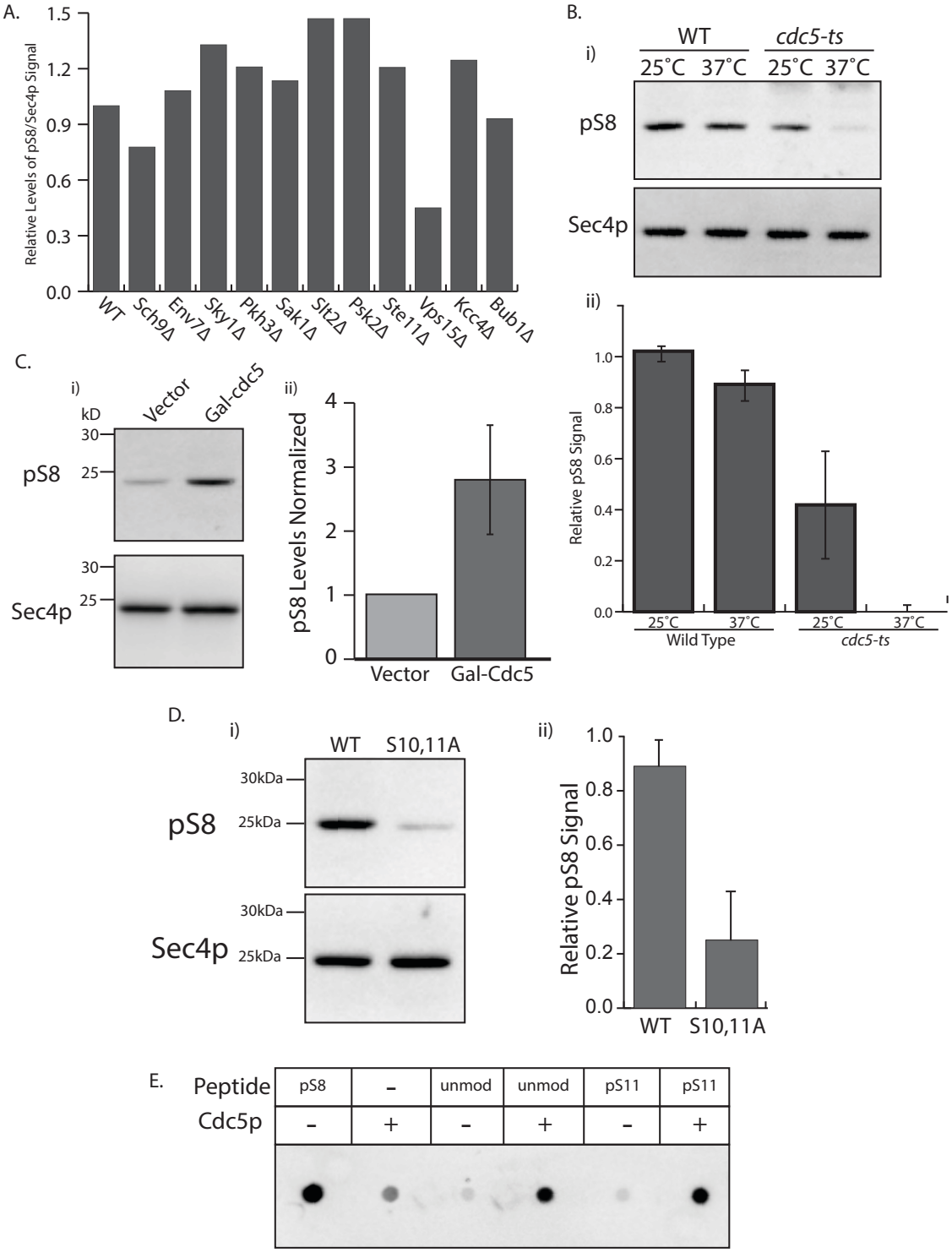
A.
Relative Levels of pS8/Sec4p Signal
1.5
1.2
0.9
0.6
0.3
0.0
WT
Sch9Δ
Env7Δ
Sky1Δ
Pkh3Δ
Sak1Δ
Slt2Δ
Psk2Δ
Ste11Δ
Vps15Δ
Kcc4Δ
Bub1Δ
B.
i)
WT
cdc5-ts
25˚C 37˚C 25˚C 37˚C
pS8
Sec4p
ii)
Relative pS8 Signal
1.0
0.8
0.6
0.4
0.2
0.0
25˚C 37˚C 25˚C 37˚C
Wild Type
cdc5-ts
C.
i)
kD
Vector
Gal-cdc5
30
25
pS8
30
25
Sec4p
ii)
pS8 Levels Normalized
4
3
2
1
0
Vector
Gal-Cdc5
D.
i)
WT S10,11A
30kDa
25kDa
pS8
30kDa
25kDa
Sec4p
ii)
Relative pS8 Signal
1.0
0.8
0.6
0.4
0.2
0.0
WT S10,11A
E.
Peptide
Cdc5p
pS8 - unmod unmod pS11 pS11
- + - + - +

cellular processes including, but not limited to, progression of cytokinesis via recruitment of Rho1p, timely mitotic exit, nuclear shape during mitosis, and Cdc14p release during anaphase (Botchkarev et al., 2014; Walters et al., 2014; Yoshida et al., 2006). Cdc5p was also identified in the landmark cell division cycle screen, thus a temperature sensitive allele is available for further study (Hartwell et al., 1973). Using the *cdc5*^{ts} allele, we sought to determine if Cdc5p activity was required for Sec4p phosphorylation. Indeed, at the restrictive temperature, Sec4p phosphorylation was almost completely ablated in the *cdc5*^{ts} strain (figure 2.9B). Additionally, there does appear to be a slight decrease in pS8 levels even at the permissive temperature, consistent with a partially impaired Cdc5p protein.

Ranking kinases from greatest to least increase in Sec4p phosphorylation, Cdc5p was the 9th highest kinase, doubling pS8 levels relative to total Sec4p. However, Cdc5p's activity is regulated by localization and degradation throughout different stages of the cell cycle, and we felt that the observed increase in Sec4p phosphorylation from the screen could be significantly improved upon. Additionally, overexpression of Cdc5p has been shown to be toxic to cells, thus there may be selective pressure to keep the plasmid copy number lower to reduce Cdc5p expression (Sopko et al., 2006). We put Cdc5p expression under the control of a GAL4 promoter to transiently, but substantially increase Cdc5p expression. Indeed, upon induction of Cdc5p expression with galactose, we observed a significant increase in Sec4p phosphorylation that was greater than that observed from the screen (figure 2.9C).

The activity of Cdc5p is regulated by its spatial and temporal sub-cellular localization throughout cell-cycle progression (Cheng et al., 1998; Park et al., 2004). Cdc5p protein levels are controlled in an APC dependent way, peaking in S/G2 and being actively degraded in G1 (Visintin et al., 2008). Furthermore, Cdc5p is targeted to its substrates via a polo-box domain

(PBD) through recognition of a core S-pS/pT-P/X phospho-peptide motif (Elia et al., 2003; Song et al., 2000). Examination of the mass-spectrometry data confirmed phosphorylation sites on Sec4p reveals a hypothetical core PBD recognition site in the NH_2 terminus of Sec4p (figure 2.1A). Disruption of this hypothetical PBD recognition motif via alanine mutagenesis (S10, 11A) shows a dramatic decrease in Sec4p phosphorylation (figure 2.9D). Additionally, based on the characterization of the pS8 antibody, we are confident that mutagenesis of S10 and S11 does affect substrate recognition.

In order to show that Cdc5p directly modifies Sec4p, Cdc5p was purified from *S. cerevisiae* and used for *in vitro* kinase assays with $Sec4p^{3-14}$ peptides as substrates. Peptides were analyzed for modifications via a dot-blot and subsequent probing with the pS8 antibody. Cdc5p was able to directly modify Sec4p peptide substrates (figure 2.9E). The addition of a phosphate on S11 to mimic the hypothetical polo-box binding phospho-peptide did not affect the final total of phosphorylated Sec4p as compared to an un-modified Sec4p peptide; however, the rates of phosphorylation were not addressed in this study.

Cdc5p over-expression toxicity is not rescued by an unphosphorylatable Sec4p

Since Cdc5p activity is required for Sec4p phosphorylation and over-expression of Cdc5p is both toxic and increases Sec4p phosphorylation, we wondered whether an unphosphorylatable Sec4p mutant could rescue this phenotype. To answer this question, we created multiple yeast strains with various Sec4p unphosphorylatable mutants and partial phosphomimetics, and induced Cdc5p overexpression using a controllable Gal4 promoter (figure 2.10). We found that Cdc5p over-expression is indeed toxic to cells, relative to a vector only control, but no Sec4p mutant was able to rescue or exacerbate this phenotype. As previously mentioned, Cdc5p is

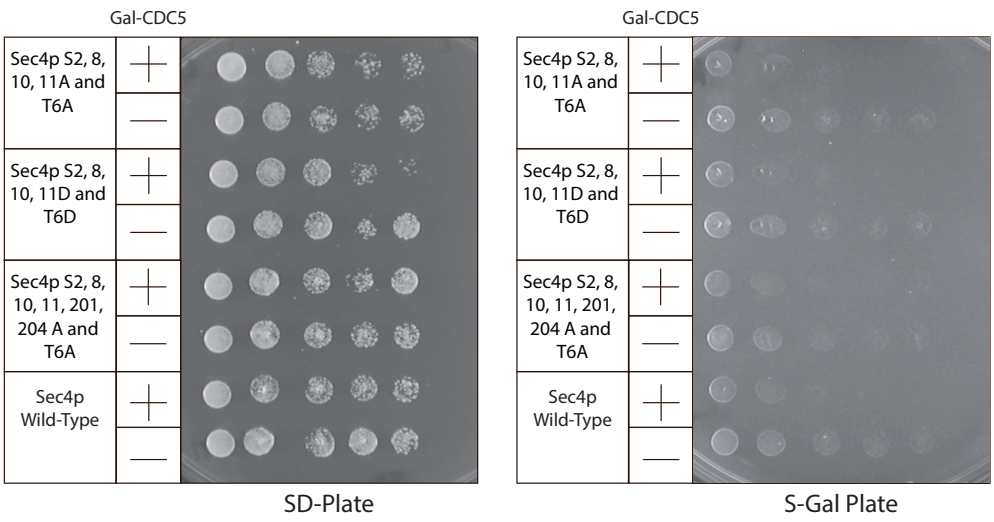

Figure 2.10: Cdc5p over-expression is toxic to cells

Dilution and spot test of yeast strains expressing different phospho-mimetic or unphosphorylatable mutants of Sec4p on SD plates or on S-Gal (2% galactose as the sole carbon source) plates in the presence or absence of a galactose driven Cdc5p over-expression plasmid.

known to control many different cellular processes, so it is likely that the toxicity observed is a combination of many different proteins/pathways being affected, not just Sec4p.

Sec4p phosphorylation is a dynamic cell-cycle sensitive modification

To determine the physiological relevance of phosphorylation of Sec4p by Cdc5p, we examined the spatial and temporal localization of Cdc5p. Both Cdc5p and Sec4p change subcellular localization throughout the cell cycle, with Sec4p localizing to the bud-tip, the periphery of the growing bud, and to the bud neck for cytokinesis and Cdc5p localizing to the nucleus, spindle-pole bodies, and site of cytokinesis (Song et al., 2000). Using a GFP-tagged Sec4p and a 3x-mCherry-tagged Cdc5p, we examined the localization of both proteins at various stages of cell cycle (figure 2.11A). Early budded cells in G1 show Sec4p at the tip of the growing bud, while Cdc5p is either not visible or appears to be in the vacuole, consistent with Cdc5p being actively degraded. In S/G2, Cdc5p becomes localized to the nucleus or spindle pole bodies, while Sec4p is more distributed throughout the daughter cell for isotropic growth. During late M-phase or cytokinesis, we find that Sec4p and Cdc5p co-localize at the bud neck. Not only does this show that Cdc5p is in a position to phosphorylate Sec4p *in vivo*, but it also suggests that Sec4p is phosphorylated at a specific time point in the mitotic cell cycle.

To confirm whether or not Sec4p phosphorylation is a cell-cycle dependent modification, we performed cell synchrony and release experiments via two independent methods; the mating pheromone α-factor to halt cells in G1, and the microtubule de-polymerizing agent nocodazole to halt cells in metaphase. In both cases, Sec4p phosphorylation was found to be a highly dynamic process, and only showing pS8 phosphorylation for around 30 minutes per each cell cycle (figure 2.11). The localization of Sec4p during synchrony and release experiments was monitored by GFP-tagged Sec4p (nocodazole release) and immunofluorescence (alpha-factor release) and, in

Figure 2.11: Sec4p phosphorylation peaks during co-localization of Sec4p and Cdc5p during cytokinesis

A. Microscopy of GFP-Sec4p and Cdc5p-3xmCherry at various stages of cell cycle based on bud size and Sec4p localization.

B. i) Nocodazole synchrony and release of GFP-Sec4p expressing cells. Approximately 100 cells were counted for each time point and Sec4p localization was categorized to either bud tip, bud neck, or diffuse localization. The graph shows the percentage of each category of Sec4p localization status at each time point. ii) Nocodazole synchrony and release for wild type cells, where cells were pelleted and frozen in liquid nitrogen for each time point.

C. i) Alpha-factor synchrony and release of *bar1Δ* cells. At each indicated time point, cells were fixed in 2% paraformaldehyde and Sec4p localization was imaged by immunofluorescence. Approximately 100 cells were counted for each time point and Sec4p localization was categorized to either bud tip, bud neck, or diffuse localization. The graph shows the percentage of each category of Sec4p localization status at each time point. ii) Cells were taken from the same culture and time points and frozen in liquid nitrogen for western blot analysis.

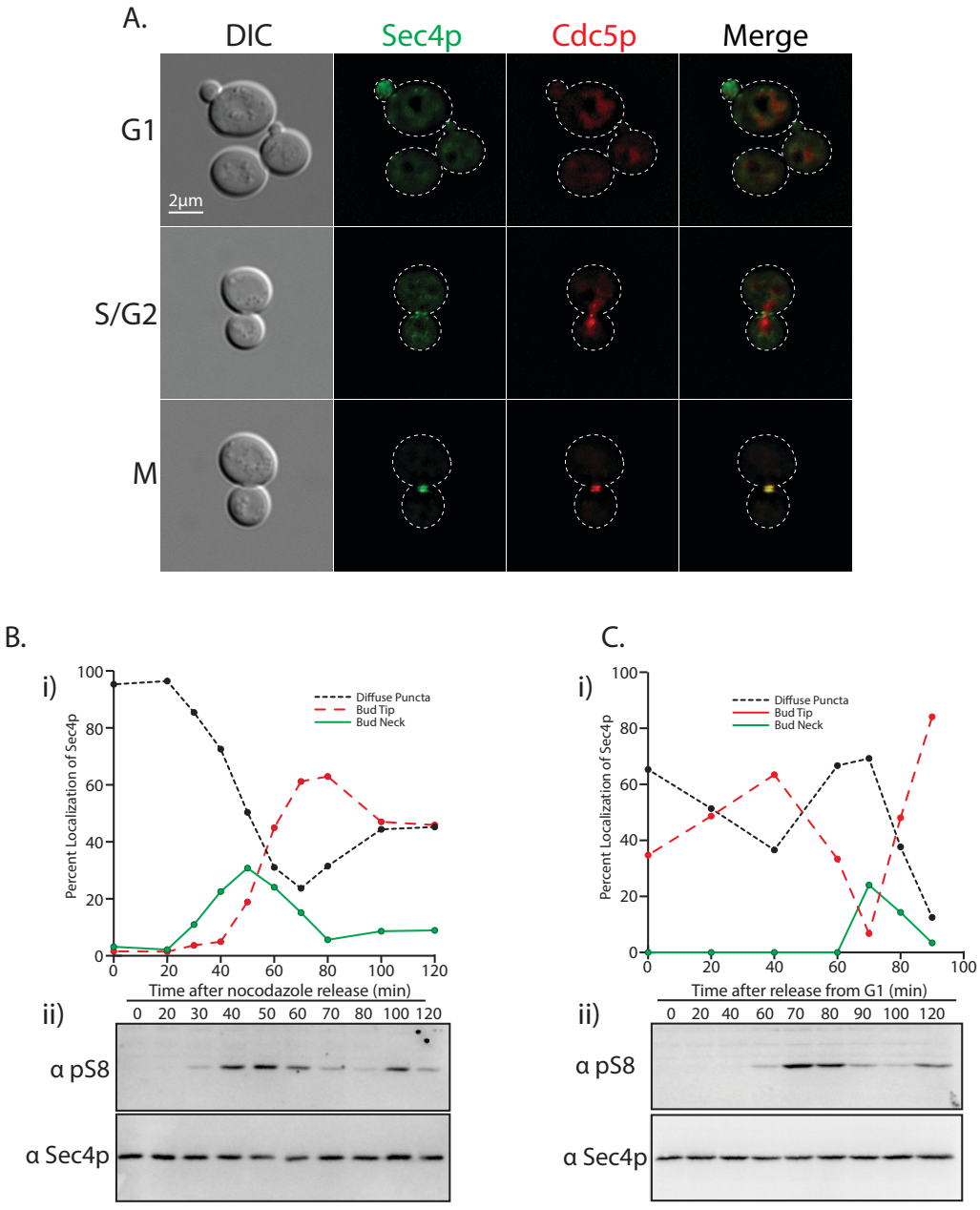
A.
DIC
Sec4p
Cdc5p
Merge
G1
S/G2
M
2µm
B.
i)
Percent Localization of Sec4p
Diffuse Puncta
Bud Tip
Bud Neck
Time after nocodazole release (min)
ii)
0 20 30 40 50 60 70 80 100 120
α pS8
α Sec4p
C.
i)
Percent Localization of Sec4p
Diffuse Puncta
Bud Tip
Bud Neck
Time after release from G1 (min)
ii)
0 20 40 60 70 80 90 100 120
α pS8
α Sec4p

both cases, the rise and fall of bud-neck localization of Sec4p corresponds with pS8 phosphorylation (figure 2.11B-C). These data show that phosphorylation of Sec4p in a cell cycle dependent manner and specifically when Sec4p is at the bud neck where it was previously shown to co-localize with Cdc5p.

Phosphorylation is not required for Sec4p localization changes during cell-cycle progression

The observation that phosphorylation of Sec4p only occurs during a specific spatial and temporal location begs the question as to whether phosphorylation is responsible for this localization change or if it is a result of the localization change. To answer this question, we investigated the localization of a GFP-Sec4p^{Ala} compared to a GFP-Sec4p^{WT} as the sole copies of the protein after a nocodazole synchrony and release experiment (figure 2.12). We found that either version of Sec4p was able to efficiently move to the bud neck, bud tip, or to the periphery of the growing bud. This suggests that phosphorylation is a result of Sec4p co-localizing with Cdc5p at the bud neck, rather than being responsible for this localization change. As such, phosphorylation is likely controlling Sec4p's activity after arrival at the bud neck.

Sec4p phosphorylation is induced upon cytokinetic defects and regulates cell size.

To explore the function of Sec4p phosphorylation in relation to cytokinesis, we investigated the effects of cytokinetic defects on Sec4p phosphorylation. We hypothesized that Sec4p phosphorylation may act as a checkpoint to regulate timely cytokinesis and provide a mechanism to link cellular growth with cytokinesis. To induce cytokinetic defects, we used *myo1Δ* and *hof1Δ* cell lines, which have been shown to be defective in cell separation, but still viable (Korinek et al., 2000; Lippincott and Li, 1998; Watts et al., 1987). Myo1p is a type II myosin heavy chain, and localizes to the actomyosin ring for cell separation, while Hof1p regulates the

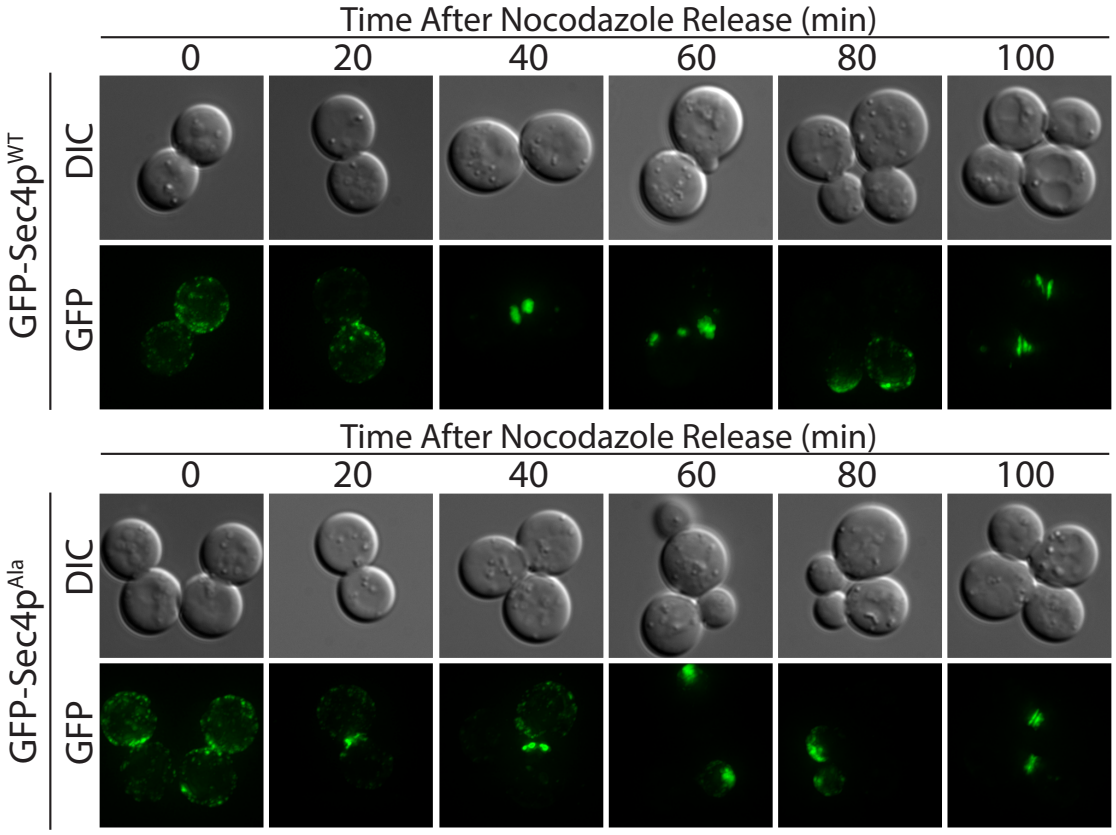

Figure 2.12: Microscopy of GFP-Sec4p and GFP-Sec4p^{Ala} after release from nocodazole

Microscopy of GFP-Sec4^{WT} and GFP-Sec4p^{Ala} as the sole copy of Sec4p at various time points after release from nocodazole block.

actin cytoskeleton and the formin Bnr1p (Oh et al., 2013). Hof1p is a known Cdc5p substrate (Meitinger et al., 2011). *Hof1Δ* cells also have enlarged cell size and defects in apical growth (Graziano et al., 2014). We found that in *hof1Δ* cells, but not *myo1Δ* cells, there is a very large increase in Sec4p phosphorylation (figure 2.13A,B). Furthermore, Sec4p localization in a *hof1Δ* cell line is in agreement with Graziano et al., and bud neck localization can be seen in groups of cells that have not completed budding (figure 2.13C). Since phosphorylation was increased in the *hof1Δ* background, we next investigated the effects of removing Sec4p phosphorylation. However, new phosphorylation sites on Sec4p have been discovered since the beginning of this work on S2 and T6 (Sadowski et al., 2013). Therefore, we created a mutant Sec4p with positions S2, 8, 10, 11, 201, 204, and T6 all converted to alanine residues, and refer to this mutant as Sec4p^{A7}. When we expressed this Sec4p^{A7} as the sole copy of Sec4p in *hof1Δ*, we saw that cells were significantly smaller, thus partially rescuing the *hof1Δ* phenotype although the cytokinetic defects remain (figure 2.13D). Additionally, in a wild-type genetic background, expressing Sec4p^{A7} as the sole copy, we also observed that cells were significantly smaller (figure 2.13E). These results suggest that Sec4p phosphorylation may be a mechanism to coordinate cell growth/size with cytokinesis.

Conclusion/Discussion

Sec4p phosphorylation had previously been characterized to negatively regulate function, however the signaling pathways involved, molecular mechanism by which function is disrupted, the dynamics of these modifications, and kinase/s involved were unclear (Heger et al., 2011). In this chapter, we demonstrate that Sec4p phosphorylation is a dynamic modification and is sensitive to nutrient availability. Nutrient starvation elicits numerous cellular responses, including halting cells in G1 (Barbet et al., 1996; Rohde et al., 2001), and here we show that it

Figure 2.13: Sec4p phosphorylation is stimulated upon cytokinetic stress and is required for proper cell size maintenance

A. Sec4p phosphorylation status in *myo1*Δ strain compared to wild-type. Total Sec4p and Pgk1p were also probed for loading controls. Quantification of 3 independent measurements are illustrated in a bar graph. Error bars are standard deviation and samples were normalized to the ratio of pS8 levels over total Sec4p levels.

B. Sec4p phosphorylation status in *hof1*Δ strain compared to wild-type. Total Sec4p and Pgk1p were also probed for loading controls. Quantification of 3 independent measurements are illustrated in a bar graph. Error bars are standard deviation.

C. Microscopy of GFP-Sec4p in a *hof1*Δ background.

D. DIC microscopy of *hof1*Δ cells expressing wild-type Sec4p and Sec4p^{A7}.

E. Quantification of cell size using 150 cells for each strain. Cell size was measured using ImageJ to take the area of the mother cell exclusively, as the size of the bud is more indicative of position within the cell-cycle as opposed to overall cell size. Error bars are standard error and significance was calculation using a two-tailed students T-test.

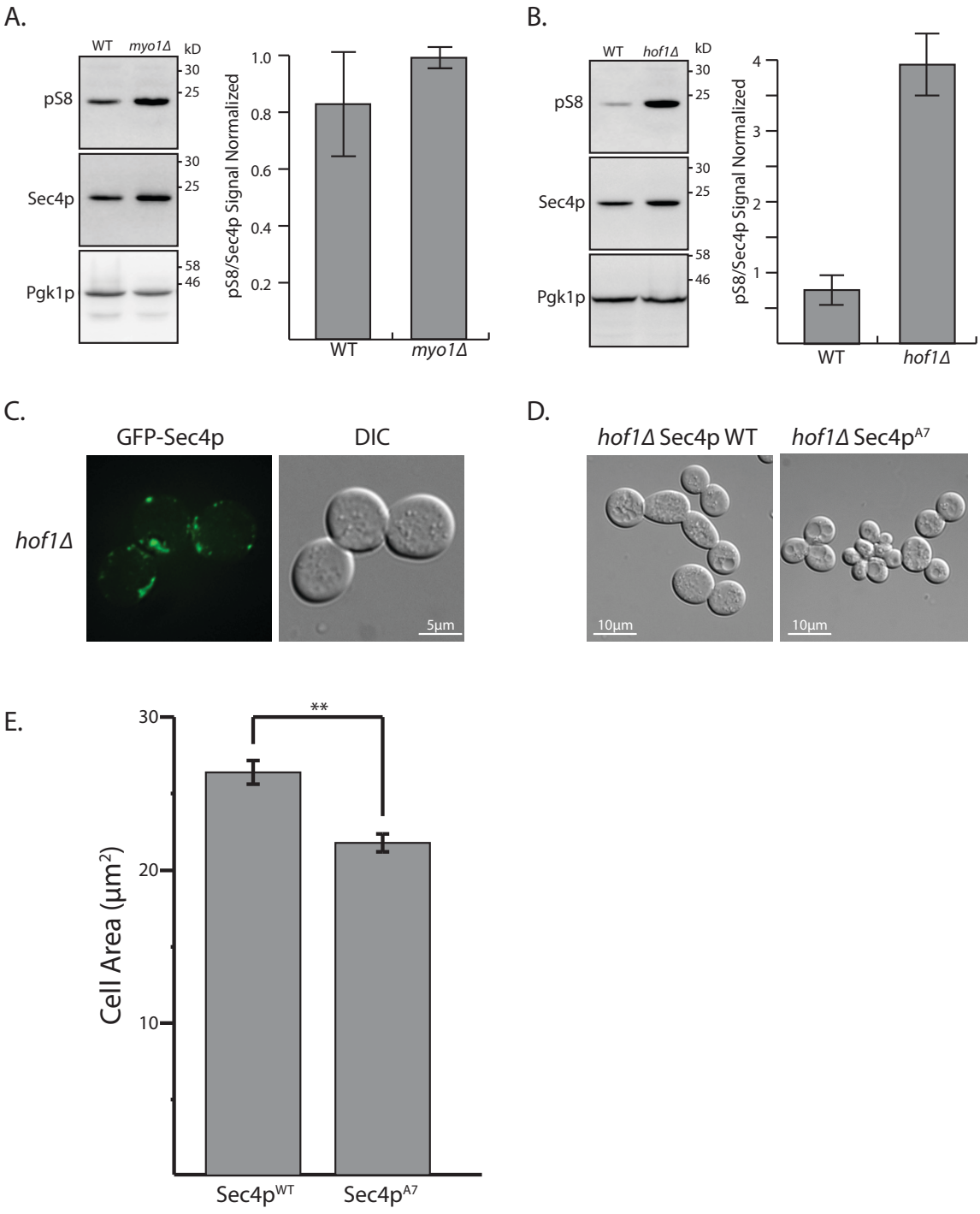
A.
WT
myo1Δ
kD
pS8
Sec4p
Pgk1p
30
25
58
46
pS8/Sec4p Signal Normalized
1.0
0.8
0.6
0.4
0.2
WT
myo1Δ
B.
hof1Δ
4
3
2
1
C.
GFP-Sec4p
DIC
hof1Δ
5μm
D.
hof1Δ Sec4p WT
hof1Δ Sec4p^A7
10μm
E.
**
Cell Area (μm^2)
30
20
10
Sec4p^WT
Sec4p^A7

also negatively affects Sec4p phosphorylation. Further investigation revealed that Sec4p phosphorylation is a cell-cycle dependent modification that peaks during late M phase, specifically cytokinesis, and is removed during G1, suggesting that data showing lack of phosphorylation during nutrient starvation is primarily a function of cell cycle arrest. Additionally, a genomic kinase screen identified several mitotic cell-cycle kinases that significantly increased Sec4p phosphorylation when overexpressed, further supporting the idea that Sec4p phosphorylation is controlled by cell-cycle progression.

The molecular mechanism by which phosphorylation negatively affects function appears to be via disrupting the interaction between Sec4p and the Exocyst complex via Sec15p. Indeed, phosphorylation is enriched on the membrane bound pool of Sec4p relative to the cytosolic fraction and is in a physiologically relevant location to modulate the interaction between Sec4p and the exocyst complex. Temperature sensitive phosphomimetic Sec4p accumulates on vesicles that build-up inside the cell, which is a phenotype similar to that observed in Sec15p temperature sensitive mutants (Salminen and Novick, 1989). Furthermore, biochemical analysis of a full phosphomimetic shows reduced affinity for Sec15p relative to the wild type and the complimentary alanine mutant. It is important to note that detection of phosphorylated Sec4p in this study was measured using pS8 as a marker, however the phosphomimetic mutant has five sites mutated. It is possible that additional intermediate species of phosphorylated Sec4p exist and have specific functions, but in this study, we were unable to observe multiple differentially phosphorylated isoforms.

We also identified Cdc5p as a potential Sec4p kinase via a kinase overexpression screen and further demonstrated that Cdc5p activity is responsible for Sec4p phosphorylation and Cdc5p is capable of directly modifying Sec4p *in vitro*. Additionally, the spatial and temporal co-

localization of Cdc5p and Sec4p corresponds to the rise of Sec4p phosphorylation during cytokinesis, and loss of phosphorylation correlates with the degradation of Cdc5p and Sec4p localization change to the newly forming bud tip. Additionally, phosphorylation is not required for the localization of Sec4p to the bud neck, suggesting phosphorylation is a result of the localization change.

The phosphatase required for removing Sec4p phosphorylation still remains to be confirmed. Previous work suggests that PP2A in complex with Cdc55p is a Sec4p phosphatase (Heger et al., 2011), however we found that *cdc55Δ* cells did not have any changes in Sec4p phosphorylation levels (figure 2.14). This result however does not definitely exclude PP2A and Cdc55p from being the phosphatase, especially considering that *cdc55Δ* cells have elongated buds due to excessive polarized exocytosis (Healy et al., 1991). This would cause Sec4p to have decreased bud neck localization, which could offset any expected rise Sec4p phosphorylation due to a lack of Cdc55p.

Several interesting possibilities suggest themselves to understand the physiological role of Sec4p phosphorylation at the bud neck during cytokinesis. In animal cells, there is a specific requirement for the exocyst complex during cytokinesis (Neto et al., 2013), and this complex also participates in membrane delivery at the site of division in *S. cerevisiae* (Heider and Munson, 2012; Novick et al., 2006). In animal cells, the exocyst provides a link between cell surface delivery and retrieval and represents an ideal nexus for the integration of different physiological signals (Bodemann et al., 2011; Lipschutz et al., 2000; Wiederkehr et al., 2003), some of which are already know to be subject to phosphorylation control (Mace et al., 2005). We show that cell cycle dependent phosphorylation of Sec4p reduces the affinity for the exocyst component Sec15p, and thus provides an intervention point for the integration of post-Golgi

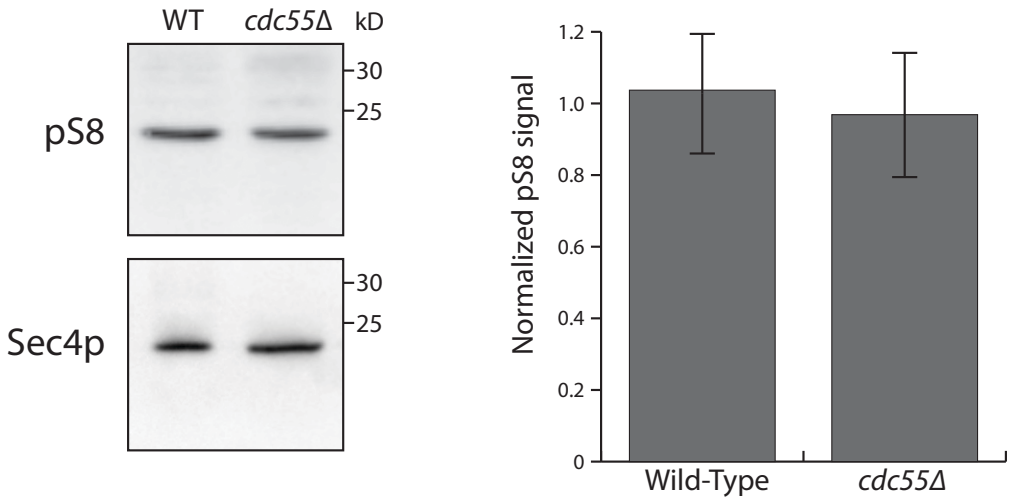

Figure 2.14: pS8 levels in *cdc55*Δ genetic background

Western blot analysis of pS8 and Sec4p levels in wild-type and *cdc55*Δ cells. Bar graph shows average measurements of three independent samples. Error bars are standard deviation (n=3).

vesicle traffic and membrane tethering with cytokinesis (figure 2.15). Additionally, Cdc42p, which (like Sec4p) preferentially interacts with the exocyst complex in its GTP-bound state (Wu et al., 2010), is inhibited in a Cdc5p dependent mechanism during mitotic exit (Atkins et al., 2013). Cdc42p interacts with exocyst subunit Exo70p when Cdc42p is directly associated with the plasma membrane. The Cdc5p dependent inhibition of Cdc42p was also shown to be important for proper cytokinesis, and would affect the ability of the exocyst to tether vesicles to the plasma membrane. General disruptions to membrane trafficking, particularly endocytosis, have been noted to occur during mitosis (Fielding et al., 2012; Warren et al., 1984). Additionally, phosphorylation of the exocyst component Exo84 by Cdc28p has been shown to cause dissociation of the exocyst complex (Luo et al., 2013). Exo84 phosphorylation occurs as early as metaphase, whereas Sec4p phosphorylation was found to occur after release from metaphase, suggesting that Exo84 phosphorylation to inhibit cell growth happens slightly before Sec4p phosphorylation. Furthermore, Cdc28p, which phosphorylates Exo84p, also phosphorylates Cdc5p leading to its activation and may link Sec4p and Exo84p phosphorylation (Simpson-Lavy and Brandeis, 2011).

Rab phosphorylation in general may provide a mechanism to halt membrane trafficking during mitosis. Indeed, Rab1 and Rab4 have previously been shown to be preferentially phosphorylated during mitosis (Bailly et al., 1991). Further work to characterize the phosphorylation status of other Rab proteins is needed to address the true functional significance of Rab phosphorylation during mitosis and to demonstrate such modifications represent a regulatory mechanism by which cell-cycle signaling pathways can impinge upon critical membrane trafficking pathways that remodel cell shape and size.

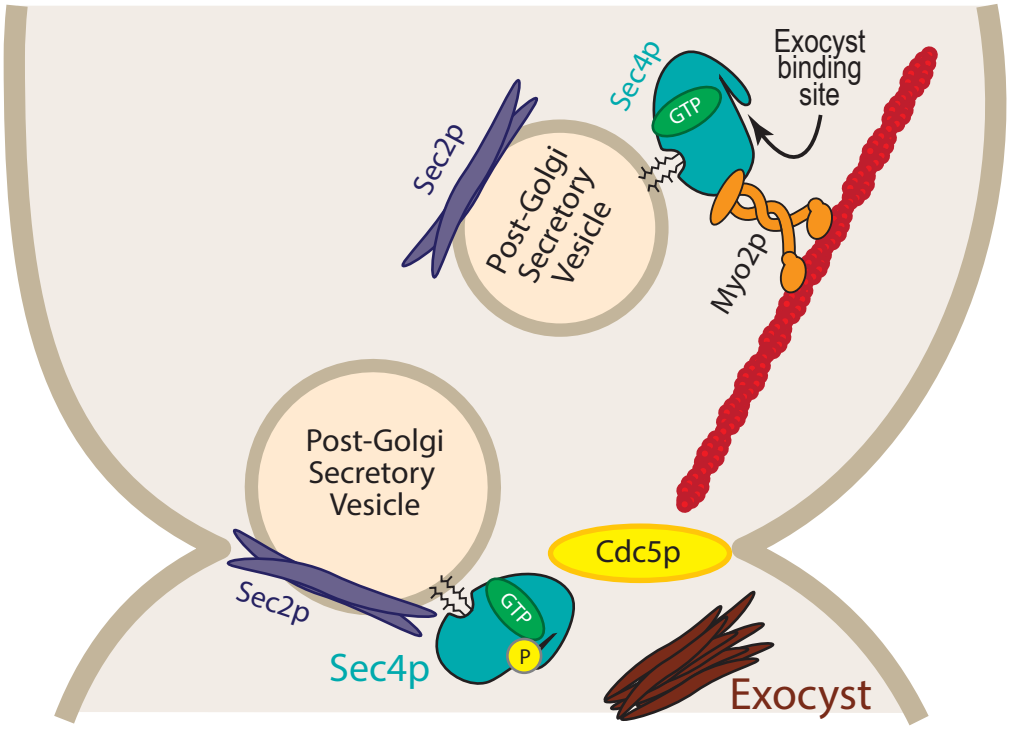

Figure 2.15: Cartoon model for Sec4p phosphorylation by Cdc5p during cytokinesis

As the cell prepares for cytokinesis at the end of mitosis, Cdc5p kinase phosphorylates Sec4p on secretory vesicles at the side of future cell division. This phosphorylation event will block interaction with Sec15p, the downstream effector and halt the addition of new plasma membrane at this location. Plasma membrane traffic is not halted at other locations so the cells can continue to enlarge during this period. As cytokinesis progresses, Sec4p dephosphorylation will facilitate exocyst function and allow the cells to form the new plasma membrane at the site of cytokinesis.

References

Atkins, B.D., S. Yoshida, K. Saito, C.F. Wu, D.J. Lew, and D. Pellman. 2013. Inhibition of Cdc42 during mitotic exit is required for cytokinesis. *J Cell Biol*. 202:231-240.

Bailly, E., M. McCaffrey, N. Touchot, A. Zahraoui, B. Goud, and M. Bornens. 1991. Phosphorylation of two small GTP-binding proteins of the Rab family by p34cdc2. *Nature*. 350:715-718.

Bao, Y., J.A. Lopez, D.E. James, and W. Hunziker. 2007. Snapin interacts with the Exo70 subunit of the exocyst and modulates GLUT4 trafficking. *J. Biol. Chem*. 283:324-331.

Barbet, N.C., U. Schneider, S.B. Helliwell, I. Stansfield, M.F. Tuite, and M.N. Hall. 1996. TOR controls translation initiation and early G1 progression in yeast. *Mol Biol Cell*. 7:25-42.

Blankenship, J.T., M.T. Fuller, and J.A. Zallen. 2007. The Drosophila homolog of the Exo84 exocyst subunit promotes apical epithelial identity. *J Cell Sci*. 120:3099-3110.

Bodemann, B.O., A. Orvedahl, T. Cheng, R.R. Ram, Y.H. Ou, E. Formstecher, M. Maiti, C.C. Hazelett, E.M. Wauson, M. Balakireva, J.H. Camonis, C. Yeaman, B. Levine, and M.A. White. 2011. RalB and the exocyst mediate the cellular starvation response by direct activation of autophagosome assembly. *Cell*. 144:253-267.

Botchkarev, V.V., Jr., V. Rossio, and S. Yoshida. 2014. The budding yeast Polo-like kinase Cdc5 is released from the nucleus during anaphase for timely mitotic exit. *Cell Cycle*. 13:3260-3270.

Cardenas, M.E., N.S. Cutler, M.C. Lorenz, C.J. Di Como, and J. Heitman. 1999. The TOR signaling cascade regulates gene expression in response to nutrients. *Genes Dev*. 13:3271-3279.

Chang, L., S.H. Chiang, and A.R. Saltiel. 2004. Insulin signaling and the regulation of glucose transport. *Mol Med*. 10:65-71.

Cheng, L., L. Hunke, and C.F. Hardy. 1998. Cell cycle regulation of the Saccharomyces cerevisiae polo-like kinase cdc5p. *Mol Cell Biol*. 18:7360-7370.

Chien, Y., S. Kim, R. Bumeister, Y.M. Loo, S.W. Kwon, C.L. Johnson, M.G. Balakireva, Y. Romeo, L. Kopelovich, M. Gale, Jr., C. Yeaman, J.H. Camonis, Y. Zhao, and M.A. White. 2006. RalB GTPase-

mediated activation of the IkappaB family kinase TBK1 couples innate immune signaling to tumor cell survival. *Cell*. 127:157-170.

Collins, R.N. 2005. Application of phylogenetic algorithms to assess Rab functional relationships. *Methods Enzymol*. 403:19-28.

Elia, A.E., L.C. Cantley, and M.B. Yaffe. 2003. Proteomic screen finds pSer/pThr-binding domain localizing Plk1 to mitotic substrates. *Science*. 299:1228-1231.

Ficarro, S.B., M.L. McCleland, P.T. Stukenberg, D.J. Burke, M.M. Ross, J. Shabanowitz, D.F. Hunt, and F.M. White. 2002. Phosphoproteome analysis by mass spectrometry and its application to Saccharomyces cerevisiae. *Nat. Biotechnol*. 20:301-305.

Fielding, A.B., A.K. Willox, E. Okeke, and S.J. Royle. 2012. Clathrin-mediated endocytosis is inhibited during mitosis. *Proc Natl Acad Sci U S A*. 109:6572-6577.

Gancedo, J.M. 1998. Yeast carbon catabolite repression. *Microbiol Mol Biol Rev*. 62:334-361.

Geng, J., U. Nair, K. Yasumura-Yorimitsu, and D.J. Klionsky. 2010. Post-Golgi Sec proteins are required for autophagy in Saccharomyces cerevisiae. *Mol Biol Cell*. 21:2257-2269.

Goehring, A.S., B.S. Pedroja, S.A. Hinke, L.K. Langeberg, and J.D. Scott. 2007. MyRIP Anchors Protein Kinase A to the Exocyst Complex. *J Biol Chem*. 282:33155-33167.

Goud, B., A. Salminen, N.C. Walworth, and P.J. Novick. 1988. A GTP-binding protein required for secretion rapidly associates with secretory vesicles and the plasma membrane in yeast. *Cell*. 53:753-768.

Graziano, B.R., H.Y. Yu, S.L. Alioto, J.A. Eskin, C.A. Ydenberg, D.P. Waterman, M. Garabedian, and B.L. Goode. 2014. The F-BAR protein Hof1 tunes formin activity to sculpt actin cables during polarized growth. *Mol Biol Cell*. 25:1730-1743.

Gromley, A., C. Yeaman, J. Rosa, S. Redick, C.T. Chen, S. Mirabelle, M. Guha, J. Sillibourne, and S.J. Doxsey. 2005. Centriolin anchoring of exocyst and SNARE complexes at the midbody is required for secretory-vesicle-mediated abscission. *Cell*. 123:75-87.

Grosshans, B.L., and P. Novick. 2008. Identification and verification of Sro7p as an effector of the Sec4p Rab GTPase. *Methods Enzymol*. 438:95-108.

Guo, W., D. Roth, C. Walch-Solimena, and P. Novick. 1999. The exocyst is an effector for Sec4p, targeting secretory vesicles to sites of exocytosis. *Embo J*. 18:1071-1080.

Hartwell, L.H., R.K. Mortimer, J. Culotti, and M. Culotti. 1973. Genetic Control of the Cell Division Cycle in Yeast: V. Genetic Analysis of cdc Mutants. *Genetics*. 74:267-286.

He, B., F. Xi, X. Zhang, J. Zhang, and W. Guo. 2007. Exo70 interacts with phospholipids and mediates the targeting of the exocyst to the plasma membrane. *Embo J*. 26:4053-4065.

Healy, A.M., S. Zolnierowicz, A.E. Stapleton, M. Goebl, A.A. DePaoli-Roach, and J.R. Pringle. 1991. CDC55, a Saccharomyces cerevisiae gene involved in cellular morphogenesis: identification, characterization, and homology to the B subunit of mammalian type 2A protein phosphatase. *Mol Cell Biol*. 11:5767-5780.

Heger, C.D., C.D. Wrann, and R.N. Collins. 2011. Phosphorylation provides a negative mode of regulation for the yeast Rab GTPase Sec4p. *PLoS One*. 6:e24332.

Heider, M.R., and M. Munson. 2012. Exorcising the exocyst complex. *Traffic*. 13:898-907.

Herman, P.K., J.H. Stack, J.A. DeModena, and S.D. Emr. 1991. A novel protein kinase homolog essential for protein sorting to the yeast lysosome-like vacuole. *Cell*. 64:425-437.

Hornbeck, P.V., B. Zhang, B. Murray, J.M. Kornhauser, V. Latham, and E. Skrzypek. 2015. PhosphoSitePlus, 2014: mutations, PTMs and recalibrations. *Nucleic Acids Res*. 43:D512-520.

Hutagalung, A.H., and P.J. Novick. 2011. Role of Rab GTPases in membrane traffic and cell physiology. *Physiol Rev*. 91:119-149.

Jahn, R., and R.H. Scheller. 2006. SNAREs--engines for membrane fusion. *Nat Rev Mol Cell Biol*. 7:631-643.

Jiang, L., S.L. Rogers, and S.T. Crews. 2007. The Drosophila Dead end Arf-like3 GTPase controls vesicle trafficking during tracheal fusion cell morphogenesis. *Dev Biol*.

Jin, Y., A. Sultana, P. Gandhi, E. Franklin, S. Hamamoto, A.R. Khan, M. Munson, R. Schekman, and L.S. Weisman. 2011. Myosin V transports secretory vesicles via a Rab GTPase cascade and interaction with the exocyst complex. *Dev Cell*. 21:1156-1170.

Kamada, Y., T. Funakoshi, T. Shintani, K. Nagano, M. Ohsumi, and Y. Ohsumi. 2000. Tor-mediated induction of autophagy via an Apg1 protein kinase complex. *J Cell Biol*. 150:1507-1513.

Kim, J., W.P. Huang, P.E. Stromhaug, and D.J. Klionsky. 2002. Convergence of multiple autophagy and cytoplasm to vacuole targeting components to a perivacuolar membrane compartment prior to de novo vesicle formation. *J Biol Chem*. 277:763-773.

Klionsky, D.J. 2011. For the last time, it is GFP-Atg8, not Atg8-GFP (and the same goes for LC3). *Autophagy*. 7:1093-1094.

Klionsky, D.J., A.M. Cuervo, and P.O. Seglen. 2007. Methods for monitoring autophagy from yeast to human. *Autophagy*. 3:181-206.

Korinek, W.S., E. Bi, J.A. Epp, L. Wang, J. Ho, and J. Chant. 2000. Cyk3, a novel SH3-domain protein, affects cytokinesis in yeast. *Curr Biol*. 10:947-950.

Lippincott, J., and R. Li. 1998. Dual function of Cyk2, a cdc15/PSTPIP family protein, in regulating actomyosin ring dynamics and septin distribution. *J Cell Biol*. 143:1947-1960.

Lipschutz, J.H., W. Guo, L.E. O'Brien, Y.H. Nguyen, P. Novick, and K.E. Mostov. 2000. Exocyst is involved in cystogenesis and tubulogenesis and acts by modulating synthesis and delivery of basolateral plasma membrane and secretory proteins. *Mol Biol Cell*. 11:4259-4275.

Luo, G., J. Zhang, F.C. Luca, and W. Guo. 2013. Mitotic phosphorylation of Exo84 disrupts exocyst assembly and arrests cell growth. *J Cell Biol*. 202:97-111.

Mace, G., M. Miaczynska, M. Zerial, and A.R. Nebreda. 2005. Phosphorylation of EEA1 by p38 MAP kinase regulates mu opioid receptor endocytosis. *EMBO J*. 24:3235-3246.

Meitinger, F., M.E. Boehm, A. Hofmann, B. Hub, H. Zentgraf, W.D. Lehmann, and G. Pereira. 2011. Phosphorylation-dependent regulation of the F-BAR protein Hof1 during cytokinesis. *Genes Dev*. 25:875-888.

Mizuno-Yamasaki, E., M. Medkova, J. Coleman, and P. Novick. 2010. Phosphatidylinositol 4-phosphate controls both membrane recruitment and a regulatory switch of the Rab GEF Sec2p. *Dev Cell*. 18:828-840.

Mizushima, N., and M. Komatsu. 2011. Autophagy: renovation of cells and tissues. *Cell*. 147:728-741.

Munson, M., X. Chen, A.E. Cocina, S.M. Schultz, and F.M. Hughson. 2000. Interactions within the yeast t-SNARE Sso1p that control SNARE complex assembly. *Nat Struct Biol*. 7:894-902.

Munson, M., and F.M. Hughson. 2002. Conformational regulation of SNARE assembly and disassembly in vivo. *J Biol Chem*. 277:9375-9381.

Nejsum, L.N., and W.J. Nelson. 2007. A molecular mechanism directly linking E-cadherin adhesion to initiation of epithelial cell surface polarity. *J Cell Biol*. 178:323-335.

Neto, H., G. Balmer, and G. Gould. 2013. Exocyst proteins in cytokinesis: Regulation by Rab11. *Commun Integr Biol*. 6:e27635.

Novick, P., and P. Brennwald. 1993. Friends and family: the role of the Rab GTPases in vesicular traffic. *Cell*. 75:597-601.

Novick, P., S. Ferro, and R. Schekman. 1981. Order of events in the yeast secretory pathway. *Cell*. 25:461-469.

Novick, P., C. Field, and R. Schekman. 1980. Identification of 23 complementation groups required for post-translational events in the yeast secretory pathway. *Cell*. 21:205-215.

Novick, P., M. Medkova, G. Dong, A. Hutagalung, K. Reinisch, and B. Grosshans. 2006. Interactions between Rabs, tethers, SNAREs and their regulators in exocytosis. *Biochem Soc Trans*. 34:683-686.

Oh, Y., J. Schreiter, R. Nishihama, C. Wloka, and E. Bi. 2013. Targeting and functional mechanisms of the cytokinesis-related F-BAR protein Hof1 during the cell cycle. *Mol Biol Cell*. 24:1305-1320.

Ortiz, D., M. Medkova, C. Walch-Solimena, and P. Novick. 2002. Ypt32 recruits the Sec4p guanine nucleotide exchange factor, Sec2p, to secretory vesicles; evidence for a Rab cascade in yeast. *J Cell Biol*. 157:1005-1015.

Park, J.E., C.J. Park, K. Sakchaisri, T. Karpova, S. Asano, J. McNally, Y. Sunwoo, S.H. Leem, and K.S. Lee. 2004. Novel functional dissection of the localization-specific roles of budding yeast polo kinase Cdc5p. *Mol Cell Biol*. 24:9873-9886.

Reggiori, F., and D.J. Klionsky. 2013. Autophagic processes in yeast: mechanism, machinery and regulation. *Genetics*. 194:341-361.

Rinaldi, F.C., M. Packer, and R. Collins. 2015. New insights into the molecular mechanism of the Rab GTPase Sec4p activation. *BMC Struct Biol*. 15:14.

Rohde, J., J. Heitman, and M.E. Cardenas. 2001. The TOR kinases link nutrient sensing to cell growth. *J Biol Chem*. 276:9583-9586.

Sadowski, I., B.J. Breitkreutz, C. Stark, T.C. Su, M. Dahabieh, S. Raithatha, W. Bernhard, R. Oughtred, K. Dolinski, K. Barreto, and M. Tyers. 2013. The PhosphoGRID Saccharomyces cerevisiae protein phosphorylation site database: version 2.0 update. *Database (Oxford)*. 2013:bat026.

Salminen, A., and P.J. Novick. 1987. A ras-like protein is required for a post-Golgi event in yeast secretion. *Cell*. 49:527-538.

Salminen, A., and P.J. Novick. 1989. The Sec15 protein responds to the function of the GTP binding protein, Sec4, to control vesicular traffic in yeast. *J Cell Biol*. 109:1023-1036.

Simpson-Lavy, K.J., and M. Brandeis. 2011. Phosphorylation of Cdc5 regulates its accumulation. *Cell Div*. 6:23.

Song, S., T.Z. Grenfell, S. Garfield, R.L. Erikson, and K.S. Lee. 2000. Essential function of the polo box of Cdc5 in subcellular localization and induction of cytokinetic structures. *Mol Cell Biol*. 20:286-298.

Sopko, R., D. Huang, N. Preston, G. Chua, B. Papp, K. Kafadar, M. Snyder, S.G. Oliver, M. Cyert, T.R. Hughes, C. Boone, and B. Andrews. 2006. Mapping pathways and phenotypes by systematic gene overexpression. *Mol Cell*. 21:319-330.

St-Pierre, J., M. Douziech, F. Bazile, M. Pascariu, E. Bonneil, V. Sauve, H. Ratsima, and D. D'Amours. 2009. Polo kinase regulates mitotic chromosome condensation by hyperactivation of condensin DNA supercoiling activity. *Mol Cell*. 34:416-426.

Stolz, A., A. Ernst, and I. Dikic. 2014. Cargo recognition and trafficking in selective autophagy. *Nat Cell Biol*. 16:495-501.

Stuart, L.M., J. Boulais, G.M. Charriere, E.J. Hennessy, S. Brunet, I. Jutras, G. Goyette, C. Rondeau, S. Letarte, H. Huang, P. Ye, F. Morales, C. Kocks, J.S. Bader, M. Desjardins, and R.A. Ezekowitz. 2007. A systems biology analysis of the Drosophila phagosome. *Nature*. 445:95-101.

Suzuki, K., T. Kirisako, Y. Kamada, N. Mizushima, T. Noda, and Y. Ohsumi. 2001. The pre-autophagosomal structure organized by concerted functions of APG genes is essential for autophagosome formation. *EMBO J*. 20:5971-5981.

Urban, J., A. Soulard, A. Huber, S. Lippman, D. Mukhopadhyay, O. Deloche, V. Wanke, D. Anrather, G. Ammerer, H. Riezman, J.R. Broach, C. De Virgilio, M.N. Hall, and R. Loewith. 2007. Sch9 is a major target of TORC1 in Saccharomyces cerevisiae. *Mol Cell*. 26:663-674.

Visintin, C., B.N. Tomson, R. Rahal, J. Paulson, M. Cohen, J. Taunton, A. Amon, and R. Visintin. 2008. APC/C-Cdh1-mediated degradation of the Polo kinase Cdc5 promotes the return of Cdc14 into the nucleolus. *Genes Dev*. 22:79-90.

Walters, A.D., C.K. May, E.S. Dauster, B.P. Cinquin, E.A. Smith, X. Robellet, D. D'Amours, C.A. Larabell, and O. Cohen-Fix. 2014. The yeast polo kinase Cdc5 regulates the shape of the mitotic nucleus. *Curr Biol*. 24:2861-2867.

Warren, G., J. Davoust, and A. Cockcroft. 1984. Recycling of transferrin receptors in A431 cells is inhibited during mitosis. *EMBO J*. 3:2217-2225.

Watson, K., G. Rossi, B. Temple, and P. Brennwald. 2015. Structural basis for recognition of the Sec4 Rab GTPase by its effector, the Lgl/tomosyn homologue, Sro7. *Mol Biol Cell*. 26:3289-3300.

Watts, F.Z., G. Shiels, and E. Orr. 1987. The yeast MYO1 gene encoding a myosin-like protein required for cell division. *EMBO J*. 6:3499-3505.

Wiederkehr, A., Y. Du, M. Pypaert, S. Ferro-Novick, and P. Novick. 2003. Sec3p is needed for the spatial regulation of secretion and for the inheritance of the cortical endoplasmic reticulum. *Mol Biol Cell*. 14:4770-4782.

Wu, H., C. Turner, J. Gardner, B. Temple, and P. Brennwald. 2010. The Exo70 subunit of the exocyst is an effector for both Cdc42 and Rho3 function in polarized exocytosis. *Mol Biol Cell*. 21:430-442.

Yoshida, S., K. Kono, D.M. Lowery, S. Bartolini, M.B. Yaffe, Y. Ohya, and D. Pellman. 2006. Polo-like kinase Cdc5 controls the local activation of Rho1 to promote cytokinesis. *Science*. 313:108-111.

Chapter 3: A Conserved Rab Phosphorylation Site Affects Membrane Association and Prenylation

Introduction

NH_2 and COOH-terminal phosphorylation events in Rabs were investigated using Sec4p as a model (Chapter 2). Rab phosphorylation is enriched in the NH_2 and COOH terminal extensions, however these phosphorylation events are not well conserved among members of the Rab family of small GTPases. Phosphorylation is not solely restricted to these regions and does occur in the GTPase domain itself. Specifically, we noticed a conserved serine/threonine residue in the switch II region of the GTPase domain (figure 1.5), which is phosphorylated in over a dozen different Rabs. The switch II region undergoes different structural conformations depending upon the nucleotide-bound state of the Rab and facilitates the interaction with GEFs, GDIs, and Rab Escort Proteins or REPs. As such, modification of this region may affect the nucleotide bound state of Rabs, recycling of Rabs on and off membranes, and the prenylation status of Rabs. To investigate this modification, we chose to use the *S. cerevisiae* Rab Ypt7p as a model.

Ypt7p is the only yeast Rab GTPase to contain a mass spectrometry confirmed phosphorylation event in the switch II region, and this phosphorylation site is conserved in the human ortholog Rab 7 (Sadowski et al., 2013; Shinde and Maddika, 2016). Ypt7p is involved in homeotypic fusion of vacuoles and is thus required for the maintenance of vacuolar morphology (Haas et al., 1995; Wada et al., 1992). Ypt7p is a non-essential Rab GTPase, and, due to the dynamic nature of vacuolar fission and fusion, loss of Ypt7p results in highly fragmented vacuoles (Haas et al., 1995; LaGrassa and Ungermann, 2005).

In addition to Ypt7p, other proteins are required for vacuolar homeotypic tethering and fusion, including the HOPS complex (a Ypt7p effector complex), Mon1p/Ccz1p (a Ypt7p GEF

complex), vacuolar SNAREs, and SNARE disassembly proteins Sec17p and Sec18p (Cabrera et al., 2014; Hickey and Wickner, 2010; Stroupe et al., 2009). The GEF complex Mon1p/Ccz1p is required for Ypt7p vacuolar localization and activation, but is not required for general association with cellular membranes (Cabrera and Ungermann, 2013). Once nucleotide exchange has been completed, Ypt7p in its GTP bound state interacts with the HOPS complex to mediate vesicle tethering and organize SNARE mediated fusions (Seals et al., 2000).

Phosphorylation of the Ypt7p GEF subunit Mon1p by Yck3p has already been characterized to release Mon1p from vacuolar membrane (Lawrence et al., 2014), and demonstrates phosphorylation as a mechanism to apply addition regulatory control over vacuolar fusion. Based on this information, we wondered if phosphorylation of Ypt7p would have similar effects in controlling vacuolar fusion. Additionally, based on the crystal structure of the human ortholog of Ypt7p (Rab7) the conserved phosphorylation occurs on the interface

Methods and Materials

Yeast strains, media and reagents

The *S. cerevisiae* strains and plasmids used in this study are listed in Table 3.1 and Table 3.2 respectively. Strains were created using standard genetic manipulations and lithium acetate transformations. For Western blot analysis, gels were transferred to PVDF Immobilon membrane (Millipore) prior to probing with antibodies including anti-GFP antibody abcam ab6556 and anti-His antibody Thermo Pierce™ 6x-His Epitope Tag (His.H8).

Membrane fractionation

GFP-Ypt7p wild type, GFP-Ypt7p^{S73A}, and GFP-Ypt7p^{S73E} were grown to mid-log phase OD, and 15 OD units of cells were lysed using glass beads into 10mM Tris pH 7.5, 10mM NaN_3, 200mM

sorbitol, 1mM PMSF, 1mM benzamidine, 0.2mM DTT, 5mM β-glycerol phosphate, 50mM NaF, and 2mM EDTA. Samples were clarified for 10 min at 4˚C 10,000xg. The supernatant was then spun for 1 hour at 100,000xg to separate the insoluble membrane fraction from the cytosolic fraction. The supernatant was removed and the membrane was re-suspended in the original lysis buffer prior to preparation for western blot.

Fluorescence microscopy

Fluorescence microscopy and differential interference contrast microscopy were achieved using an Eclipse E600 Nikon microscopy, 1X optivar (0.08μm/pixel), 60X Oil objective (1.4 numerical aperture), 10X/25 Nikon eye piece (CFIUW), and imaged with a Clara CCD camera from Andor Technology (DR-328G-C01-SIL). A C-FL GFP HC HISN zero shift filter set and C-FL Texas Red HC HISN zero shift filter set was used for GFP and mCherry image acquisition respectively. Images were taken as a series of z-stacks in 0.6μm increments over 8μm using NIS-Elements Advanced Research imaging software. Images were deconvolved using AutoQuant X software.

GFP-Atg8p Autophagy Assay

Yeast strains of RCY2193 expressing Ypt7p or Ypt7p mutants (pRC5488 and pRC5489) and pRC5411A were grown in SCD-Leu-Ura until mid-log phase. Each sample was then sub-cultured into either YPD (yeast peptone extract with 2% glucose) and SD-N (0.17% yeast nitrogen base without amino acids, 2% glucose) for 3 hours at 23˚C. Samples were then harvested, and 10 OD units of cells were spun down, washed in TAZ buffer (10mM Tris pH 7.5, 10mM NaN_3) then resuspended in 10mM Tris pH 7.5, 10mM NaN_3, 1mM PMSF, 1mM benzamidine, 0.2mM DTT, 5mM β-glycerol phosphate, 50mM NaF, and 2mM EDTA for glass

Table 3.1: Strain list

Strain	Genotype	Source
NY605	*MAT*a *ura3-52 leu2-3,112*	Novick Lab
RCY2193	MATa/α *ypt7Δ/ypt7Δ ura3Δ0/ura3 leu2Δ0/leu2 his3Δ0/his3 LYS2/lys2Δ0 MET15/met15Δ0*	Resgen
RCY5105	*MAT*α *his3Δ1 leu2Δ0 ura3Δ0 mon1ΔKAN^R*	Resgen

Table 3.2: Plasmid List

Plasmid ID	Description	Source
pRC5487	pRS426 vph1-mCherry	This study
pRC5488	pRS315 ypt7	This study
pRC5489	pRS315 ypt7^{S73A}	This study
pRC5490	pRS315 ypt7^{S73E}	This study
pRC5491	pRS315 GFP-ypt7	This study
pRC5492	pRS315 GFP-ypt7^{S73A}	This study
pRC5493	pRS315 GFP-ypt7^{S73E}	This study
pRC5494	pET28a ypt7	This study
pRC5495	pET28a ypt7^{S73A}	This study
pRC5496	pET28a ypt7^{S73E}	This study
pRC5411A	pRS316 GFP-atg8	This study
pRC5478	pRS315 GFP-ypt1^{T73E}	This study
pRC5479	pRS315 GFP-ypt1	This study
pRC5480	pRS315 GFP-sec4^{T84E}	This study
pRC651	pRS315 GFP-sec4	Collins lab
pRC5481	pRS315 GFP-ypt6^{S74E}	This study
pRC5482	pRS315 GFP-ypt6	This study
pRC5467	pRS316 Mon1-3xmCherry	This study

bead lysis. GFP-Atg8p degradation status was evaluated via western blot analysis using anti-GFP antibody abcam ab6556.from the cytosolic fraction. The supernatant was removed and the membrane was re-suspended in the original lysis buffer prior to preparation for western blot.

Fluorescence microscopy

Fluorescence microscopy and differential interference contrast microscopy were achieved using an Eclipse E600 Nikon microscopy, 1X optivar (0.08μm/pixel), 60X Oil objective (1.4 numerical aperture), 10X/25 Nikon eye piece (CFIUW), and imaged with a Clara CCD camera from Andor Technology (DR-328G-C01-SIL). A C-FL GFP HC HISN zero shift filter set and C-FL Texas Red HC HISN zero shift filter set was used for GFP and mCherry image acquisition respectively. Images were taken as a series of z-stacks in 0.6μm increments over 8μm using NIS-Elements Advanced Research imaging software. Images were deconvolved using AutoQuant X software.

GFP-Atg8p Autophagy Assay

Yeast strains of RCY2193 expressing Ypt7p or Ypt7p mutants (pRC5488 and pRC5489) and pRC5411A were grown in SCD-Leu-Ura until mid-log phase. Each sample was then sub-cultured into either YPD (yeast peptone extract with 2% glucose) and SD-N (0.17% yeast nitrogen base without amino acids, 2% glucose) for 3 hours at 23˚C. Samples were then harvested, and 10 OD units of cells were spun down, washed in TAZ buffer (10mM Tris pH 7.5, 10mM NaN_3) then resuspended in 10mM Tris pH 7.5, 10mM NaN_3, 1mM PMSF, 1mM benzamidine, 0.2mM DTT, 5mM β-glycerol phosphate, 50mM NaF, and 2mM EDTA for glass bead lysis. GFP-Atg8p degradation status was evaluated via western blot analysis using anti-GFP antibody abcam ab6556.

Protein purification

Ypt7p and subsequent mutant variations were purified from BL21 (DE3) *E. coli* using a 6x-His tag purification scheme. Briefly, protein expression was induced with 0.2mM IPTG overnight at 4˚C, bacterial pellets were resuspended in a lysis buffer (20mM Tris-HCl pH 8.0, 300mM NaCl and 5mM $MgCl_2$, 1mM benzamidine and 1mM PMSF), lysed by sonication, and clarified by centrifugation at 12,000xg for 30min. Affinity purification was achieved using a Cobalt conjugated agarose resin (Gold Biotechnology Inc.), and protein eluted with imidazole. Protein samples were dialyzed into 20mM Tris-HCl pH 8.0, 300mM NaCl, and 5mM $MgCl_2$ prior to nucleotide exchange assays and protein affinity pull-down assays. GST-Tagged Gdi1p was also purified from BL21 (DE3) cells using 50μM IPTG induction. Cells were pelleted, resuspended in 20mM Tris pH 8.0, 300mM NaCl, 10mM beta-mercaptoethanol, 5% glycerol, 1mM benzamidine, and 1mM PMSF. Affinity purification was achieved using Glutathione agarose resin from Gold Biotechnology, and eluted with 10mM glutathione in 20mM Tris pH 8.0, 300mM NaCl, 10mM beta-mercaptoethanol, 5% glycerol. Protein samples were dialyzed to remove glutathione.

Nucleotide Exchange Assay

This assay was based on the protocol described by Eberth et al. 2009 (Eberth and Ahmadian, 2009). Using a Spectra max Gemini XPS plate reader to measure fluorescence, Ypt7p and mutant samples were added to 10mM Tris HCl pH 7.5, 150mM NaCl, 2.5mM $MgCl_2$, 10mM EDTA, and 600nM mant-GTP at a final concentration of 600nM to begin the reaction. An excitation wavelength of 360nm and emission wavelength of 400nm was used to monitor the state of mant-GTP as either protein bound or free in solution. The reaction was monitored until fluorescent measurements plateaued.

Pull-down assay

Purified recombination 6x-His tagged Ypt7p mutants and GST-Gdi1p from bacteria were mixed together at a concentration of 75μg/mL and 160μg/mL respectively in a final volume of 500μL 20mM Tris pH 7.5, 250mM NaCl, and 3mM $MgCl_2$. Using glutathione agarose resin from Gold Biotechnology, samples were incubated in batch at 4˚C for 30min, then washed three times in 1mL 20mM Tris pH 7.5, 250mM NaCl, and 3mM $MgCl_2$. Samples were eluted through the addition of 50μL of 5X sample buffer with DTT and boiled at 95˚C for 10minutes prior to loading onto 12% SDS PAGE gels. Coomassie staining was used to visualize bound GST-Gdi1p and input Ypt7p samples, while western blot using anti-His antibody Thermo Pierce™ 6x-His Epitope Tag (His.H8) was used to assess bound Ypt7p mutants.

Maleimide PEG Assay

Maleimide PEG 2,000MW from Laysan Bio Inc. was used to modify cell lysates from RCY2193 with either pRC5491, pRC5492, pRC5493, or pRS315. Cells were grown to mid-log phase (0.2-0.8OD_{600}) and 10 OD_{600} units of cells were measured, pelleted, and resuspended in 100μL of 10mM HEPES pH 7.4, 1mM PMSF, and 1mM benzamidine. Individual 25μL aliquots from this protein lysate were used for each reaction. Briefly, 3μL of 0.1M maleimide PEG or 3μL of DMSO were added to each tube and the reaction was allowed to proceed for 30min at 30˚C. Reactions were stopped by adding 25μL of 2X SSB with DTT and boiling for 10min. For the denaturing conditions, an extra 2.5μL of 10% SDS was added to the reaction prior to maleimide PEG. Protein samples were resolved on 10% SDS PAGE gels, and subsequent western blots were performed as described using Abcam anti-GFP antibody (Ab6556).

Results

Phosphomimetic Ypt7p fails to associate with the vacuolar membrane

To investigate Ypt7p phosphorylation, we first attempted to mimic the constitutively phosphorylated state of the protein by converting serine 73 to a glutamic acid residue ($Ypt7p^{S73E}$). Conversely, we also mutated serine 73 to an alanine to prevent phosphorylation ($Ypt7p^{S73A}$). The phosphorylation event on serine 73 occurs in the switch II domain of Ypt7p, and, based on the structure of human homolog Rab7 REP-1 complex (Rak et al., 2004), is predicted to occur at the interface between REP and Ypt7p (figure 3.1). Using GFP tagged Ypt7p mutants and ectopically expressing them in wild type cells, we sought to determine if membrane association was disrupted (figure 3.2A). Indeed, $Ypt7p^{S73E}$, but not $Ypt7p^{S73A}$, completely failed to localize to any particular membrane structure and appeared to be completely cytosolic. This raises several possibilities as to the effect of phosphorylation, such as membrane recruitment being lost, rate of dissociation from the membrane significantly increased (but still capable of binding membrane), nucleotide-binding capacity disrupted, or aberrant protein folding.

To determine whether or not $Ypt7p^{S73E}$ was capable of associating with membranes at all and able to fold properly without being degraded, we performed membrane fractionation experiments with GFP tagged Ypt7p constructs as the sole copy of the protein (figure 3.2B). While the majority of $Ypt7p^{WT}$ and $Ypt7p^{S73A}$ associates with the membrane-bound fraction, no detectable amount of $Ypt7p^{S73E}$ was found to associate with membranes. Additionally, no degradation of $Ypt7p^{S73E}$ was detected, so protein folding does not appear to be significantly disrupted. The ability of Ypt7p to mediate vacuolar fusion requires membrane recruitment and

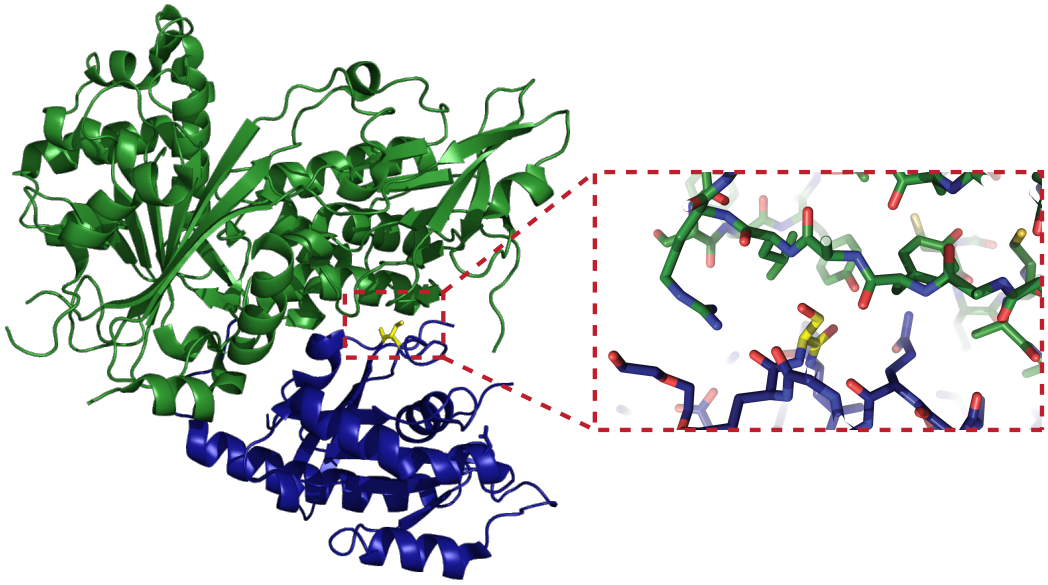

Figure 3.1: Conserved phosphorylated serine/threonine is at the Rab-REP interface

Rab7 REP-1 crystal structure (PDB: 1VG0) (Rak et al., 2004). Rab7 is in blue and REP-1 is in green. Serine 72, which is known to be phosphorylated (Hornbeck et al., 2015; Shinde and Maddika, 2016), is highlighted in yellow. The interface is magnified to show serine 72 tightly packed at the interface between Rab7 and REP-1.

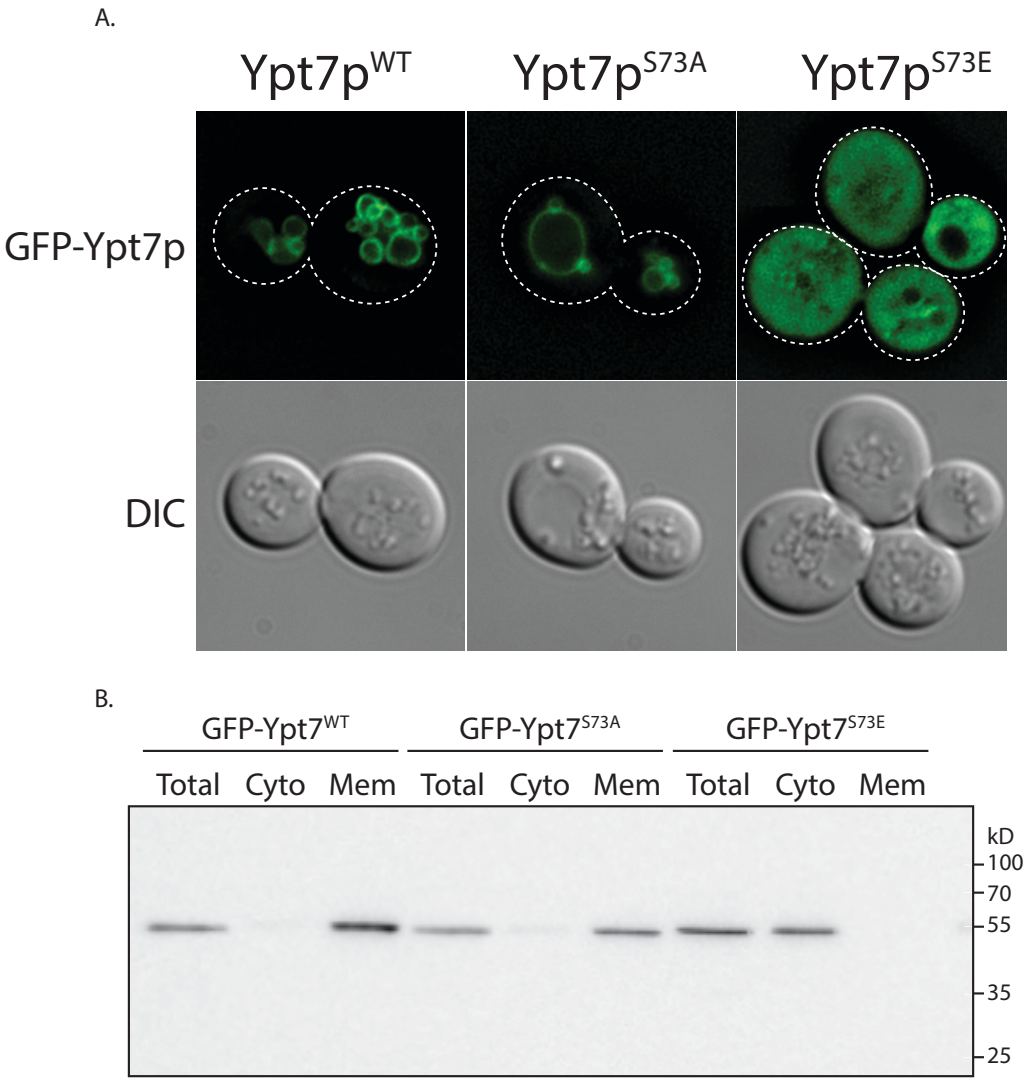

Figure 3.2: Phosphomimetic Ypt7p fails to associate with membranes

A. Microscopy of ectopically expressed, GFP tagged Ypt7p, Ypt7p^{S73A}, and Ypt7p^{S73E}. Cells were grown in SCD-Leu to mid-log phase prior to live cell imaging.

B. Membrane fractionation experiment using GFP tagged Ypt7p, Ypt7p^{S73A}, and Ypt7p^{S73E} as the sole copies of the protein in each respective cell line. After a 100,000xg spin, the soluble cytosolic fraction and the insoluble membrane fraction were separated and analyzed via western blot using GFP antibodies.

subsequent nucleotide exchange (Nordmann et al., 2010; Stroupe et al., 2009; Zick and Wickner, 2014). Based on the membrane association data, we hypothesized that phosphomimetic Ypt7p would be nonfunctional.

Phosphomimetic Ypt7p fails to mediate vacuolar fusion and autophagy

To determine if phosphomimetic and unphosphorylatable versions of Ypt7p were functional, we took advantage of the fact that Ypt7p is one of the few non-essential Rabs, and that loss of Ypt7p function results in fragmented vacuoles (Haas et al., 1995). Using a *ypt7Δ* strain, we tested whether or not Ypt7p^{S73E} and/or Ypt7p^{S73A} could rescue this phenotype. As a vacuolar membrane marker, we used an mcherry tagged Vph1 construct (Manolson et al., 1992). Indeed, in a vector only control, we noticed severe vacuolar fragmentation, however both the Ypt7p^{WT} and Ypt7p^{S73A} were able to rescue this phenotype (figure 3.3A). Ypt7p^{S73E} failed to rescue this phenotype, and vacuolar morphology was indistinguishable from the vector only control.

Additionally, Ypt7p is also required for autophagy (Hyttinen et al., 2013; Kim et al., 1999; Kirisako et al., 1999; Meiling-Wesse et al., 2002) like Sec4p (see chapter 2). As such, we wanted to address if phosphomimetic Ypt7p failed to rescue autophagy defects or whether phosphorylation is required for autophagy. To answer this question, we performed a GFP-Atg8p assay (Klionsky, 2011) (see chapter 2) using untagged Ypt7p mutants in a *ypt7Δ* genetic background (figure 3.3B). Using a vector only control, we saw autophagosome formation was indeed lost, but both Ypt7p^{WT} and Ypt7p^{S73A} were able to rescue this phenotype. Ypt7p^{S73E} failed to rescue autophagosome formation, so phosphorylation appears to completely compromise the ability of Ypt7p to mediate membrane fusion.

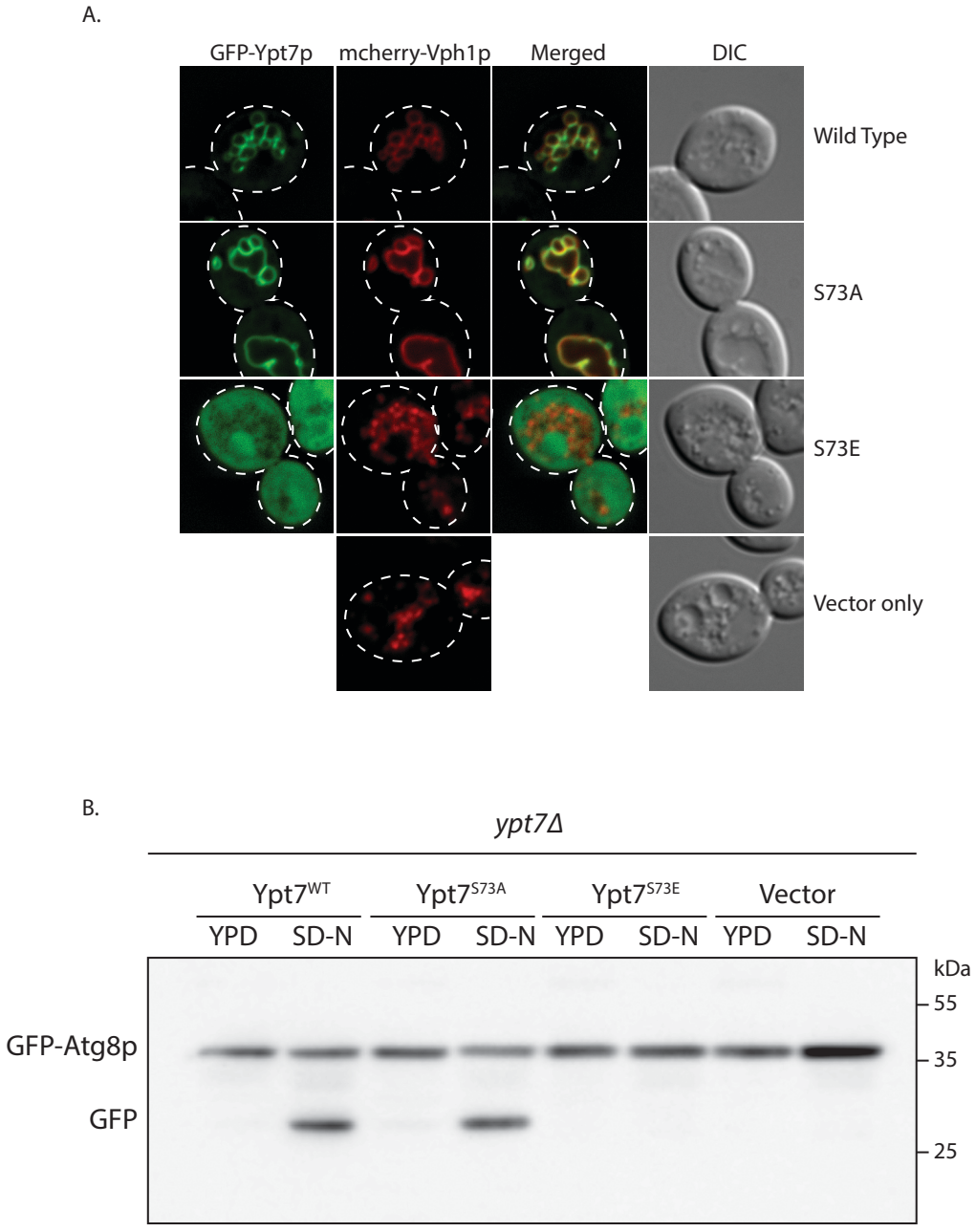

Figure 3.3: Phosphomimetic Ypt7p is non-functional for vacuolar fusion and autophagy

A. Live cell-imaging of GFP tagged Ypt7p, Ypt7p^{S73A}, and Ypt7p^{S73E} and mCherry tagged Vph1p as a vacuolar marker. GFP tagged Ypt7p constructs are the sole copy of the protein and there function is assayed by vacuolar fragmentation. Images were taken by Olya Spassibojko.

B. GFP-Atg8p autophagy assay of RCY2193 cells expressing either Ypt7p, Ypt7p^{S73A}, or Ypt7p^{S73E} on a pRS315 plasmid. Western blot of GFP tagged Atg8p to assess autophagosome formation as indicated by GFP (27 kD band) degradation product. Autophagy was induced by nitrogen starvation growth conditions (SD-N) and YPD medium was used as a negative control.

Intrinsic nucleotide binding and exchange is not affected by phosphorylation

To understand the molecular mechanism inhibiting the function of phosphomimetic Ypt7p, we wanted to determine if the protein itself was still capable of undergoing intrinsic nucleotide exchange. Failure to fold properly to accommodate a nucleotide could explain the phenotypes, but would likely be more of an artifact of the point mutation as opposed to a reasonable physiological role of phosphorylation. To answer this question, Ypt7p, Ypt7p^{S73A}, and Ypt7p^{S73E} were purified from bacteria, and a nucleotide exchange assay using mant-GTP was performed (figure 3.4). Intrinsic nucleotide exchange simply shows the capacity of the protein to bind and exchange a nucleotide and not the ability to interact with the GEF for catalyzed exchange (Eberth and Ahmadian, 2009). For Ypt7p, the GEF Mon1p/Ccz1p requires membrane associated Ypt7p for full activity (Cabrera et al., 2014). Based on the membrane fractionation experiments, Ypt7p^{S73E} fails to associate with membranes at all, which would indirectly affect GEF catalyzed nucleotide exchange. Thus, purification of membrane-bound Ypt7p from yeast would not provide a clear answer if this mutation directly affects nucleotide exchange. Bacteria lack GGTase II, thus all purified Ypt7p constructs will be soluble and lack prenylation (the ability to bind directly to membranes is also lost). Using this *in vitro* assay, we sought to determine if the phosphomimetic mutation directly affected intrinsic nucleotide exchange of Ypt7p. We found that Ypt7p^{S73E} was able to undergo intrinsic nucleotide exchange as efficiently as Ypt7^{S73A} and Yptp^{WT}. This illustrates that the point mutation does not significantly alter the protein folding of the GTPase domain, as it does not preclude the ability to bind and exchange nucleotide.

We next wondered if the GEF interaction was lost due to phosphorylation, and if that was preventing Ypt7p to be recruited to the membrane. Previous studies have already shown that

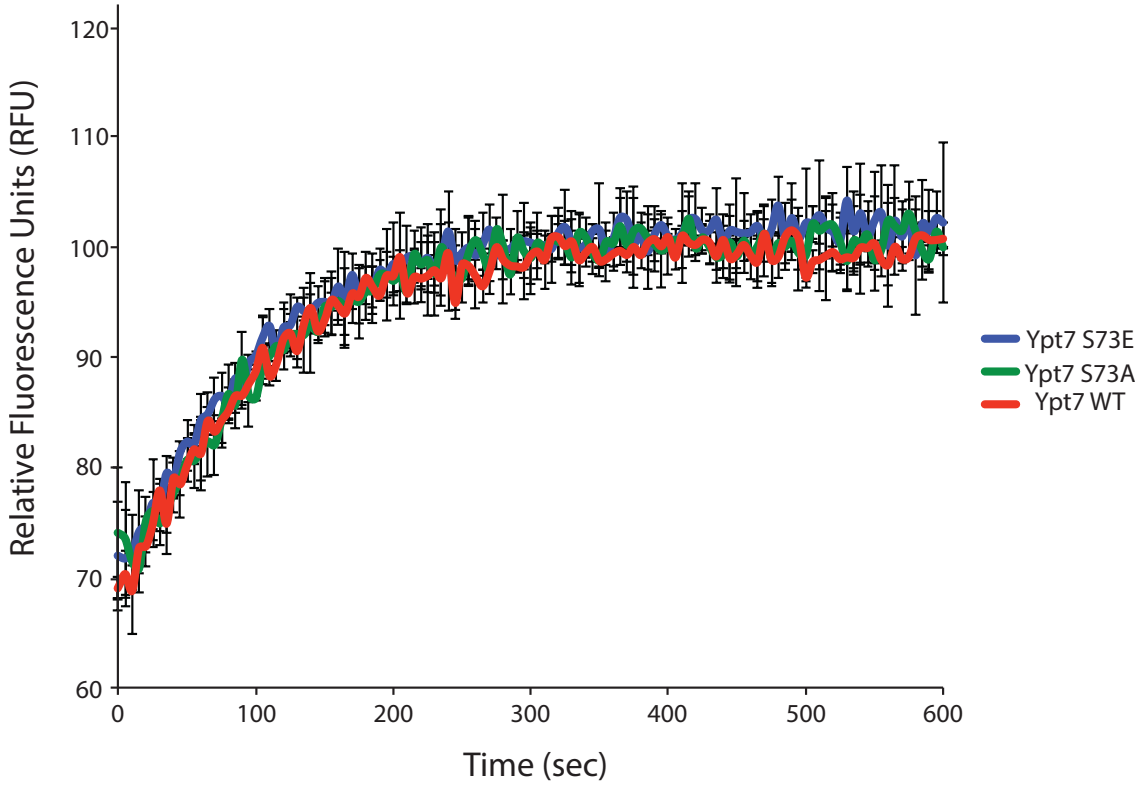

Figure 3.4: Intrinsic nucleotide exchange assay for Ypt7p

Graph showing intrinsic nucleotide exchange of Ypt7p, Ypt7p^{S73A}, and Ypt7p^{S73E}. Preloaded GDP bound Ypt7p proteins were mixed with mant-GTP and the rate of mant-GTP exchanging GDP is measured by an increase in fluorescence. Each reaction was performed in triplicate and the average relative fluorescent values for each time point are plotted above. The error bars are the standard deviation of the three different measurements.

deletion of the GEF subunit Mon1p results in a loss of Ypt7p localization to vacuolar membranes, but it does not prevent Ypt7p from associating with other membrane organelles (Cabrera and Ungermann, 2013). We sought to investigate the effects of a *mon1Δ* genetic background on cells solely expressing different Ypt7p mutants (figure 3.5). We found that, in agreement with Cabrera et al, *mon1Δ* results in Ypt7p failing to associate with vacuoles, but not with other membrane structures throughout the cell. Indeed, this was also true of Ypt7p^{S73A}, but Ypt7p^{S73E} was still completely cytosolic. These results show that lack of GEF activity does not solely explain the failure of phosphomimetic Ypt7p to associate with membranes.

Phosphomimetic Ypt7p fails to undergo prenylation

Since it appeared the nucleotide cycling of Ypt7p was not directly affected by phosphorylation, we next wondered if phosphomimetic Ypt7p was at all capable of anchoring to membranes. All Rabs require prenylation to associate with membranes, and this is accomplished through REPs directing Rabs to GGTase II for modification (Baron and Seabra, 2008). REP binds Rabs in a very similar fashion to GDI, and uses the switch II domain to have specificity for GDP-bound Rabs (Ignatev et al., 2008; Pylypenko et al., 2006; Sasaki et al., 1990; Waldherr et al., 1993). Prenylation of Rabs is thought to occur fairly rapidly after synthesis, and the modification is permanent (Kohnke et al., 2013). Since phosphomimetic Ypt7p results in complete membrane dissociation, we sought to determine whether the prenylation status of Ypt7p was disrupted or rather the protein was locked in a soluble complex with GDI.

To investigate the prenylation status of Ypt7p, we conducted a maleimide PEG experiment to modify free cysteine residues (Burgoyne et al., 2013). Prenylation occurs on two COOH-terminal cysteine residues, and being that this is a stable modification, *in vitro* modification of

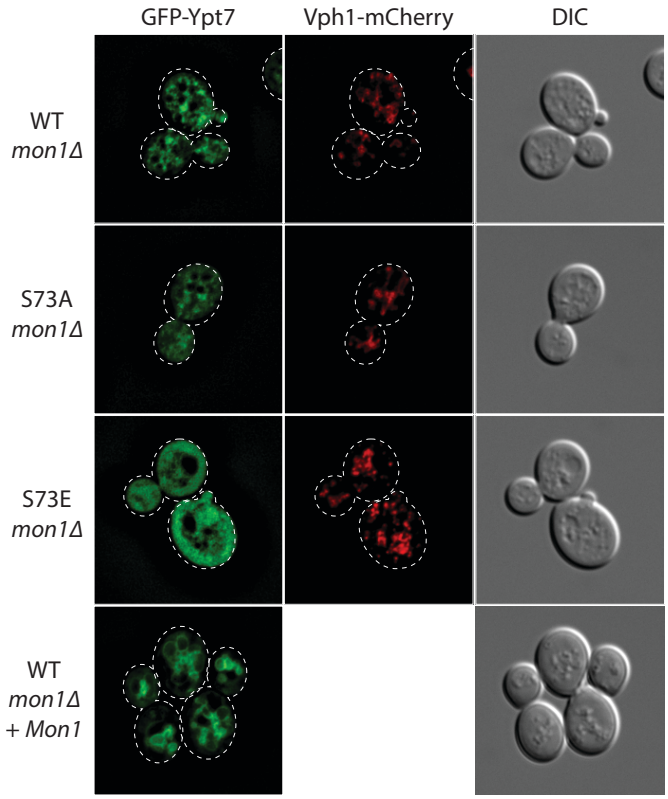

Figure 3.5: Ypt7p localization in GEF deletion background

Live cell imaging of GFP tagged Ypt7p, Ypt7p^{S73A}, and Ypt7p^{S73E} in a *mon1*Δ background strain. Vacuolar morphology is assessed using mCherry tagged Vph1p. Vacuolar morphology can be recused by adding in a normal copy of *mon1* on an episomal plasmid.

cysteine residues is blocked if prenylation is present. There are only a total of four cysteine residues on Ypt7p, and the other two are buried in the hydrophobic core of the protein according to structural information, and thus were not expected to be modified when the protein is folded (Constantinescu et al., 2002). Using this experiment to address the prenylation state of Ypt7p mutants, we found that indeed, modification of folded wild type protein does not occur, but we observed a significant shift in size, indicative of maleimide PEG modification, when the protein is unfolded and the interior free cysteine residues are exposed (figure 3.6). Furthermore, Ypt7p^{S73E}, but not Ypt7p^{S73A}, was significantly modified while folded, showing that the COOH-terminal cysteine residues were indeed free of prenylation. This explains the loss in membrane association and loss of function, as without prenylation, Ypt7p will not be able to anchor directly to membranes and thus be unable to mediate vacuolar fusion.

Gdi1p fails to interact with phosphomimetic Ypt7p

Based on structural data (figure 3.1) and lack of prenylation, it appears that Ypt7p^{S73E} fails to interact with REP, and thus fails to be modified. This suggests that there could be a role of phosphorylation in Rab prenylation, but based on the unphosphorylatable mutant, phosphorylation is not required for prenylation. Combined with the knowledge the prenylation is permanent and that there doesn't appear to be a normal detectable pool of non-prenylated Rabs *in vivo* (figure 3.6), it is likely the physiological role of phosphorylation is not to control prenylation (although this cannot be ruled out). However, since GDI and REP both bind Rabs in a similar fashion, GDI binding may be disrupted by phosphorylation, which would have a significantly different physiological role than what is observed in a constitutively phosphorylated mutant protein. However, testing this effect is complicated by the fact that prenylation increases the affinity of a Rab for GDI, and phosphomimetic Ypt7p lacks prenylation. To work around

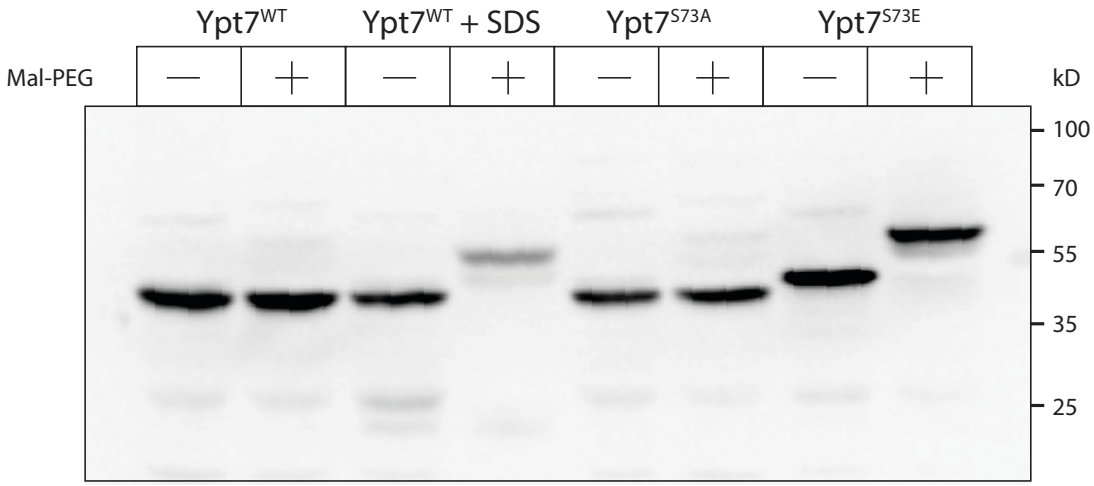

Figure 3.6: Prenylation status of phosphomimetic and unphosphorylatable Ypt7p

Maleimide PEG modification of surface exposed, reduced cysteine residues and subsequent western blot analysis. GFP tagged Ypt7p, Ypt7p^{S73A}, and Ypt7p^{S73E} is the only cellular copy of the protein in each strain. Modification of Ypt7p by maleimide to indicate reduced cysteine residues is visualized by a molecular weight shift (2kD for each cysteine). SDS was added to a final concentration of 1% to denature proteins and to expose two buried cysteine residues where indicated.

this, we used recombinant Ypt7p, Ypt7p^{S73A}, and Ypt7^{S73E} with recombinant GDI in an *in vitro* pull-down assay to determine the effects of these mutations on GDI binding. This way, Ypt7p binding to GDI can be assessed independent from the prenylation status of the protein. Using affinity tag purification of GST tagged Gdi1p and His tagged Ypt7p proteins, we found that Ypt7p^{S73E} completely lost its ability to bind Gdi1p (figure 3.7). Interestingly, Ypt7p^{S73A} had a significantly increased affinity for Gdi1p when compared to wild type protein. This suggests that phosphorylation could control Ypt7p membrane association, but in the opposite way than the microscopy of phosphomimetic protein would suggest. If phosphorylation occurs on membrane-bound (previously prenylated) Ypt7p, then it would act as a signal to remain on that membrane and fail to be extracted by Gdi1p. Furthermore, phosphorylation could facilitate release of Ypt7p from Gdi1p directly prior to membrane association. However, it should be noted that prenylation significantly increases GDI interaction, and the difference in GDI interaction between the wild type protein and Ypt7p^{S73A} may not as significant as what we observe in the absence of prenylation.

Conserved Rab phosphomimetic mutation leads to membrane dissociation

Ypt7p phosphorylation was studied as a model for a conserved Rab phosphorylation event. After establishing that phosphomimetic mutations ablate membrane association, we sought to investigate whether this same mutation would have similar consequences among other Rab proteins. To answer this question, we mutated the conserved S/T residue in the Rabs Sec4p, Ypt1p, and Ypt6p even though there is not a mass spectrometry confirmed phosphorylation event yet recorded at these positions. We found that, nearly identical to Ypt7p, all mutated Rabs exhibited a dramatic loss of membrane association (figure 3.8). Interestingly, Sec4p appears to display a slight membrane localization to what appears to be ER or other membrane bound

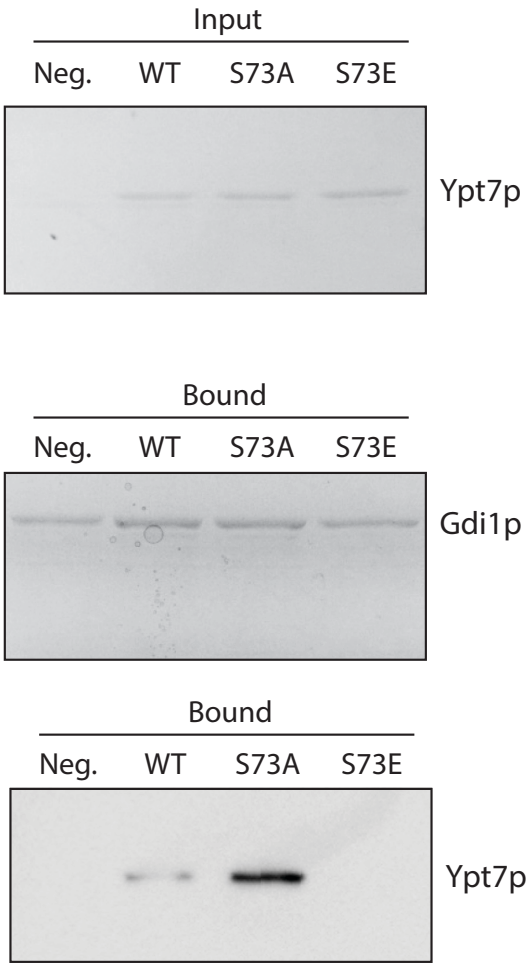

Figure 3.7: Phosphomimetic Ypt7p fails to interact with Gdi1p

Coomassie stained SDS PAGE gels showing input 6x-His tagged Ypt7p, Ypt7p^{S73A}, and Ypt7p^{S73E} and GST-resin bound GST tagged Gdi1p. Western blot of bound samples using 6x-His antibody was used to determine Ypt7p interaction with Gdi1p.

Figure 3.8: Microscopy of Rab GTPases with conserved phosphomimetic mutation

Live cell imaging of Ypt1p, Sec4p, and Ypt6p both with and without the conserved phosphorylation site mutated to mimic the constitutively phosphorylated state of the protein.

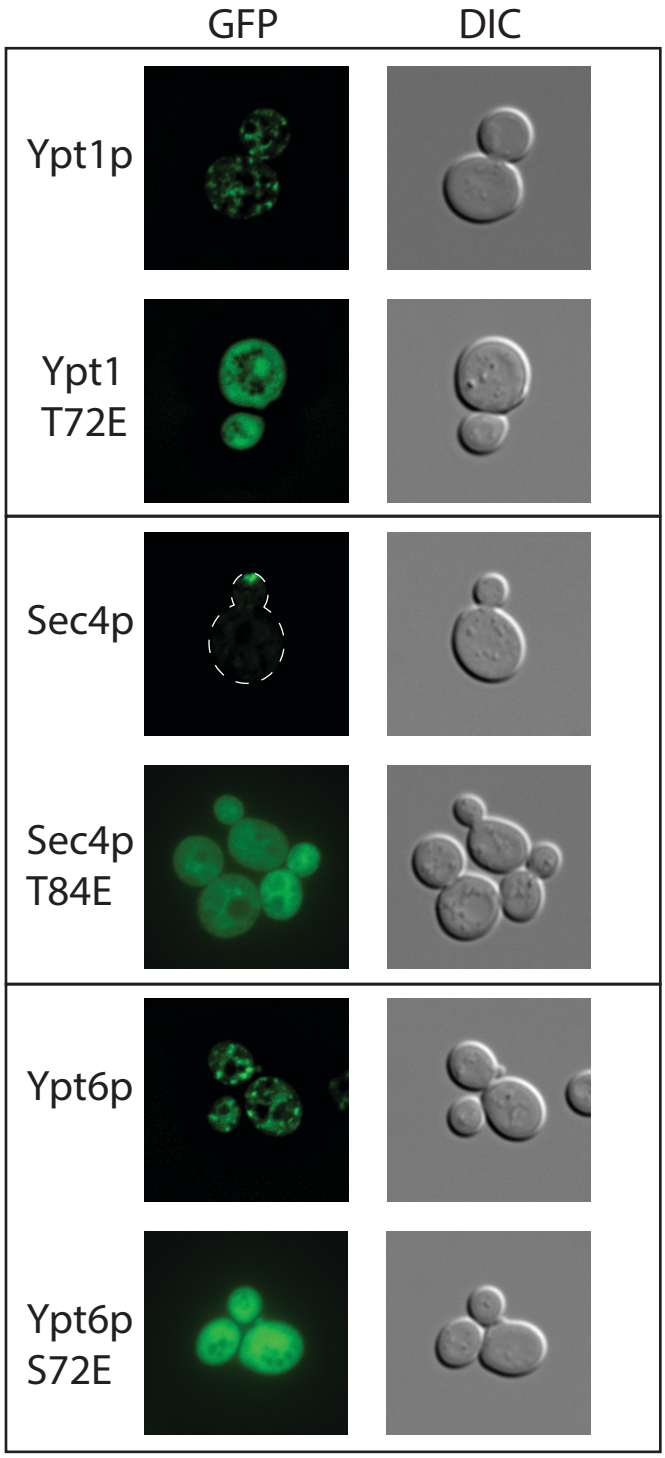
GFP
DIC
Ypt1p
Ypt1
T72E
Sec4p
Sec4p
T84E
Ypt6p
Ypt6p
S72E

organelles, but the majority of the protein is still cytosolic and Sec4p's normal membrane localization to sites of polarized exocytosis is completely lost. Based on these data, it appears we have found a conserved residue in Rabs in the switch II domain that is necessary for proper membrane association, and likely prenylation.

Conclusion/Discussion

Alignment of Rab GTPases and superimposition of mass spectrometry confirmed phosphorylation sites revealed a conserved serine/threonine residue in the switch II region that is often phosphorylated. Exploration of this modification using Ypt7p as a model suggests phosphorylation would disrupt the interaction between REPs and/or GDI proteins. Indeed, phosphomimetic Ypt7p fails to associate with membranes, is non-functional in both vacuolar fusion and autophagy, and fails to undergo prenylation. *In vitro* interaction with Gdi1p is also disrupted by this phosphomimetic mutation, while an unphosphorylatable mutant has a much greater affinity for Gdi1p. Finally, in all Rabs tested, phosphomimetic mutation of this conserved serine/threonine causes a failure to associate with membrane. Overall, these results implicate phosphorylation as a regulatory mechanism to control the membrane association of Rabs.

While this study was underway, it was reported that the ortholog of Ypt7p in humans, Rab7, displays almost identical membrane localization phenotypes when the conserved serine residue is mutated to mimic constitutive phosphorylation (Shinde and Maddika, 2016). They also went on to show that GDI interaction was disrupted as we reported, but they add that GEF binding was also disrupted. However, they failed to investigate the prenylation status of Rab7, which is likely obstructed and contributing to the loss of interaction with the GEF and GDI protein. Overall, several Rabs (Ypt7p, Rab7, Sec4p, Ypt1p, and Ypt6p) have been shown to lose membrane

association when this conserved phosphorylation site is mutated, suggesting a common mechanism among Rab family members.

It still remains to be determined whether phosphorylation has a role to play in prenylation itself, or rather if phosphorylation could stabilize Rabs on membranes by blocking GDI mediated membrane extraction. We attempted to detect *in vivo* phosphorylation of Ypt7p by a gel mobility shift using Phos-tag™ (Kinoshita et al., 2009), however we were not successful (Figure 3.9). Based on our experience with Sec4p phosphorylation however, we know that such a technique to detect phosphorylation may not be ideal.

Overall, we report a conserved Rab mutation that causes membrane dissociation. This conserved mutation may prove useful as a research tool to ablate Rab localization. This phosphomimetic mutation may have a physiological role in prenylation or GDI extraction of Rabs, however future work is required to detect and characterize *in vivo* phosphorylation.

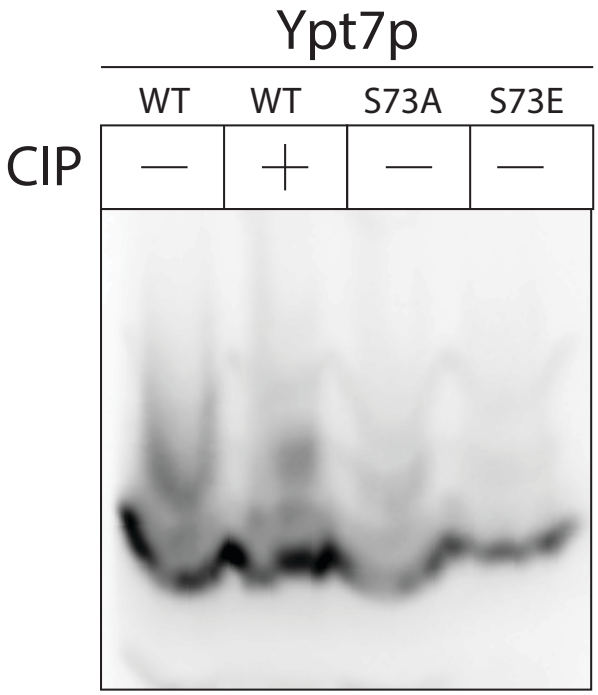

Figure 3.9: Phos-Tag™ SDS-PAGE fails to resolve Ypt7p phosphorylation

Western blot of GFP tagged Ypt7p containing yeast lysates treated with or without calf-intestinal alkaline phosphatase. Samples were resolved on phos-tag™ SDS polyacrylamide gels (experiment was carried out following manufacture's instructions). A concentration of 50μmol/L of Phos-tag™ acrylamide was used in a final 12% acrylamide gel.

References:

Baron, R.A., and M.C. Seabra. 2008. Rab geranylgeranylation occurs preferentially via the pre-formed REP-RGGT complex and is regulated by geranylgeranyl pyrophosphate. *Biochem J*. 415:67-75.

Burgoyne, J.R., O. Oviosu, and P. Eaton. 2013. The PEG-switch assay: a fast semi-quantitative method to determine protein reversible cysteine oxidation. *J Pharmacol Toxicol Methods*. 68:297-301.

Cabrera, M., M. Nordmann, A. Perz, D. Schmedt, A. Gerondopoulos, F. Barr, J. Piehler, S. Engelbrecht-Vandre, and C. Ungermann. 2014. The Mon1-Ccz1 GEF activates the Rab7 GTPase Ypt7 via a longin-fold-Rab interface and association with PI3P-positive membranes. *J Cell Sci*. 127:1043-1051.

Cabrera, M., and C. Ungermann. 2013. Guanine nucleotide exchange factors (GEFs) have a critical but not exclusive role in organelle localization of Rab GTPases. *J Biol Chem*. 288:28704-28712.

Constantinescu, A.T., A. Rak, K. Alexandrov, H. Esters, R.S. Goody, and A.J. Scheidig. 2002. Rab-subfamily-specific regions of Ypt7p are structurally different from other RabGTPases. *Structure*. 10:569-579.

Eberth, A., and M.R. Ahmadian. 2009. In vitro GEF and GAP assays. *Curr Protoc Cell Biol*. Chapter 14:Unit 14 19.

Haas, A., D. Scheglmann, T. Lazar, D. Gallwitz, and W. Wickner. 1995. The GTPase Ypt7p of Saccharomyces cerevisiae is required on both partner vacuoles for the homotypic fusion step of vacuole inheritance. *EMBO J*. 14:5258-5270.

Hickey, C.M., and W. Wickner. 2010. HOPS initiates vacuole docking by tethering membranes before trans-SNARE complex assembly. *Mol Biol Cell*. 21:2297-2305.

Hornbeck, P.V., B. Zhang, B. Murray, J.M. Kornhauser, V. Latham, and E. Skrzypek. 2015. PhosphoSitePlus, 2014: mutations, PTMs and recalibrations. *Nucleic Acids Res*. 43:D512-520.

Hyttinen, J.M., M. Niittykoski, A. Salminen, and K. Kaarniranta. 2013. Maturation of autophagosomes and endosomes: a key role for Rab7. *Biochim Biophys Acta*. 1833:503-510.

Ignatev, A., S. Kravchenko, A. Rak, R.S. Goody, and O. Pylypenko. 2008. A structural model of the GDP dissociation inhibitor rab membrane extraction mechanism. *J Biol Chem*. 283:18377-18384.

Kim, J., V.M. Dalton, K.P. Eggerton, S.V. Scott, and D.J. Klionsky. 1999. Apg7p/Cvt2p is required for the cytoplasm-to-vacuole targeting, macroautophagy, and peroxisome degradation pathways. *Mol Biol Cell*. 10:1337-1351.

Kinoshita, E., E. Kinoshita-Kikuta, H. Ujihara, and T. Koike. 2009. Mobility shift detection of phosphorylation on large proteins using a Phos-tag SDS-PAGE gel strengthened with agarose. *Proteomics*. 9:4098-4101.

Kirisako, T., M. Baba, N. Ishihara, K. Miyazawa, M. Ohsumi, T. Yoshimori, T. Noda, and Y. Ohsumi. 1999. Formation process of autophagosome is traced with Apg8/Aut7p in yeast. *J Cell Biol*. 147:435-446.

Klionsky, D.J. 2011. For the last time, it is GFP-Atg8, not Atg8-GFP (and the same goes for LC3). *Autophagy*. 7:1093-1094.

Kohnke, M., C. Delon, M.L. Hastie, U.T. Nguyen, Y.W. Wu, H. Waldmann, R.S. Goody, J.J. Gorman, and K. Alexandrov. 2013. Rab GTPase prenylation hierarchy and its potential role in choroideremia disease. *PLoS One*. 8:e81758.

LaGrassa, T.J., and C. Ungermann. 2005. The vacuolar kinase Yck3 maintains organelle fragmentation by regulating the HOPS tethering complex. *J Cell Biol*. 168:401-414.

Lawrence, G., C.C. Brown, B.A. Flood, S. Karunakaran, M. Cabrera, M. Nordmann, C. Ungermann, and R.A. Fratti. 2014. Dynamic association of the PI3P-interacting Mon1-Ccz1 GEF with vacuoles is controlled through its phosphorylation by the type 1 casein kinase Yck3. *Mol Biol Cell*. 25:1608-1619.

Manolson, M.F., D. Proteau, R.A. Preston, A. Stenbit, B.T. Roberts, M.A. Hoyt, D. Preuss, J. Mulholland, D. Botstein, and E.W. Jones. 1992. The VPH1 gene encodes a 95-kDa integral membrane polypeptide required for in vivo assembly and activity of the yeast vacuolar H(+)-ATPase. *J Biol Chem*. 267:14294-14303.

Meiling-Wesse, K., H. Barth, C. Voss, G. Barmark, E. Muren, H. Ronne, and M. Thumm. 2002. Yeast Mon1p/Aut12p functions in vacuolar fusion of autophagosomes and cvt-vesicles. *FEBS Lett*. 530:174-180.

Nordmann, M., M. Cabrera, A. Perz, C. Brocker, C. Ostrowicz, S. Engelbrecht-Vandre, and C. Ungermann. 2010. The Mon1-Ccz1 complex is the GEF of the late endosomal Rab7 homolog Ypt7. *Curr Biol*. 20:1654-1659.

Pylypenko, O., A. Rak, T. Durek, S. Kushnir, B.E. Dursina, N.H. Thomae, A.T. Constantinescu, L. Brunsveld, A. Watzke, H. Waldmann, R.S. Goody, and K. Alexandrov. 2006. Structure of doubly prenylated Ypt1:GDI complex and the mechanism of GDI-mediated Rab recycling. *EMBO J*. 25:13-23.

Rak, A., O. Pylypenko, A. Niculae, K. Pyatkov, R.S. Goody, and K. Alexandrov. 2004. Structure of the Rab7:REP-1 complex: insights into the mechanism of Rab prenylation and choroideremia disease. *Cell*. 117:749-760.

Sadowski, I., B.J. Breitkreutz, C. Stark, T.C. Su, M. Dahabieh, S. Raithatha, W. Bernhard, R. Oughtred, K. Dolinski, K. Barreto, and M. Tyers. 2013. The PhosphoGRID Saccharomyces cerevisiae protein phosphorylation site database: version 2.0 update. *Database (Oxford)*. 2013:bat026.

Sasaki, T., A. Kikuchi, S. Araki, Y. Hata, M. Isomura, S. Kuroda, and Y. Takai. 1990. Purification and characterization from bovine brain cytosol of a protein that inhibits the dissociation of GDP from and the subsequent binding of GTP to smg p25A, a ras p21-like GTP-binding protein. *J Biol Chem*. 265:2333-2337.

Seals, D.F., G. Eitzen, N. Margolis, W.T. Wickner, and A. Price. 2000. A Ypt/Rab effector complex containing the Sec1 homolog Vps33p is required for homotypic vacuole fusion. *Proc Natl Acad Sci U S A*. 97:9402-9407.

Shinde, S.R., and S. Maddika. 2016. PTEN modulates EGFR late endocytic trafficking and degradation by dephosphorylating Rab7. *Nat Commun*. 7:10689.

Stroupe, C., C.M. Hickey, J. Mima, A.S. Burfeind, and W. Wickner. 2009. Minimal membrane docking requirements revealed by reconstitution of Rab GTPase-dependent membrane fusion from purified components. *Proc Natl Acad Sci U S A*. 106:17626-17633.

Wada, Y., Y. Ohsumi, and Y. Anraku. 1992. Genes for directing vacuolar morphogenesis in Saccharomyces cerevisiae. I. Isolation and characterization of two classes of vam mutants. *J Biol Chem*. 267:18665-18670.

Waldherr, M., A. Ragnini, R.J. Schweyer, and M.S. Boguski. 1993. MRS6--yeast homologue of the choroideraemia gene. *Nat Genet*. 3:193-194.

Zick, M., and W.T. Wickner. 2014. A distinct tethering step is vital for vacuole membrane fusion. *Elife*. 3:e03251.

Chapter 4: Discussion and Future Directions for Investigating Rab Phosphorylation

Rab phosphorylation is an interesting cellular phenomenon that adds further regulation to membrane trafficking events. Despite Rabs already possessing the ability to switch between an active and inactive conformation (GTP and GDP bound respectively), phosphorylation appears to add another mechanism to control Rab activity. We demonstrated that phosphorylation negatively affects the function Sec4p and Ypt7p via separate mechanisms. NH_2 and COOH terminal phosphorylation of Sec4p disrupts the interaction with the essential effector protein and exocyst component Sec15p, while Ypt7p phosphomimetic mutation in the switch II region causes prenylation defects and failure to interact with GDI, rendering the protein nonfunctional in both homeotypic vacuolar fusion and autophagy. Interestingly, phosphorylation of Sec4p human orthologs Rab8A, Rab8B, and Rab13 on serine 111 via PTEN-induced kinase 1 (PINK1) was recently shown to impair function through disrupting GEF interaction, and Ypt7p ortholog Rab7 phosphorylation was also shown to impair function in a strikingly similar fashion to what we found in this study (Lai et al., 2015; Shinde and Maddika, 2016). It appears phosphorylation in general may negatively impact Rab activity, but more information is needed to establish if this trend holds true for the entire family of proteins. However, these finding do suggest that the examples of phosphorylation demonstrated in this work are conserved in humans and warrant further investigation.

There are still several challenges in studying Rab phosphorylation that need to be addressed. First, detection of Rab phosphorylation has proven difficult for both Sec4p and Ypt7p. Sec4p phosphorylation could only reliably be detected through developing phospho-specific antibodies, and even that technique fell short to detect phosphorylation on the COOH terminus of Sec4p.

Ypt7p phosphorylation also appears to be sub-stoichiometric as it cannot be resolved as a separate band via SDS-PAGE even with the addition of Phos-tag™ (Figure 3.9). Development of phospho-specific antibodies for Ypt7p is a possibility, as there is sufficient sequence variation to differentiate between other Rabs, but phosphorylation may be below the limit of detection. To overcome this difficulty, it may be helpful to first screen cellular conditions or genetic backgrounds that enrich Rab phosphorylation using very sensitive techniques such as mass spectrometry. It would be interesting to investigate Ypt7p phosphorylation status in certain abnormal vacuolar morphology genetic backgrounds such as *yck3Δ* and *mon1Δ/ccz1Δ* that result in the formation of large interconnected vacuoles and small fragmented vacuoles respectively (LaGrassa and Ungermann, 2005; Meiling-Wesse et al., 2002). Alternatively, altering the salt concentration of the growth media can induce vacuolar fusion (low salt) or fission (high salt) (Bone et al., 1998; Li and Kane, 2009)

Several questions also remain concerning both Sec4p and Ypt7p phosphorylation. First, Sec4p phosphorylation was shown to be a cell cycle dependent modification associated with cytokinesis and required for the maintenance of cell size and normal growth, however, only phosphorylation on serine 8 was monitored *in vivo*. It would be very interesting to determine if there are any changes in COOH terminal phosphorylation throughout the cell cycle as there are with phosphorylation of serine 8. Cell cycle synchrony and subsequent Sec4p purification coupled with mass spectrometry experiments would be ideal for measuring such changes and could identify what phosphorylated Sec4p isoforms exist *in vivo*.

Ypt7p phosphorylation was implicated in GDI binding and Rab prenylation, however Ypt7p phosphorylation was only investigated through the use of phosphomimetic mutations. These experiments have their merits and provide crucial information, however they fail to account for

the context of phosphorylation within the cell. Phosphorylation is a dynamic modification, while constitutively phosphomimetic mutants are not, thus creating issues such as a permanent loss in prenylation. The question still remains as to whether Ypt7p phosphorylation affects prenylation timing or rather GDI interaction *in vivo*. This question can be quickly answered using membrane fractionation techniques coupled to mass spectrometry to determine if Ypt7p phosphorylation exists solely in the cytosolic fraction of the protein (prenylation delay) or if it exists at all on the membrane (GDI interaction is being affected). Furthermore, the conserved phosphorylation event studied using Ypt7p was found to have similar phenotypes in several other Rabs, raising the possibility of a conserved mechanism among Rab family members. Only four Rabs were examined in this study, and only via microscopy. Maleimide PEG experiments will also need to be performed to confirm prenylation defects.

Overall, the work presented herein demonstrates Rab phosphorylation to be an important regulatory control mechanism extending to many Rab family members. Sec4p phosphorylation as a model for NH_2 and COOH terminal phosphorylation reveals a mechanism controlling effector protein recruitment in addition to the nucleotide-bound state. Although not fully investigated here, phosphorylation may allow Rabs to differentiate between different effector proteins or may recruit as of yet undiscovered effector proteins. Ypt7p phosphorylation does appear to be highly conserved not only in human homologs, but also to the Rab family in general. Similar to nucleotide hydrolysis or exchange deficient conserved Rab mutations (Feig, 1999), this S73E mutation may be a prenylation defective Rab mutation that extends to all members of the family. As such, this may be a valuable research tool. Although our understanding of Rab phosphorylation is still limited, it appears phosphorylation has conserved

mechanisms of action across many Rab family members and adds to our understanding of membrane trafficking.

References:

Bone, N., J.B. Millar, T. Toda, and J. Armstrong. 1998. Regulated vacuole fusion and fission in Schizosaccharomyces pombe: an osmotic response dependent on MAP kinases. *Curr Biol*. 8:135-144.

Feig, L.A. 1999. Tools of the trade: use of dominant-inhibitory mutants of Ras-family GTPases. *Nat Cell Biol*. 1:E25-27.

LaGrassa, T.J., and C. Ungermann. 2005. The vacuolar kinase Yck3 maintains organelle fragmentation by regulating the HOPS tethering complex. *J Cell Biol*. 168:401-414.

Lai, Y.C., C. Kondapalli, R. Lehneck, J.B. Procter, B.D. Dill, H.I. Woodroof, R. Gourlay, M. Peggie, T.J. Macartney, O. Corti, J.C. Corvol, D.G. Campbell, A. Itzen, M. Trost, and M.M. Muqit. 2015. Phosphoproteomic screening identifies Rab GTPases as novel downstream targets of PINK1. *EMBO J*. 34:2840-2861.

Li, S.C., and P.M. Kane. 2009. The yeast lysosome-like vacuole: endpoint and crossroads. *Biochim Biophys Acta*. 1793:650-663.

Meiling-Wesse, K., H. Barth, C. Voss, G. Barmark, E. Muren, H. Ronne, and M. Thumm. 2002. Yeast Mon1p/Aut12p functions in vacuolar fusion of autophagosomes and cvt-vesicles. *FEBS Lett*. 530:174-180.

Shinde, S.R., and S. Maddika. 2016. PTEN modulates EGFR late endocytic trafficking and degradation by dephosphorylating Rab7. *Nat Commun*. 7:10689.